Università degli Studi di Padova

Administrative unit: **Università degli Studi di Padova**

Department: **Territorio e Sistemi Agro-Forestali (TESAF)**

PhD Program : **Land, Environment, Resources, Health**

Batch: XXIX

New lines in tree-ring research

PhD Program Coordinator: **Prof. Davide Matteo Pettenella**

Supervisor: **Prof. Marco Carrer**

Co-supervisor: **Dr. Jesus Julio Camarero Martínez**

PhD candidate: **Elena Pellizzari**

Università degli Studi di Padova

Sede Amministrativa: **Università degli Studi di Padova**

Dipartimento di **Territorio e Sistemi Agro-Forestali (TESAF)**

Corso di Dottorato di Ricerca in: **Territorio, Ambiente, Risorse e Salute**

Ciclo: XXIX

New lines in tree-ring research

Coordinatore: **Prof. Davide Matteo Pettenella**

Supervisore: **Prof. Marco Carrer**

Co-Supervisore: **Dr. Jesus Julio Camarero Martínez**

Dottorando: **Elena Pellizzari**

CONTENTS

SUMMARY

Natural archives, and tree-rings in particular, are fundamental tools to investigate on pre-instrumental climate variability. Tree-ring research, indeed, covers a wide field of applications, however several woody species are still overlooked and investigating just at yearly resolution, we might miss important intra-annual information. To fill these gaps, the main objective of this thesis is to undertake new lines in tree-ring research testing i) the dendrochronological potential of a marginal species to detect different climatic signal respect the usual tree species and ii) a quantitative wood anatomy approach to investigate whether with multiple cell traits is possible to extract information not visible at annual level in tree-ring series. With the new species, the common juniper (*Juniperus communis, L.*), I found a clear winter precipitation signal in ring-width series in the Alps, and a decoupling in the tree-ring to climate responses and growth between trees and shrubs across all the biomes investigated (Mediterranean, Alpine and Polar). With wood anatomy, I assessed the importance to use several related proxies as a diagnostic tool to detect hydraulic deterioration and mortality due to drought stress in Scots pine (*Pinus sylvestris L.)* and Silver fir (*Abies alba*) in Spain. In addition, at high latitudes, still on Scots pine I was built a 1000-year long chronology with anatomical parameters which could permit to investigate long-term temperature fluctuations. This work highlights the importance to use different species and different approaches to extract new information out of the tree-ring series. These first analysis show the possibility to reconstruct winter precipitation in the Alps and to adopt anatomical data as a surrogate of densitometric measurements or as a valid diagnostic tool for a retrospective assessment of trees health. Prediction on the future status of our forests would benefit from such an information.

RIASSUNTO

Applicazione di nuove linee di ricerca dendrocronologiche

Archivi naturali, in particolare gli anelli legnosi, sono strumenti fondamentali per studiare la variabilità climatica antecedente la strumentazione meteorologica. La ricerca sugli anelli legnosi copre un ampio campo di applicazioni, ciononostante molte specie vegetali non sono ancora state esplorate dal punto di vista dendrocronologico, e in aggiunta l'analisi solo a livello annuale, potrebbe non evidenziare diverse importanti informazioni intra-annuali. Per colmare queste mancanze, l'obiettivo principale di questa tesi è di intraprendere nuove linee di ricerca dendrocronologica testando i) il potenziale di una specie marginale per individuare un segnale climatico differente e non identificato in altre specie arboree e ii) un approccio di dendro-anatomia quantitativa per verificare se attraverso molteplici tratti cellulari è possibile estrarre informazioni non visibili a livello annuale nelle serie di anelli legnosi. Con l'utilizzo di una nuova specie in dendrocronologia, il ginepro comune (*Juniperus communis, L.*), ho identificato un chiaro segnale di precipitazione invernale nelle serie anulari nella regione Alpina, e un disaccoppiamento negli incrementi sulla risposta clima-accrescimento tra alberi e arbusti in diversi biomi (Mediterraneo, Alpino e Polare). Attraverso l'anatomia del legno, ho definito l'importanza di utilizzare diversi "proxy" relativi a queste misure come strumenti diagnostici per individuare la deteriorazione idraulica e mortalità a causa di stress idrico e siccità su pino silvestre (*Pinus sylvestris L.*) e abete bianco (*Abies alba*) in Spagna. In aggiunta, ad elevate latitudini, sempre su pino silvestre ho costruito una cronologia lunga 1000 anni con parametri anatomici che potrebbero permettere di studiare fluttuazioni di lungo termine. Questo lavoro evidenzia l'importanza di utilizzare diverse specie in dendrocronologia e differenti approcci per estrarre nuove informazioni da serie di anelli legnosi. Queste prime analisi dimostrano la possibilità di ricostruire la precipitazione nevosa sulle Alpi e di adottare dati anatomici come sostituti di misure densitometriche o come validi strumenti diagnostici per un'analisi retrospettiva della salute degli alberi. Queste nuove informazioni possono essere di beneficio per comprendere il futuro status delle nostre foreste.

GENERAL INTRODUCTION

Dendrochronology and new frontiers in tree-ring research

The growing interest on recent global warming (IPCC, 2014) rises the emergent demand to investigate on past climate to model future trends. It is well-known that natural archives such as ice cores, pollens, ocean sediments, corals, and tree rings, store a huge amount of information about pre-instrumental climate and environmental variability, and thanks to them it is possible to reconstruct long-term climatic fluctuations (Bradley, 2014).

Tree ring in particular, is by far one of the most common and used proxy record to reconstruct past climate variation (Fritts, 1976; Jones *et al.*, 2009; IPCC, 2014). Dendrochronology is properly the science used to date tree rings through crossdating and thanks to this method, also considered a basic principle within this discipline, it is possible to move one step ahead the normal ring counting. In fact, with crossdating it is feasible to objectively compare different records with the possibility to absolutely date relic or historical wood material and to extend back the time frame of the analysis. These chances turn the tree-ring sequences one of the most accurate and precise paleorecord available.

Collecting samples from both living trees and death wood material it is clear the potential to build reliable centuries to millennia long chronologies. In fact, although some living trees (*Pinus Longeva*) can reach up to 5000 years (Brown, 1996), also processing dead individuals like snags and logs or wood samples submerged in lakes, in peat bogs or from ancient buildings, it is possible to create very long chronologies (Esper *et al.*, 2002; Guiot *et al.*, 2005; Büntgen *et al.*, 2008a; Jones *et al.*, 2009). Wisely distilling the target information out of this kind of datasets, many researches and climatologist were able to reconstruct millennia-scale climate variability in temperature- or water-limited environments (Büntgen *et al.*, 2005, 2006, 2008a; Corona *et al.*, 2010), especially at high latitudes or altitudes around the globe (Esper *et al.*, 2002, 2007, 2014; Büntgen *et al.*, 2008b; Zhu *et al.*, 2008).

Together with the most widely and classically adopted ring width there are several other parameters that can be extracted from the same wood sample which, in the last decades, proved to be very valuable proxies: stable isotopes and wood density. Stable isotopes in tree rings, are used to infer plants physiological responses to environmental variability (McCarroll & Loader, 2004a; Loader *et al.*, 2007) according to parallel variation in Carbon and Oxygen isotopes concentration in wood cellulose. From them it is possible to derive changes in plant water use efficiency or soil moisture deficit, and they have been efficiently adopted to build long term precipitation reconstructions (Treydte *et al.*, 2006, 2014; Rinne *et*

al., 2013; Sidorova *et al.*, 2013). Furthermore, high resolution density profiles can be extracted by x-ray densitometry (Schweingruber *et al.*, 1978). Among the various parameters that can be extracted, maximum latewood density has been found highly conditioned by summer temperatures, and due to this association the densitometric approach is preferred respect to tree-ring measurements in many climate reconstruction studies especially at high latitudes (Esper *et al.*, 2010, 2014; Linderholm *et al.*, 2014).

Nonetheless, despite the widespread use and the high potential there are still several drawbacks and possibilities to improve the type and quality of the information extracted from wood samples. For example, i) trees are active just during the growing season, implying a lack of information related to the winter or dormancy period; ii) tree rings have an inherent yearly resolution which, usually, hampers the possibility of a detailed analysis at intra annual level; iii) isotopes and densitometric measurements still lack shared protocols with the negative result that data are not or hardly comparable among different laboratories. Further, these approaches are rather expensive and time consuming (Mannes *et al.*, 2007; Michener & Lajtha, 2007)(McCarroll & Loader, 2004b) usually limiting sample replication.

Starting from these weaknesses and with the constant need to improve the research through more exhaustive data, emerges the need to associate the classical dendrochronological method with new research lines, including the use of different species or a different approach in samples measuring.

Testing the potential of an underrepresented species in tree-ring research

Tree-ring analysis and dendrochronology has been widely applied to many shrub and tree species distributed all over the world (Grissino-Mayer, 1993) however, some species are well known for the critical crossdating and for this reason they are not or poorly adopted. For example, common juniper (*Juniperus communis, L.*), even though it has the largest geographical range of any woody plant, is considered rather challenging to work with, and for this reason until now it has not been thoroughly considered for dendrochronological studies. Nonetheless, being a shrub, it might potentially be sensitive to different climatic drivers respect the coexisting tree species.

In this work I aimed to apply the classical dendrochronological approach to common juniper which, as already mentioned, has a marginal role in dendrochronology due to the complexities in crossdating derived from the irregular and lobate growth form, for the frequent presence of wedging and missing rings and for the reduce growth rates (Hantemirov *et al.*, 2011; Wilmking *et al.*, 2012; Myers-Smith *et al.*, 2014).

The Alps are one of the most studied area for dendrochronological investigations and tree-rings climate reconstructions (Carrer & Urbinati, 2001; Frank & Esper, 2005; Corona *et al.*, 2010). Here conifers are dominant and represent the target species for investigations considering also that they are usually long-lived and with a marked temperature signal. Nonetheless, coexisting shrub species have not been thoroughly explored in this region. Indeed, just few studies involved common juniper, and more in general the genus *Juniperus* worldwide (Esper, 2000; Hantemirov *et al.*, 2000, 2011; Esper *et al.*, 2007; Hallinger *et al.*, 2010; Liang *et al.*, 2011). To fill this gap, I tried to explore the dendrochronological potential of common juniper first in the Alpine range, and then extending the analysis at national and European level. In addition, considering that a potential decoupling should be present in climate sensitivity between shrubs and trees living at the treeline (Körner, 2012), I hypothesise that trees, having an erected growth form should be sensitive to temperatures being more coupled with atmospheric air, in contrast to shrubs, characterized by prostrate growth form which should be influenced by different climate drivers. This dichotomy between erected and prostrate growth form could assume an important role in a climate warming scenario.

Testing the informative and diagnostic potential of quantitative wood anatomical parameters

Analysis on the recent climate warming demonstrate that the global air temperature over the period of 1880-2012 has increased of an average of 0.85 [0.65 to 1.06] °C and the last 30 years was the warmest period over the last 1400 years in the northern hemisphere (IPCC, 2014). In particular the effect of rising temperatures in Mediterranean biome, can be detrimental for plant growth (Linares & Camarero, 2012; Vicente-Serrano *et al.*, 2015) especially in the drought-prone areas. Further, in this region the presence of extreme drought events has been projected to increase (Allen, 2009; Allen *et al.*, 2010). Two ecophysiological mechanisms are assumed to play a key role in drought-induced forest dieback: i) carbon starvation, due to stomata closure to avoid evapotranspiration (typical to isohydric species), but at the cost of reducing carbon uptake or ii) hydraulic failure, related to the very high evapotranspiration rate coupled with water shortage. This can induce vessel cavitation or a general deterioration in the hydraulic performances especially in the anisohydric species (McDowell, 2011). Within this framework, I tried to test the diagnostic skills of dendroanatomy in growth declining and tree dieback phenomena.

As previously mentioned, the classical dendrochronological approach usually does not permit to go beyond the typical annual resolution, though I must underline that it is almost the only natural archive that always reach such a high time definition. With dendroanatomy, i.e. the application of dendrochronological techniques to wood anatomical time series, it could be possible to concurrently i) increase the time resolution of the inferences, ii) benefit from the wealth of data and parameters (e.g. lumen area, cell wall thickness, hydraulic conductivity, etc.) that it is possible to retrieve out of the same sample and iii) have a better understanding of the underlying physiological processes related to the tree growth (Fonti *et al.*, 2010; Carrer *et al.*, 2015). Recently tree-ring anatomy has much improved, and thanks to new techniques (von Arx *et al.*, 2016) and image analysis software (von Arx & Carrer, 2014) now the time spent to obtain the data has been significantly reduced.

Zooming at anatomical and the intra-annual level can permit to assess the change in tree sensitivity to climate along the growing season and therefore to disentangle the role of earlywood cells, usually larger with the highest hydraulic conductivity, from the latewood ones characterized by thicker cell walls with the usual imprint of the plant C-sink activity throughout the growing season. This explains why latewood density, has been proved to be one of the most powerful tool to reconstruct past summer temperatures at temperature-limited environments (Tuovinen, 2005; Büntgen *et al.*, 2006; Helama *et al.*, 2008; Esper *et al.*, 2010, 2012; Chen *et al.*, 2012). With dendroanatomy I also tried to use cell-wall thickness as a potential surrogate for wood density measurement and in particular latewood cell-wall thickness as an objective and standard measure for maximum density.

AIMS OF THE THESIS

Starting from the classical dendrochronological approaches and with the general target to increase the type and quality of the information that we can extract from tree rings, in this thesis work I aimed to come along two new research lines: i) investigating the potential of a new species but still adopting the classical approach (1-2) and ii) to fully exploit and assess the new improvements and potentials of tree-ring anatomy (3-4).

1. I apply the classical dendrochronological approach to a new (or very underrepresented) species: the common juniper (*Juniperus communis, L.*). I aimed to test first of all the potential of this species to encode a different climatic signal respect the coexisting conifer trees. Firstly I performed a pilot study with a regional network in North-Eastern Alps and then, after the confirm of the initial hypothesis, I enlarged the investigation throughout the whole Alpine region.

2. Considering the widespread distribution of common juniper (Farjon, 2013), I also aimed to verify the climate response of this species through a 5000 km latitudinal transect, including different biomes, Polar, Alpine and Mediterranean across the European continent. Even in this second step I still targeted to investigate whether divergent responses are present between prostrate and erected (*Larix spp.* and *Pinus spp.*) growth forms in a much wider context.
3. I tested the potential of dendrochronological techniques applied to wood anatomical traits in two contrasting environments and two species, Scots pine (*Pinus sylvestris, L.*) and Silver fir (*Abies alba*). In particular, in the Iberian Peninsula, in stands where water is the key limiting factor and evident processes of drought-induced forest dieback are ongoing, I verified the two main hypothesis related to tree mortality: the hydraulic failure and the carbon starvation.
4. Still on Scots pine but in a temperature-limited area at high latitudes I tried to build a millennium-long chronology using anatomical features. To date the maximum length of wood anatomical time series is few decades or centuries. Lengthening this time frame would allow a wider perspective to better explore long-term climatic fluctuation. In addition, I tried to extract a surrogate of maximum latewood density from wood anatomical data.

REFERENCES

Allen CD (2009) Climate-induced forest dieback: An escalating global phenomenon? In: *Unasylva*, Vol. 60, pp. 43–49.

Allen CD, Macalady AK, Chenchouni H et al. (2010) A global overview of drought and heat-induced tree mortality reveals emerging climate change risks for forests. *Forest Ecology and Management*, **259**, 660–684.

von Arx G, Carrer M (2014) ROXAS – A new tool to build centuries-long tracheid-lumen chronologies in conifers. *Dendrochronologia*, **32**, 290–293.

von Arx G, Crivellaro A, Prendin AL, Čufar K, Carrer M (2016) Quantitative Wood Anatomy—Practical Guidelines. *Frontiers in Plant Science*, **7**, 781.

Bradley R (2014) *Paleoclimatology: Reconstructing Climates of the Quaternary*, 3rd edn. Academic Press, 696 pp.

Brown PM (1996) OLDLIST: A database of maximum tree ages. In: *J.S. Dean, D.M. Meko, and T.W. Swetnam, eds., Tree Rings, Environment, and Humanity: Proceedings of the International ConferenceTree Rings, Environment, and Humanity*, pp. 727–731. Tucson, Arizona, 17-21 May, 1994. Radiocarbon 1996.

Büntgen U, Esper J, Frank DC, Nicolussi K, Schmidhalter M (2005) A 1052-year tree-ring proxy for Alpine summer temperatures. *Climate Dynamics*, **25**, 141–153.

Büntgen U, Frank DC, Nievergelt D, Esper J (2006) Summer temperature variations in the European Alps, A.D. 755-2004. *Journal of Climate*, **19**, 5606–5623.

Büntgen U, Frank D, Wilson R, Carrer M, Urbinati C, Esper J (2008a) Testing for tree-ring divergence in the European Alps. *Global Change Biology*, **14**, 2443–2453.

Büntgen U, Frank D, Grudd H, Esper J (2008b) Long-term summer temperature variations in the Pyrenees. *Climate Dynamics*, **31**, 615–631.

Carrer M, Urbinati C (2001) Spatial analysis of structural and tree-ring related parameters in a timberline forest in the Italian Alps. *Journal of Vegetation Science*, **12**, 643–652.

Carrer M, Arx G Von, Castagneri D, Petit G (2015) Distilling allometric and environmental information from time series of conduit size : the standardization issue and its relationship to tree hydraulic architecture. *Tree Physiology*, **35**, 27–33.

Chen F, Yuan Y jiang, Wei W shou et al. (2012) Temperature reconstruction from tree-ring maximum latewood density of Qinghai spruce in middle Hexi Corridor, China. *Theoretical and Applied Climatology*, **107**, 633–643.

Corona C, Guiot J, Edouard JL, Chalié F, Büntgen U, Nola P, Urbinati C (2010) Millennium-long summer temperature variations in the European Alps as reconstructed from tree rings. *Climate of the Past*, **6**, 379–400.

Esper J (2000) Long-term tree-ring variations in Juniperus at the upper timber-line in the Karakorum (Pakistan). *The Holocene*, **10**, 253–260.

Esper J, Cook ER, Schweingruber FH (2002) Low-frequency signals in long tree-ring chronologies for reconstructing past temperature variability. *Science (New York, N.Y.)*, **295**, 2250–2253.

Esper J, Frank D, Wilson RS, Büntgen U, Treydte K (2007) Uniform growth trends among central Asian low- and high-elevation juniper tree sites. *Trees*, **21**, 141–150.

Esper J, Frank D, Büntgen U, Verstege A, Hantemirov R, Kirdyanov A V. (2010) Trends and uncertainties in Siberian indicators of 20th century warming. *Global Change Biology*, **16**, 386–398.

Esper J, Frank DC, Timonen M et al. (2012) Orbital forcing of tree-ring data. *Nature Clim. Change*, **2**, 862–866.

Esper J, Düthorn E, Krusic PJ, Timonen M, Büntgen U (2014) Northern European summer temperature variations over the Common Era from integrated tree-ring density records. *Journal of Quaternary Science*, **29**, 487–494.

Farjon A (2013) Juniperus communis. *The IUCN Red List of Threatened Species. Version 2015.2*.

Fonti P, Von Arx G, García-González I, Eilmann B, Sass-Klaassen U, Gärtner H, Eckstein D (2010) Studying global change through investigation of the plastic responses of xylem anatomy in tree rings. *New Phytologist*, **185**, 42–53.

Frank D, Esper J (2005) Characterization and climate response patterns of a high-elevation, multi-species tree-ring network in the European Alps. *Dendrochronologia*, **22**, 107–121.

Fritts HC (1976) *Tree rings and Climate*. Academic Press, London, UK.

Grissino-Mayer H d. (1993) An updated list of species used in tree-ring research. *Tree-Ring Bulletin*, **53**, 17–43.

Guiot J, Nicault A, Rathgeber C, Edouard JL, Guibal F, Pichard G, Till C (2005) Last-millennium summer-temperature variations in western Europe based on proxy data. *The Holocene*, **15**, 489–500.

Hallinger M, Manthey M, Wilmking M (2010) Establishing a missing link: warm summers and winter snow cover promote shrub expansion into alpine tundra in Scandinavia. *New Phytologist*, **186**, 890–899.

Hantemirov RM, Gorlanova LA, Shiyatov SG (2000) Pathological tree-ring structures in Siberian juniper (juniperus sibirica burgsd.) and their use for reconstructing extreme climatic events. *Russian Journal of Ecology*, **31**, 167–173.

Hantemirov R, Shiyatov S, Gorlanova L (2011) Dendroclimatic study of Siberian juniper. *Dendrochronologia*, **29**, 119–122.

Helama S, Vartiainen M, Kolström T, Peltola H, Meriläinen J (2008) X-ray microdensitometry applied to subfossil tree-rings: Growth characteristics of ancient pines from the southern boreal forest zone in Finland at intra-annual to centennial time-scales. *Vegetation History and Archaeobotany*, **17**, 675–686.

IPCC (2014) *Climate Change 2014: Impacts, Adaptation, and Vulnerability. Part A: Global and Sectoral Aspects. Contribution of Working Group II to the Fifth Assessment Report of the Intergovernmental Panel on Climate Change [Field, C.B., V.R. Barros, D.J. Dokken, K.J.* Cambridge University Press, Cambridge, United Kingdom and New York, NY, USA, 1132 pp.

Jones PD, Briffa KR, Osborn TJ et al. (2009) High-resolution palaeoclimatology of the last millennium: a review of current status and future prospects. *The Holocene*, **19**, 3–49.

Körner C (2012) Treelines will be understood once the functional difference between a tree and a shrub is. *Ambio*, **41**, 197–206.

Liang E, Lu X, Ren P, Li X, Zhu L, Eckstein D (2011) Annual increments of juniper dwarf shrubs above the tree line on the central Tibetan Plateau: A useful climatic proxy. *Annals of Botany*, **109**, 721–728.

Linares JC, Camarero JJ (2012) From pattern to process: Linking intrinsic water-use efficiency to drought-induced forest decline. *Global Change Biology*, **18**, 1000–1015.

Linderholm HW, Björklund J, Seftigen K, Gunnarson BE, Fuentes M (2014) Fennoscandia revisited: a spatially improved tree-ring reconstruction of summer temperatures for the last 900 years. *Climate Dynamics*, **45**, 933–947.

Loader NJ, McCarroll D, Gagen M, Robertson I, Jalkanen R (2007) Extracting Climatic Information from Stable Isotopes in Tree Rings. *Terrestrial Ecology*, **1**.

Mannes D, Lehmann E, Cherubini P, Niemz P (2007) Neutron imaging versus standard X-ray densitometry as method to measure tree-ring wood density. *Trees*, **21**, 605–612.

McCarroll D, Loader NJ (2004a) Stable isotopes in tree rings. In: *Quaternary Science Reviews*, Vol. 23, pp. 771–801.

McCarroll D, Loader NJ (2004b) Stable isotopes in tree rings. In: *Quaternary Science Reviews*, Vol. 23, pp. 771–801.

McDowell NG (2011) Mechanisms linking drought, hydraulics, carbon metabolism, and vegetation mortality. *Plant physiology*, **155**, 1051–1059.

Michener RH, Lajtha K (2007) *Stable isotopes in ecology and environmental science*. xxvi, 566 p.

Myers-Smith IH, Hallinger M, Blok D et al. (2014) Methods for measuring arctic and alpine shrub growth: A review. *Earth-Science Reviews*, **140**, 1–13.

Rinne KT, Loader NJ, Switsur VR, Waterhouse JS (2013) 400-year May-August precipitation reconstruction for Southern England using oxygen isotopes in tree rings. *Quaternary Science Reviews*, **60**, 13–25.

Schweingruber F, Fritts H, Braker O, Drew L, Schar E (1978) The Xray technique as applied to dendroclimatology. *Tree-Ring Bulletin*, **38**, 61–91.

Sidorova O V., Siegwolf RTW, Myglan VS et al. (2013) The application of tree-rings and stable isotopes for reconstructions of climate conditions in the Russian Altai. *Climatic Change*, **120**, 153–167.

Treydte K, Schleser GH, Helle G, Frank D, Winiger M, Haug GH, Esper J (2006) The twentieth century was the wettest period in northern Pakistan over the past millennium. *Nature*, **440**, 1179–1182.

Treydte K, Boda S, Graf Pannatier E et al. (2014) Seasonal transfer of oxygen isotopes from precipitation and soil to the tree ring: Source water versus needle water enrichment. *New Phytologist*, **202**, 772–783.

Tuovinen M (2005) Response of tree-ring width and density of Pinus sylvestris to climate beyond the continuous northern forest line in Finland. *Dendrochronologia*, **22**, 83–91.

Vicente-Serrano SM, Camarero JJ, Zabalza J, Sangüesa-Barreda G, López-Moreno JI, Tague CL (2015) Evapotranspiration deficit controls net primary production and growth of silver fir: Implications for Circum-Mediterranean forests under forecasted warmer and drier conditions. *Agricultural and Forest Meteorology*, **206**, 45–54.

Wilmking M, Hallinger M, Van Bogaert R et al. (2012) Continuously missing outer rings in woody plants at their distributional margins. *Dendrochronologia*, **30**, 213–222.

Zhu H, Zheng Y, Shao X, Liu X, Xu Y, Liang E (2008) Millennial temperature reconstruction based on tree-ring widths of Qilian juniper from Wulan, Qinghai Province, China. *Chinese Science Bulletin*, **53**, 3914–3920.

LIST OF PAPERS

Chapter I

Pellizzari E, Pividori M, Carrer M, 2014. **Winter precipitation effect in a mid-latitude temperature-limited environment: the case of common juniper at high elevation in the Alps**.
Environmental Research Letters, **9**, 104021.

In this pilot study we explored the dendroclimatological skills of common juniper in the Alpine range selecting three study sites. Our results call for a deeper investigation on the dendrochronological potential of common juniper (*Juniperus communis, L.*). In fact, this species is sensitive to winter precipitation, a climate signal not visible in tree species. and its tree-ring sequences could be considered a proxy for winter snow accumulation.

Chapter II

Pellizzari E., Camarero J. J., Gazol A., Granda E., Shetti R., Wilmking M., Moiseev P., Pividori M. and Carrer M. **Diverging shrub and tree growth from the Polar to the Mediterranean biomes across the European continent**
Global change biology, **in press**

After having assessed the potentiality of common juniper to detect a winter precipitation signal in the Alpine range, in this work we investigate the decoupling between shrubs (common juniper, *Juniperus communis, L.*) and coexisting trees in a wide area covering different biomes - Mediterranean, Alpine and Polar - to understand how different growth forms respond to climate warming. We first hypothesized and then proved the presence of a divergent sensitivity between shrubs and trees. Unexpectedly we found that junipers in Polar and Mediterranean biomes present an enhanced growth in the last decades. These findings may help to better understand growth trends in treeline environments under the pressure of rising temperatures.

Chapter III

Pellizzari E, Camarero JJ, Gazol A, Sangüesa-Barreda G, Carrer M, 2016. **Wood anatomy and carbon-isotope discrimination support long-term hydraulic deterioration as a major cause of drought-induced dieback.**
Global Change Biology, **22**, 2125–2137
Rising temperatures and reduced water availability has become increasingly important in Mediterranean region, where drought-induced forest mortality is getting more and more frequent. Using quantitative wood anatomy here we tested, in two Scots pine (*Pinus sulvestris, L*) and Silver fir (*Abies alba*) stands , , whether the main cause of tree mortality is linked to hydraulic failure or carbon starvation. Our results suggest that hydraulic

deterioration is the most important cause of drought-induced dieback since dead trees presented significant smaller vessels respect to living ones.

Chapter IV

Pellizzari E, Esper J. Carrer M….. **Comparing MXD and millennium-long cell-chronology in northern Finland.**
In preparation
In this work I tried to build one of the longest chronology using anatomical parameters processing both living and sub-fossil Scots pine (*Pinus sylvestris L*) samples from northern Finland. Out of more than 40 samples I built a multi-trait chronology spanning over 1000 years. Radial cell wall thickness has been proved to be the most sensitive anatomical parameter to summer temperatures, and a valuable surrogate of maximum latewood density data.

CHAPTER I

OPEN ACCESS
IOP Publishing
Environmental Research Letters
Environ. Res. Lett. 9 (2014) 104021 (9pp)
doi:10.1088/1748-9326/9/10/104021

Winter precipitation effect in a mid-latitude temperature-limited environment: the case of common juniper at high elevation in the Alps

Elena Pellizzari, Mario Pividori and Marco Carrer

Università degli studi di Padova, dip. TeSAF, Agripolis, I-35020 Legnaro, PD, Italy

E-mail: elena.pellizzari.4@studenti.unipd.it

Received 16 May 2014, revised 25 September 2014
Accepted for publication 25 September 2014
Published 27 October 2014

Abstract

Common juniper (*Juniperus communis* L.) is by far the most widespread conifer in the world. However, tree-ring research dealing with this species is still scarce, mainly due to the difficulty in crossdating associated with the irregular stem shape with strip-bark growth form in older individuals and the high number of missing and wedging rings. Given that many different species of the same genus have been successfully used in tree-ring investigations and proved to be reliable climate proxies, this study aims to (i) test the possibility to successfully apply dendrochronological techniques on common juniper growing above the treeline and (ii) verify the climate sensitivity of the species with special regard to winter precipitation, a climatic factor that generally does not affect tree-ring growth in all Alpine high-elevation tree species. Almost 90 samples have been collected in three sites in the central and eastern Alps, all between 2100 and 2400 m in elevation. Despite cross-dating difficulties, we were able to build a reliable chronology for each site, each spanning over 200 years. Climate-growth relationships computed over the last century highlight that juniper growth is mainly controlled by the amount of winter precipitation. The high variability of the climate-growth associations among sites, corresponds well to the low spatial dependence of this meteorological factor. Fairly long chronologies and the presence of a significant precipitation signal open up the possibility to reconstruct past winter precipitation.

S Online supplementary data available from stacks.iop.org/ERL/9/104021/mmedia

Keywords: *Juniperus communis*, tree-ring, climate-growth response, winter precipitation, snow cover

1. Introduction

Trees growing at their uppermost or northernmost limits have long attracted scientists. Indeed, these areas usually offer a clear representation of the activity of an environmental driver, namely temperature, which is able to set a limit to growth and distribution of the tree life form. This feature, together with other peculiarities such as the presence of a relatively undisturbed area with respect to sites at lower elevation the presence of more long-lived individuals, contributes to *tree-line* being a key topic with a very rich literature and long-standing research history in plant ecology (Körner 2012). In the last decades, the discussion on global change has further increased the attention of the scientific community on these temperature-limited ecosystems. Indeed, they are highly sensitive to even minor temperature variation related, for example, to climate variability (Körner 2012) or

microtopographical settings (Bunn *et al* 2011, Bunn *et al* 2005, Carrer and Urbinati 2001) and play a major role in various feedback mechanisms within the climate system with significant effects at global scale *e.g.* the treeline advance (Grace *et al* 2002, Devi *et al* 2008, Harsch *et al* 2009) or the change in the terrestrial albedo (Bonan *et al* 1995).

The Alps are one of the most studied areas for high elevation forests and their relationships with climate (Holtmeier 2009, Tranquillini 1979); the most investigated species are conifer trees (*Larix decidua*, *Pinus cembra*, *Picea abies*, *Pinus sylvestris*, *Abies alba*). In this area tree species usually have the typical erect life form, once they reach 2–4 m in height they become closely coupled to prevailing atmospheric conditions and for this reason temperature is generally the key limiting factor for tree growth (Carrer and Urbinati 2004, Büntgen *et al* 2005, Frank and Esper 2005, Carrer and Urbinati 2006). In the Alps, as in most of the high-latitude regions (St George 2014), precipitation, and specifically winter precipitation, is rarely a limiting factor for tree growth if we exclude some special cases where a mechanical action, linked to avalanches or slow mass movement, is involved (Holtmeier and Broll 2010, Smith *et al* 2003, Casteller *et al* 2007). This is why in the Alps almost no investigations found the clear presence of a tree growth sensitivity to precipitation or, within a long-term perspective, no clear precipitation signal has ever been detected in high elevation tree-ring sequences (Büntgen *et al* 2008, Carrer *et al* 2007, Frank and Esper 2005). Nonetheless, in many regions snow cover emerged as an important driver of tree and shrub growth by providing a constant cover and protection against frosts during the early growing season (Wipf *et al* 2009, Rixen *et al* 2010), and increasing the nutrient supply (Hallinger *et al* 2010). In contrast, massive snowpack could delay the onset of the growing season (Kirdyanov *et al* 2003, Schmidt *et al* 2006, Vaganov *et al* 1999), reducing the duration of cambial activity.

The absence of a precipitation signal in the Alps with the consequent impossibility to adopt tree-ring sequences as a proxy to infer past precipitation conditions still represents a gap in our knowledge. Indeed, short- and long-term water cycle dynamics in a densely populated mountain area such as the Alps could have major social and environmental effects, from the collapse of the glaciers mass balance (Haeberli and Beniston 1998, Beniston 2012), to freshwater resource management (Viviroli *et al* 2011) or the permanence of a winter snow pack fundamental for many alpine plant species but also for winter tourism and related activities (Elsasser and Burki 2002, Morrison and Pickering 2013). To fill this gap, we directed our attention on a different species that grows at the same elevation as or higher than the other conifer species, but which could be sensitive to winter precipitation: common juniper (*Juniperus communis L.*).

The species has a wide distribution in the Alps, as in the whole northern hemisphere, and its slow growth, associated with high longevity, are the main reasons for considering the possibility of applying dendrochronological techniques to find a reliable climatic signal within ring-width sequences.

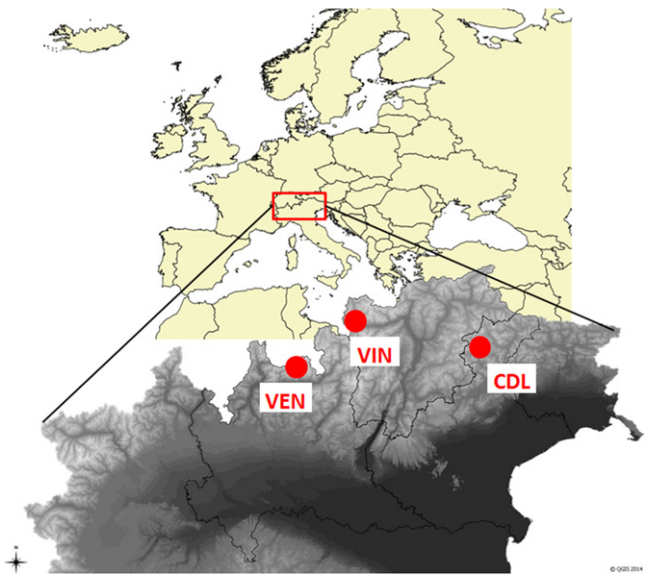

Figure 1. Location of the study sites. CDL: Croda da Lago; VIN: Vinschgau-Val Venosta; VEN: Ventina.

Our underlying hypothesis refers to the height of the species at high elevation, no taller than 0.5 meters, and therefore usually beneath the snow cover during wintertime. Since juniper does not start growing until it is free of the snowpack (Hantemirov *et al* 2000), we will test the hypothesis that shrub growth is linked to winter precipitation, based in snowpack depth. The objectives of the study are twofold: (i) to assess the possibility of building reliable juniper ring width chronologies in the Alps; (ii) verify the sensitivity of the species to precipitation, and especially to winter snowfalls.

2. Material and methods

2.1. Study area

Juniper ring chronologies were built for three sites in the central and eastern Alps (figure 1). The study areas were: Ventina (VEN, 46° 18'N, 9° 46'E, 2200 m a.s.l.), Vinschgau-Val Venosta (VIN, 46° 38'N, 10° 31'E, 2300 m a.s.l.) and Croda da Lago (CDL, 46° 28'N, 12° 07'E, 2150 m a.s.l.). The substrate differs at the sites, with dolomite and limestone with shallow rendzic leptosols at CDL, and igneous, volcanic and metamorphic silicates (i.e. granite, porphyry, gneiss and phyllite) with spodosols and podzols at VEN and VIN. Annual (and winter) precipitation also varies, with 608 (327) mm in Vinschgau, 1068 (615) mm in Croda da Lago and 1196 (681) mm in Ventina (figure S1). In our study winter was defined as the period from October through May, when precipitation normally falls as snow at our research sites.

2.2. Ring width measurements and crossdating

Most samples were collected above the treeline, between 2100 and 2400 m a.s.l., by randomly selecting the shrubs

Figure 2. The typical prostrate growth form of common juniper at high elevation.

(figure 2) and saw-cutting one of the main stems that depart from the root collar to obtain a disk. During summer 2012 we collected and measured a total of 91 samples both dead and alive, at the three sites: 22 in VIN, 27 in CDL and 42 in VEN. At the same sites we also collected cores from larch (*L. decidua*) at the timberline-treeline belt (2000–2200 m) to compare juniper growth to that of a typical high elevation tree species often used in dendroecological investigation. We sampled 121 larches, 23 in VIN, 70 in CDL and 28 in VEN, collecting two cores per tree.

At the lab, disks and cores were sanded with progressively finer gridded sandpaper for a clear visualization of the rings and measured to the nearest 0.01 mm using a sliding stage micrometer interfaced with a personal computer (Aniol 1987). Juniper stems have a typical lobate form resulting from irregular growth. For this reason, to obtain a more reliable representation of ring width, we measured two to four radii per disk. In some cases, to enhance the visibility of the ring -width sequences, we applied microscopic sample preparation through (i) cutting the disks into small pieces (3–5 cm); (ii) cutting thin sections (ca. 20 nm) with a microtome; (iii) staining them with safranin and permanently fixing with balsam (Gärtner and Schweingruber 2013). We then measured the rings as for the normal samples.

Crossdating was accomplished following the standard procedure (Stokes and Smiley 1968): first by visual comparison of the 2–4 radii within each sample, then comparing radii from different samples. In this phase the presence of event rings, i.e. rings with a conspicuous feature within a limited section of the radius (Kaennel and Schweingruber 1995) assisted in finding the correct match among the series. Lastly, after computing the individual mean growth curve, dating and measurement errors were checked using the COFECHA program (Holmes 1983). Ring-width site chronologies were obtained from the crossdated ring-width series using the ARSTAN program (Cook and Holmes 1997) that was specifically developed to remove any biologically induced age-trends and transient disturbance pulses present in raw tree-ring series and to enhance the high-frequency year to year variability often associated to climate. In both species we applied a rather conservative detrending using a spline function with 50% frequency cut-off at 100 years. Individual series were therefore standardized by fitting the spline function to measured data series and dividing observed by expected values. Several statistical parameters were calculated to compare the chronologies: (i) mean sensitivity (MS), a measure of the relative difference in ring width between consecutive years, adopted to assess the high frequency variability of the series, (ii) first order autocorrelation (ac), a measure of the influence of previous year's condition on ring formation (Fritts 1976), (iii) the variance explained by the first principal component (PC1), and (iv) the mean correlation between samples (rbar) and the 'expressed population signal' (EPS) (Wigley *et al* 1984) to estimate the level of year-by-year growth variations shared by samples in the same site. Higher values of PC1 and rbar indicate higher synchronization in the annual growth patterns among samples and better common signal strength in the mean growth chronologies, while EPS is commonly adopted as a criterion for assessing mean chronology reliability.

2.3. Climate—growth association

Rather than take records from the closest weather stations, which may not be totally representative in a mountain area, we used the HISTALP gridded dataset (Auer *et al* 2007). This dataset, valid for the Greater Alpine Region, is based on precipitation and temperature data from hundreds of weather stations firstly subjected to homogeneity tests and relative adjustments regarding elevation and changes of instrument position and type, then gridded on a 1° × 1° network and finally expressed as anomalies with respect to the 20th century mean (Auer *et al* 2005, Böhm *et al* 2001). We selected the climate data from the closest grid points to each study site and computed the growth/climate analyses over the 1876–2005 period. We investigated climate-growth associations by correlating each site chronology with monthly precipitation and temperature data from June of the previous year (t-1) to September of the current year (t). Seasonal data were also taken into account by considering the period from October to May (POM, TOM) when, at this elevation, precipitation mainly occurs as snow and the months from June to September (PJS, TJS) considered as the growing season. The bootstrap approach (Efron 1979) was applied to test the stability and significance of the outcomes. After 100 000 replications, each correlation was deemed significant at the 95% level if the ratio between the correlation coefficient (r) and the standard deviation of the bootstrap replications (s) was higher

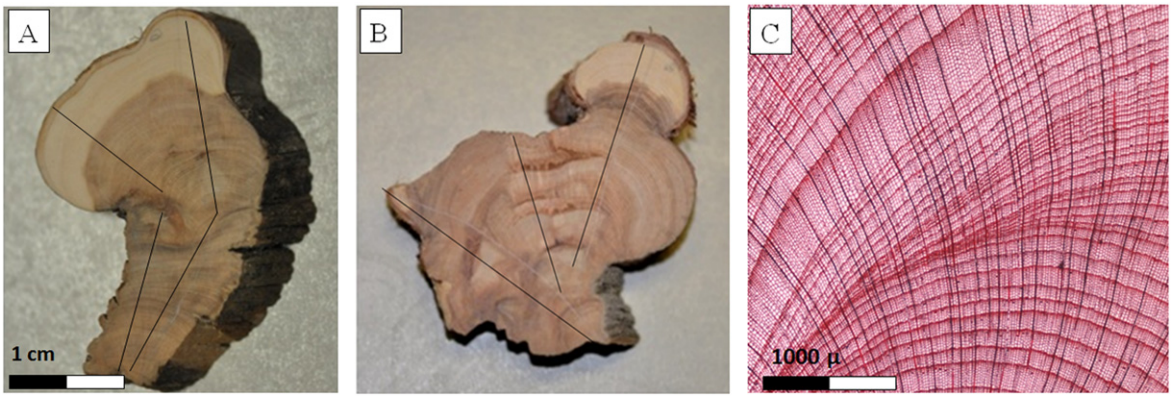

Figure 3. (A) and (B) Samples of common juniper having 401 and 180 rings respectively. (C) Microscopic image of a microtome slice taken at 40× showing many wedging rings induced by uneven cambial activity.

Table 1. Site location and chronology statistics for *Juniperus communis* and *Larix decidua* (shaded).

Site	Lat	Long	Period	Series length (years) (max-mean-min)	N	MS	AC (Indexed)	PC1	Rbar (Indexed)	Missing rings (%)	Frost rings (%)
CDL–JC	46.28	12.07	1749-2012	263-177-75	15	0.32	0.59 (0.45)	0.36	0.16 (0.18)	19 (0.73)	20 (0.77)
VEN–JC	46.18	9.46	1611-2012	402-167-94	17	0.28	0.69 (0.51)	0.33	0.19 (0.19)	14 (0.48)	33 (1.14)
VIN–JC	46.38	10.31	1765-2012	232-115-43	14	0.32	0.64 (0.49)	0.32	0.17 (0.15)	3 (0.18)	89 (5.45)
CDL–LD	46.29	12.06	1452-2009	557-270-84	70	0.39	0.66 (0.36)	0.66	0.59 (0.64)	86 (0.22)	n.d.
VEN–LD	46.18	9.46	1496-2012	514-360-234	28	0.35	0.71 (0.50)	0.57	0.41 (0.55)	29 (0.22)	n.d.
VIN–LD	46.43	10.38	1668-2004	403-220-36	23	0.34	0.73 (0.46)	0.78	0.76 (0.76)	39 (0.39)	n.d.

Note: chronology statistics include mean ring width (MRW), mean sensitivity (MS) and first-order serial autocorrelation (ac) computed on the raw (indexed) ring-width series, the variance explained by the first principal component (PC1) and the mean interseries correlation (Rbar) computed on the raw (indexed) ring-width series. Site codes CDL, VEN, VIN correspond respectively to Croda da Lago, Ventina, and Vinschgau-Val Venosta respectively.

than |2| (Guiot 1991). Analyses were performed on the complete 130-year period as well as on two 65-year sub-periods (1876–1940 and 1941–2005).

3. Results

3.1. Ring-width measurements and crossdating

The irregular and lobate growth form of juniper stems frequently induces the presence of wedging (figure 3) and missing rings (i.e. rings that are absent in a sample due to failure of cambial activity Kaennel and Schweingruber 1995). To reduce the crossdating complexity we usually selected the least problematic and most representative radii, where the rings did not wedge out. Nonetheless, almost half of the samples collected (45 samples) could not be successfully crossdated. On the 46 dated disks (17 for VEN, 14 for VIN and 15 for CDL), we selected and measured an average of 2.4 radii per disk, for a total of 210 radii and 7146 rings. Within these samples we detected 142 frost rings (i.e. distorted xylem tissue damaged by freezing in the growing season Kaennel and Schweingruber 1995) corresponding to 0.77% in CDL, 1.14% in VEN and 5.44% in VIN and 36 missing rings, which correspond to ca. 0.73%, 0.48% and 0.18% for CDL, VEN and VIN respectively. Chronology length is 402 years for VEN (from 1611 to 2012), 247 years for VIN (from 1765 to 2012), and 263 years for CDL (1749-2012) (table 1, figure S2). The larch chronologies were all longer, reaching up to 557 years for CLD, with the typical high mean sensitivity and common signal statistics of the species (Carrer and Urbinati 2006). The PC1 and rbar values of the juniper chronologies are lower than those of the larch. In juniper the expressed population signal often results as lower than the threshold level of 0.85 (figure 4).

3.2. Climate-growth association

Two of the stations, VEN and CDL, show significant negative correlations between precipitation and ring growth with *r*/*s* coefficients lower than −2. Winter months, from September to January in VEN and from November to January in CDL show the most significant correlations. With winter precipitation (POM), we obtained a much higher and significant association (figures 5, 6). Splitting the time period in two, precipitation and especially the winter seasonal sum, confirmed the previous outcomes, being always significant although with less variability (figure S3). At the third site, VIN, juniper ring widths were not related to either precipitation or temperature. We found that temperature is not a key factor for juniper growth; indeed it shows no significant coherent correlation with growth apart from for a few isolated months, corresponding to the late previous and current growing season. We found the opposite for larch, where precipitation

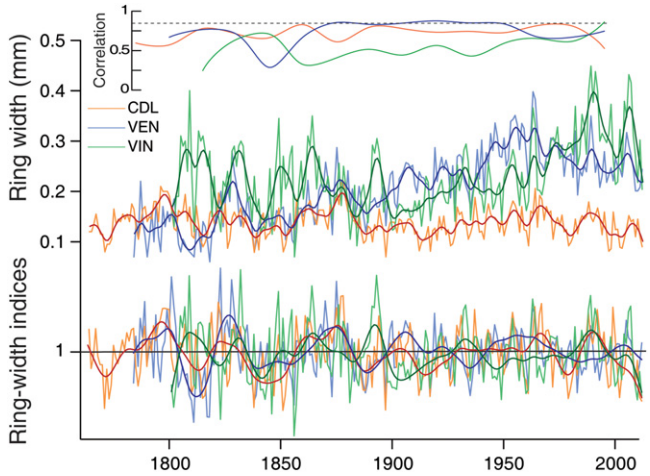

Figure 4. Raw and indexed ring-width chronologies. Smoothed lines are 20-year low-pass filter. Top-inset graph represents the 30-year running EPS with the 0.85 threshold highlighted.

seems to play a negligible role both at monthly and seasonal level, whereas temperature has a highly significant effect that is clearly homogeneous among sites (figure 5).

4. Discussion

High elevation and high latitude are considered to be the areas most sensitive to climate change (IPCC 2007, 2013). Indeed, climate is the major environmental driver of conifer growth at high altitude, where the limiting effect of temperature on tree growth is reflected in the prevailing significant correlation between tree-ring parameters and summer temperatures (Carrer and Urbinati 2004, Büntgen *et al* 2005, Frank and Esper 2005, Carrer and Urbinati 2006). At high altitude in the Alps tree growth seems not to be sensitive to precipitation, however, our study demonstrates that growth of a shrub conifer, *J. communis*, growing at the same or higher elevation, is influenced by winter precipitation. Many researchers investigated other species of the same genus (*Juniperus thurifera*, *J. excelsa*, *J. occidentalis*, etc) and the most common outcomes were a positive correlation between juniper growth and summer temperatures or precipitation when the species grew in temperature- (e.g. Tibetan plateau, Northern Scandinavia) or water- (e.g. Ethiopia and Oregon) limited environments (Sass-Klaassen *et al* 2008, Liang *et al* 2012, Knapp *et al* 2004, Hallinger *et al* 2010). Hallinger *et al* (2010) reported a positive effect of snow cover on *J. nana* at high latitude. In these regions (Northern Scandinavia), in contrast to our sites, higher snow accumulation would increase the insulation with warmer soil temperature promoting microbial activity. Shrub growth would benefit from a resulting increase in nutrient supply. Given the growing interest in the water cycle and the consequent effects at environmental level (Haeberli and Beniston 1998, Beniston 2012), this study adds a valuable contribution, by providing the first example at mid-latitude across Eurasia (St George 2014) of a long-living plant limited in growth by winter precipitation. We highlight a potential new proxy that could be useful in the Alps, an area where summer temperature has so far been the only climate signal detected in tree-ring chronologies.

4.1. Ring-width chronologies characteristics

The genus *Juniper* includes many long-living species (Brown 1996) in which ring-width chronologies have been shown to contain strong climatic signals (Treydte *et al* 2006, Knapp *et al* 2001, DeSoto *et al* 2012). As the other species of the same genus, *J. communis* in the Alps has proved to register a climatic signal at least in two sites out of three. We detected the presence of frost rings in the ring-width sequences. Juniper is considered rather vulnerable to frost damage due to its thin bark, yet the presence of frost rings does not decrease with age (Hantemirov *et al* 2000, 2004) as observed in other tree species. The total number of these event rings we recorded is low, probably because the significant snow cover and late melting at high elevation delay the onset of cambial growth reducing the chance of being injured by an abrupt freeze (Hantemirov *et al* 2000). This is likely why the highest number of frost rings are observed at VIN. This site has the lowest amount of winter precipitation, which implies a shallower snow cover that melts faster in spring increasing the chance of late frost damage. Furthermore, VIN sampling area is subjected to constant strong winds that blow away the snow cover (Whiteman and Dreiseitl 1984), in some cases leaving the shrubs with a higher probability of being exposed to frosts (Bokhorst *et al* 2009). As reported by other authors, although not always confirmed (Bär *et al* 2008), shrub growth is largely influenced by microenvironmental variability or local topography (Kivinen *et al* 2012, Hantemirov *et al* 2000, 2004) that can differ between and within the same sites, inducing a corresponding variability between individual ring-width chronologies. Some of the chronology statistics, namely rbar and to a lesser extent EPS, mirror this ring-width variability dominated by individual rather than population variability. However, the fairly low values of these statistics are likely not species- or site-specific as similar values have been reported by many authors working on the same genus (Liang *et al* 2012, Hallinger *et al* 2010, Sass-Klaassen *et al* 2008, Zhu *et al* 2008). Still, despite the difficulties in crossdating and the high individual variability (figure S2), the three site chronologies we built allowed us to compute reliable climate-growth associations. This represents a fundamental step for investigating how juniper reacts to winter precipitation.

4.2. Climate—growth association

The VEN and CDL sites demonstrate a significant negative correlation between accumulated winter precipitation and juniper ring width together with a weaker correlation with monthly precipitation. There are several reasons for the importance of using a seasonal correlation along with examining correlations with monthly data. We are dealing with a meteorological parameter, precipitation, which tends to accumulate over the winter months. Once juniper is covered

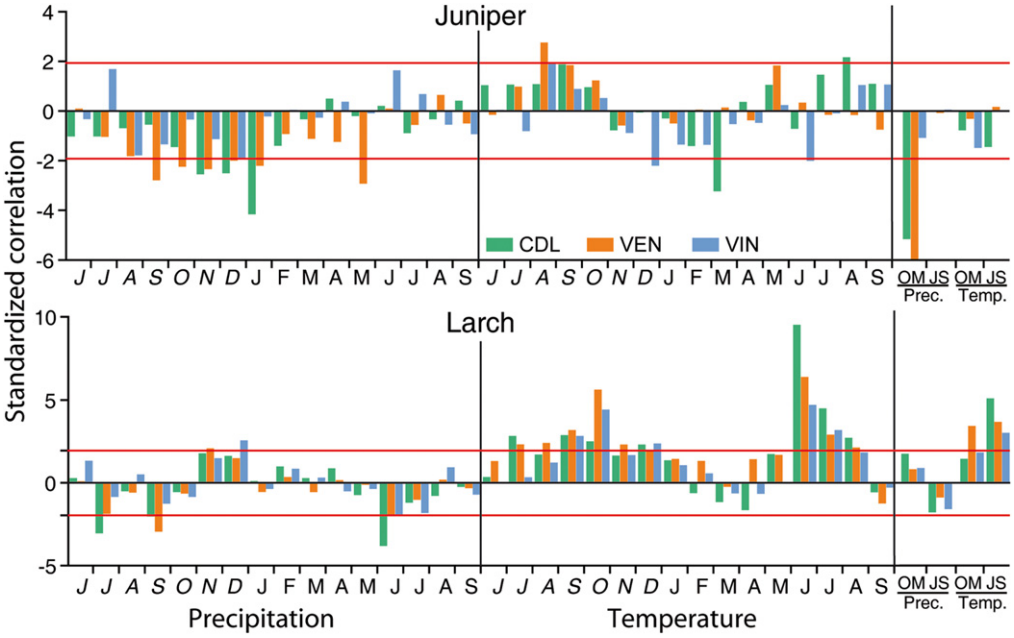

Figure 5. Climate-growth associations between the three ring-width site chronologies and total monthly precipitation and mean monthly temperatures for the previous (June–December) and current (January–September) year plus the seasonal precipitation sum and temperature mean from previous October to current May and from current June to September. Standardized coefficients were obtained by dividing the mean correlations by their standard deviations after the bootstrap replications. They express the significance of monthly parameters. Values above |2| are significant at $p < 0.05$.

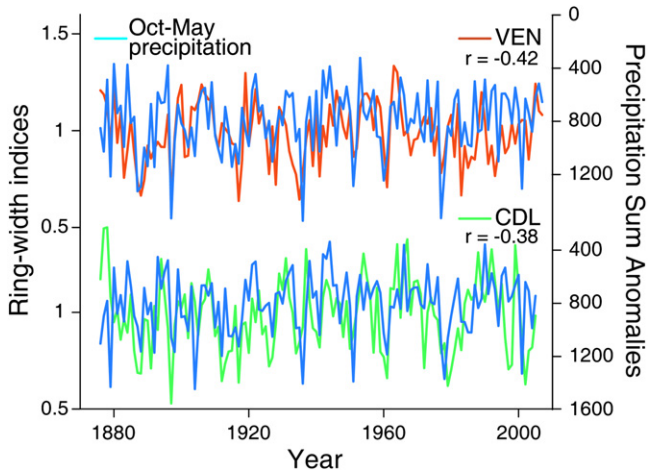

Figure 6. Comparison between the cumulative winter precipitation from October to May (blue lines) and ring-width indexed chronologies of Croda da Lago (CDL) and Ventina (VEN), the two sites that show a significant association with this precipitation parameter. The second *Y* axis related to precipitation sum has been reversed for a better visualization. Pearson correlation coefficients (*r*) are also shown, both are significant at $P < 0.001$.

by the first snowfalls in October/November, there is no direct effect from the amount of precipitation during the winter rest period. The negative correlation indicates that the higher the amount of winter precipitation is, the thicker the snowpack is and the narrower the rings are in the following growing season. This is supported by the fact that cambial activity does not start until after snowmelt (Hantemirov *et al* 2000). In fact, a thicker snowpack usually takes longer to melt thus delaying the onset of cambial activity and shortening the growing season, with the resulting narrower ring formation. Late-persisting snow could also have a detrimental effect on growth through cooler soil temperature which can delay the onset or slow down the first phases of the growing season (Schmidt *et al* 2006, Kirdyanov *et al* 2003, Vaganov *et al* 1999, Peterson and Peterson 1994). In our study larch trees did not show any sign of this negative effect. This is further confirmation that the most plausible reason for the negative precipitation correlation in juniper is the physical effect of the snow cover that filters the incoming solar radiation blocking photosynthesis, rather than the collateral reduction in soil temperature. The only area with no significant growth-climate correlation for either precipitation or temperatures is VIN. The possible reason is the rather low quality of the common signal among the ring-width series highlighted by the low EPS value of the chronology. The VIN site is a zone exposed to strong wind, as is most of the high Vinshaug valley (Whiteman and Dreiseitl 1984) and due to this, the snow falling during winter is blown away, leaving the ground almost bare. A lack of snow cover implies a potential earlier start of cambial activity, with the consequence of no correlation with winter precipitation. The higher presence of frost rings due to late frosts could also be evidence of an earlier onset of cambial activity: the probability of freezing injuries is higher with an earlier start to the growing season. Temperature did not affect ring-width formation at any of our sites, which confirms, although surprisingly, the weak influence of this factor on juniper growth. Indeed, it is well-known that temperature is the key limiting factor for tree growth at high elevation, as confirmed by our comparison with larch growing in the same areas. This is

likely due to the fact that trees are more closely coupled to air temperature. A similar result, has been recorded on another prostrate shrub, *Salix arctica*, in Greenland (Schmidt *et al* 2006). Even if other investigations at high-latitudes report that temperature, and especially summer temperature, is the key environmental factor driving shrub growth (Bär *et al* 2008, Buchwal *et al* 2013, Weijers *et al* 2013, Buras *et al* 2012, Hallinger and Wilmking 2011), at mid-latitude, at least in the Alps, common juniper is seemingly less affected than trees by air temperature. Indeed, with its prostrate growth form juniper grows within the boundary layer and is likely more influenced by soil temperature. Furthermore, the topography, aspect and landscape heterogeneity influence the persistence of snow at local level (Kivinen *et al* 2012) and this also explains to some extent the high variability between samples. However, despite this high individual and spatial variability the winter precipitation signal seems to be fairly stable in time as it is significant for both the subperiods analyzed (figure S3). The increasing or decreasing of this winter precipitation signal could likely be connected with the not uniform climate data quality and with the corresponding variability in time of the common signal as shown by the running EPS values (figure 4).

5. Conclusion

We demonstrated that, despite the challenging crossdating, it is possible to built centuries-long chronologies with common juniper. In addition, we found a significant winter precipitation signal in the ring-width chronologies of two of our three research sites. As a prostrate shrub *J. communis* seems better coupled with the soil surface rather than the air temperature. This is probably one of the reasons why the influence of air temperature on ring-width formation seems less significant. This study is just a pilot investigation. Future research will be directed to (i) enlarging the sample size, paying attention to collecting more sections along the stem to obtain a more reliable representation of plant growth and to reduce the risk of losing any information due to missing rings (Wilmking *et al* 2012); (ii) extending back in time the ring-width series, considering the high potential to generate longer chronologies than these with additional collections including also dry dead wood remains; and (iii) extending the sites network across the Alps. If the climatic signal we detected is confirmed, this will provide a baseline for a possible reconstruction of past winter precipitation variability in the region. Our results suggest that *J. communis* ring width chronologies may serve as a winter precipitation proxy in the Alps.

Acknowledgements

The authors would like to thank Paola Nola and Renzo Motta for providing the larch series from the Ventina (VEN) site and the two anonymous reviewers for their helpful comments and suggestions on the earlier version of the manuscript.

References

Aniol R W 1987 A new device for computer assisted measurement of tree-ring widths *Dendrochronologia* **5** 135–41

Auer I *et al* 2005 A new instrumental precipitation dataset for the greater alpine region for the period 1800-2002 *Int. J. Climatol.* **25** 139–66

Auer I, Bohm R, Jurkovic A, Lipa W, Orlik A, Potzmann R, Schoner W, Ungersbock M, Matulla C and Briffa K 2007 HISTALP–historical instrumental climatological surface time series of the greater alpine region *Int. J. Climatol.* **27** 17–46

Bär A, Pape R, Bräuning A and Löffler J 2008 Growth-ring variations of dwarf shrubs reflect regional climate signals in alpine environments rather than topoclimatic differences *J. Biogeogr.* **35** 625–36

Beniston M 2012 Is snow in the Alps receding or disappearing? *Wiley Interdiscip. Rev.-Clim. Change* **3** 349–58

Böhm R, Auer I, Brunetti M, Maugeri M, Nanni T and Schoner W 2001 Regional temperature variability in the European Alps: 1760-1998 from homogenized instrumental time series *Int. J. Climatol.* **21** 1779–801

Bokhorst S F, Bjerke J W, Tømmervik H, Callaghan T V and Phoenix G K 2009 Winter warming events damage sub-Arctic vegetation: consistent evidence from an experimental manipulation and a natural event *J. Ecol.* **97** 1408–15

Bonan G B, Chapin F S III and Thompson S L 1995 Boreal forest and tundra ecosystems as components of the climate system *Clim. Change* **29** 145–67

Brown P M Oldlist. A database of maximum tree ages ed J S Dean, D M Meko and T W Swetnam *Tree Rings, Environment and Humanity: Proc. Int. Conf. (17–21 May 1994 Tucson, AZ) Radiocarbon* **1996** 727–731

Buchwal A, Rachlewicz G, Fonti P, Cherubini P and Gaertner H 2013 Temperature modulates intra-plant growth of Salix polaris from a High Arctic site (Svalbard) *Polar Biol.* **36** 1305–18

Bunn A G, Hughes M K and Salzer M W 2011 Topographically modified tree-ring chronologies as a potential means to improve paleoclimate inference *Clim. Change* **105** 627–34

Bunn A G, Waggoner L A and Graumlich L J 2005 Topographic mediation of growth in high elevation foxtail pine (*Pinus balfouriana* Grev. et Balf.) forests in the Sierra Nevada, USA *Glob. Ecol. Biogeogr.* **14** 103–14

Büntgen U, Esper J, Frank D C, Nicolussi K and Schmidhalter M 2005 A 1052-year tree-ring proxy for alpine summer temperatures *Clim. Dyn.* **25** 141–53

Büntgen U, Frank D, Wilson R, Carrer M, Urbinati C and Esper J 2008 Testing for tree-ring divergence in the European Alps *Glob. Change Biol.* **14** 2443–53

Buras A, Hallinger M and Wilmking M 2012 Can shrubs help to reconstruct historical glacier retreats? *Environ. Res. Lett.* **7** 044031

Carrer M, Nola P, Eduard J L, Motta R and Urbinati C 2007 Regional variability of climate-growth relationships in *Pinus cembra* high elevation forests in the Alps *J. Ecol.* **95** 1072–83

Carrer M and Urbinati C 2001 Spatial analysis of structural and tree-ring related parameters in a timberline forest in the Italian Alps *J. Veg. Sci.* **12** 643–52

Carrer M and Urbinati C 2004 Age-dependent tree-ring growth responses to climate *Larix decidua Pinus Cembra Ecol.* **85** 730–40

Carrer M and Urbinati C 2006 Long-term change in the sensitivity of tree-ring growth to climate forcing *Larix decidua New Phytol.* **170** 861–71

Casteller A, Stöckli V, Villalba R and Mayer A C 2007 An evaluation of dendroecological indicators of snow avalanches in the Swiss Alps *Arctic Antarct. Alpine Res.* **39** 218–28

Cook E R and Holmes R L 1997 *The International Tree-Ring Data Bank Program Library, version 2.1, user's Manual* ed H D Grissino Mayer *et al* (Tucson, AZ, USA: University of Arizona Laboratory of Tree-Ring Research) pp 75–92

DeSoto L, Camarero J J, Olano J M and Rozas V 2012 Geographically structured and temporally unstable growth responses of *Juniperus thurifera* to recent climate variability in the Iberian Peninsula *Eur. J. Forest Res.* **131** 905–17

Devi N, Hagedorn F, Moiseev P, Bugmann H, Shiyatov S, Mazepa V and Rigling A 2008 Expanding forests and changing growth forms of Siberian larch at the polar urals treeline during the 20th century *Glob. Change Biol.* **14** 1581–91

Efron B 1979 Bootstrap methods: another look at the jackknife *Ann. Stat.* **7** 1–26

Elsasser H and Burki R 2002 Climate change as a threat to tourism in the Alps *Clim. Res.* **20** 253–7

Frank D and Esper J 2005 Characterization and climate response patterns of a high-elevation, multi-species tree-ring network in the European Alps *Dendrochronologia* **22** 107–21

Fritts H C 1976 *Tree Rings and Climate* (London, UK: Academic)

Gärtner H and Schweingruber F H 2013 *Microscopic Preparation Techniques for Plant Stem Analysis* (Remagen: Kessel)

Grace J, Berninger F and Nagy L 2002 Impacts of climate change on the tree line *Ann. Bot.* **90** 537–44

Guiot J 1991 The bootstrapped response function *Tree Ring Bull.* **51** 39–41

Haeberli W and Beniston M 1998 Climate change and its impacts on glaciers and permafrost in the Alps *Ambio* **27** 258–65

Hallinger M, Manthey M and Wilmking M 2010 Establishing a missing link: warm summers and winter snow cover promote shrub expansion into alpine tundra in Scandinavia *New Phytol.* **186** 890–9

Hallinger M and Wilmking M 2011 No change without a cause—why climate change remains the most plausible reason for shrub growth dynamics in Scandinavia *New Phytol.* **189** 902–8

Hantemirov R M, Gorlanova L A and Shiyatov S G 2000 Pathological tree-ring structures in Siberian juniper (*Juniperus sibirica* burgsd.) and their use for reconstructing extreme climatic events *Russ. J. Ecol.* **31** 167–73

Hantemirov R M, Gorlanova L A and Shiyatov S G 2004 Extreme temperature events in summer in northwest Siberia since AD 742 inferred from tree rings *Palaeogeogr. Palaeoclim. Palaeoecol.* **209** 155–64

Harsch M A, Hulme P E, McGlone M S and Duncan R P 2009 Are treelines advancing? A global meta-analysis of treeline response to climate warming *Ecol. Lett.* **12** 1040–9

Holmes R L 1983 Computer-assisted quality control in tree-ring dating and measurement *Tree Ring Bull.* **43** 69–78

Holtmeier F-K and Broll G 2010 Wind as an ecological agent at treelines in North America, the Alps, and the European Subarctic *Phys. Geogr.* **31** 203–33

Holtmeier F K 2009 *Mountain Timberlines: Ecology, Patchiness, and Dynamics* (Berlin: Springer)

IPCC 2007 *Climate Change 2007: The Physical Science Basis Contribution of Working Group I to the Fourth Assessment Report of the Intergovernmental Panel on Climate Change* ed S Solomon *et al* (Cambridge: Cambridge University Press) p 996

IPCC 2013 *Climate Change 2013: The Physical Science Basis Contribution of Working Group I to the Fifth Assessment Report of the Intergovernmental Panel on Climate Change* ed T Stocker *et al* (Cambridge: Cambridge Univ Press) p 1535

Kaennel M and Schweingruber F H 1995 *Multilingual Glossary of Dendrochronology* (Berne: Wsl/Fnp Birmensdorf, P. Haupt Pub)

Kirdyanov A, Hughes M, Vaganov E, Schweingruber F and Silkin P 2003 The importance of early summer temperature and date of snow melt for tree growth in the Siberian Subarctic *Trees-Struct. Funct.* **17** 61–9

Kivinen S, Kaarlejärvi E, Jylhä K and Räisänen J 2012 Spatiotemporal distribution of threatened high-latitude snowbed and snow patch habitats in warming climate *Environ. Res. Lett.* **7** 034024

Knapp P A, Soule P T and Grissino Mayer H D 2001 Detecting potential regional effects of increased atmospheric CO_2 on growth rates of western juniper *Glob. Change Biol.* **7** 903–17

Knapp P A, Soule P T and Grissino-Mayer H D 2004 Occurrence of sustained droughts in the interior pacific Northwest (AD 1733-1980) inferred from tree-ring data *J. Clim.* **17** 140–50

Körner C 2012 *Alpine Treelines: Functional Ecology of the Global High Elevation Tree Limits* (Basel: Springer)

Liang E, Lu X, Ren P, Li X, Zhu L and Eckstein D 2012 Annual increments of juniper dwarf shrubs above the tree line on the central Tibetan Plateau: a useful climatic proxy *Ann. Bot.* **109** 721–8

Miles D and Worthington M 1998 Sonora Pass junipers from California USA: construction of a 3500-year chronology *Dendrochronology and Environmental Trends. Proc. of the Int. Conf.* pp 17–21

Morrison C and Pickering C M 2013 Perceptions of climate change impacts, adaptation and limits to adaption in the Australian Alps: the ski-tourism industry and key stakeholders *J. Sustainable Tourism* **21** 173–91

Peterson D W and Peterson D L 1994 Effects of climate on radial growth of subalpine conifers in the North Cascade Mountains *Can. J. Forest Res.* **24** 1921–32

Rixen C, Schwoerer C and Wipf S 2010 Winter climate change at different temporal scales in Vaccinium myrtillus, an Arctic and alpine dwarf shrub *Polar Res.* **29** 85–94

Sass-Klaassen U, Couralet C, Sahle Y and Sterck F J 2008 Juniper from Ethiopia contains a large-scale precipitation signal *Int. J. Plant Sci.* **169** 1057–65

Schmidt N, Baittinger C and Forchhammer M 2006 Reconstructing century-long snow regimes using estimates of High Arctic *Salix arctica* radial growth *Arctic Antarct. Alpine Res.* **38** 257–62

Smith W K, Germino M J, Hancock T E and Johnson D M 2003 Another perspective on altitudinal limits of alpine timberlines *Tree Physiol.* **23** 1101–12

St. George S 2014 An overview of tree-ring width records across the Northern Hemisphere *Quat. Sci. Rev.* **95** 132–50

Stokes M A and Smiley T L 1968 *Introduction to Tree-Ring Dating* (Chicago, IL: University of Chicago Press)

Tranquillini W 1979 *Physiological Ecology of The Alpine Timberline* vol 31 (Berlin: Springer)

Treydte K, Schleser G H, Helle G, Frank D, Winiger M, Haug G H and Esper J 2006 The twentieth century was the wettest period in northern Pakistan over the past millennium *Nature* **440** 1179–82

Vaganov E A, Hughes M K, Kirdyanov A V, Schweingruber F H and Silkin P P 1999 Influence of snowfall and melt timing on tree growth in subarctic Eurasia *Nature* **400** 149–51

Viviroli D *et al* 2011 Climate change and mountain water resources: overview and recommendations for research, management and policy *Hydrol. Earth Syst. Sci.* **15** 471–504

Weijers S, Wagner-Cremer F, Sass-Klaassen U, Broekman R and Rozema J 2013 Reconstructing High Arctic growing season intensity from shoot length growth of a dwarf shrub *The Holocene* **23** 721–31

Whiteman C D and Dreiseitl E 1984 *Alpine Meteorology: Translations of Classic Contributions* ed A Wagner, E Ekhart and F Defant p 129

Wigley T M L, Briffa K R and Jones P D 1984 On the average value of correlated time series with applications in dendroclimatology and hydrometeorology *J. Clim. Appl. Meteorol.* **23** 201–13

Wilmking M, Hallinger M, Van Bogaert R, Kyncl T, Babst F, Hahne W, Juday G P, de Luis M, Novak K and Vollm C 2012 Continuously missing outer rings in woody plants at their distributional margins *Dendrochronologia* **30** 213–22

Wipf S, Stoeckli V and Bebi P 2009 Winter climate change in alpine tundra: plant responses to changes in snow depth and snowmelt timing *Clim. Change* **94** 105–21

Zhu H, Zheng Y, Shao X, Liu X, Xu Y and Liang E 2008 Millennial temperature reconstruction based on tree-ring widths of Qilian juniper from Wulan, Qinghai Province, China *Chin. Sci. Bull.* **53** 3914–20

Supplementary material

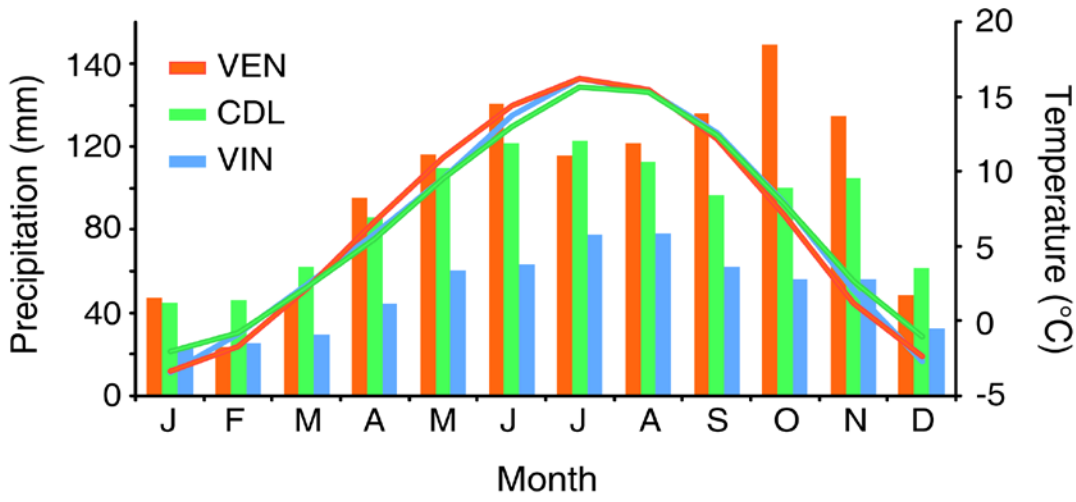

Figure S1: Climatic diagrams for the three sites. Whether records come from the closest meteorological stations: VEN (Lanzada, 46°3'N 9°85'E, 1983 m a.s.l., 1921-1990 for precipitation and from 1926-1990 for temperature), CDL (Cortina d'Ampezzo, 46°19'N 12°48'E, 1275 m a.s.l., 1925-2010 both for precipitation and temperature), VIN (Tubre/Rivaira, 46°64'N 10°46'E, 1119m a.s.l., 1922-2010 for precipitation and 1935-2010 for temperature).

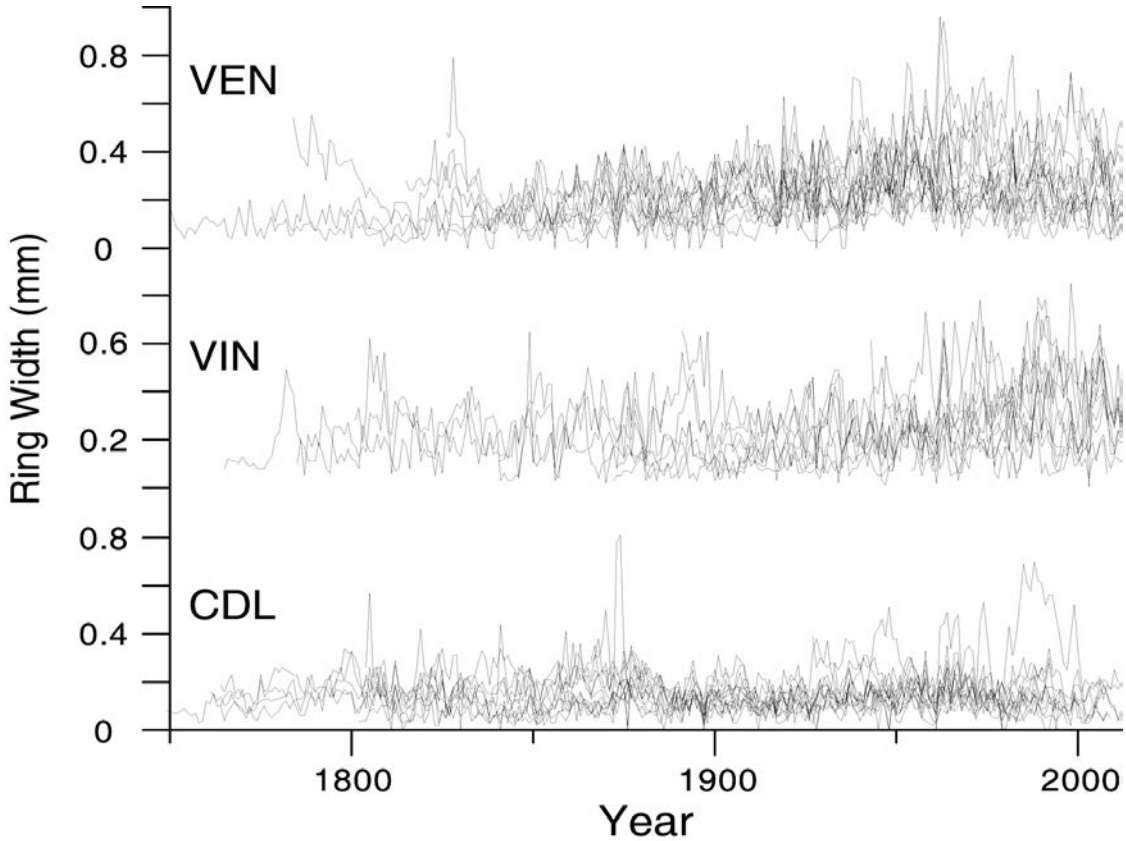

Figure S2: Raw individual ring-width series for all the samples crossdated at each site.

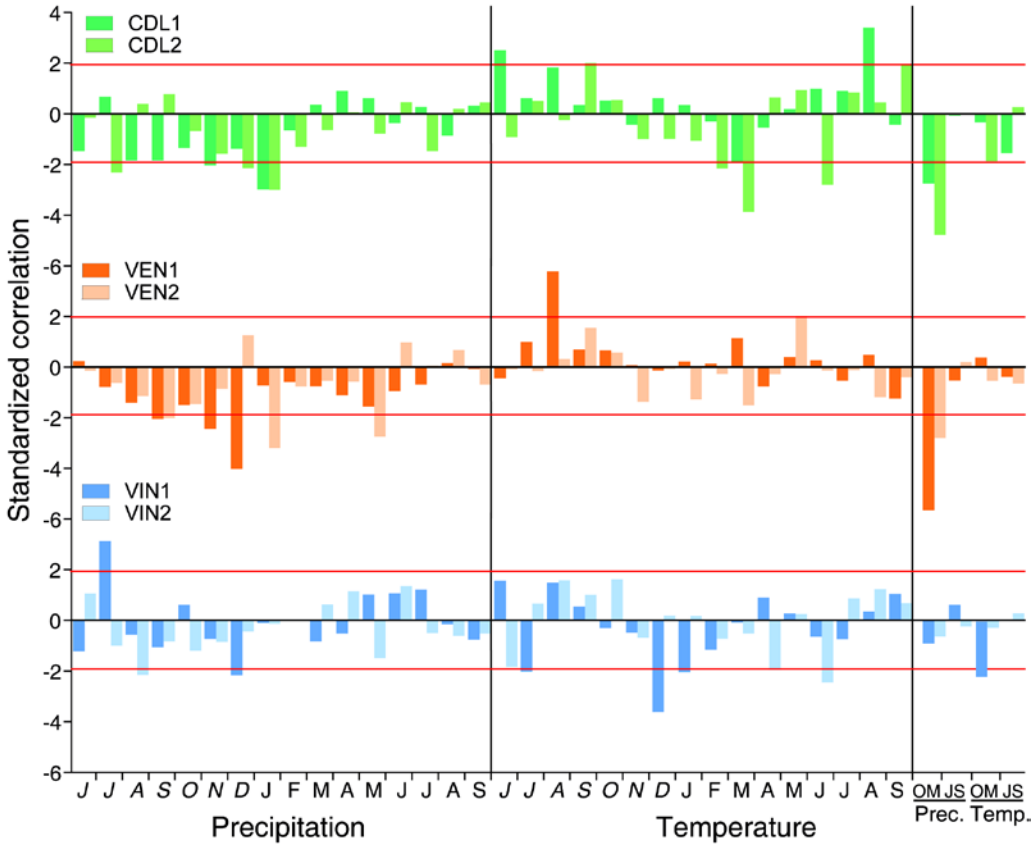

Figure S3: Climate-growth associations between the three ring-width site chronologies and total monthly precipitation and mean monthly temperatures for the previous (June to December) and current (January to September) growth year plus the seasonal precipitation sum and temperature mean from previous October to current May and from current June to September, computed splitting the meteorological record into two 65-year subperiods (1: 1876-1940 and 2: 1941-2005). Standardized coefficients were obtained by dividing the mean correlations by their standard deviations after the bootstrap replications. They express the significance of monthly parameters. Values above |2| are significant at $p < 0.05$.

CHAPTER II

Diverging shrub and tree growth from the Polar to the Mediterranean biomes across the European continent

Running head: growth forms diverge in different biomes.

Elena Pellizzari[1], J. Julio Camarero[2*], Antonio Gazol[2], Elena Granda[2], Rohan Shetti[3], Martin Wilmking[3], Pavel Moiseev[4], Mario Pividori[1] and Marco Carrer[1]

[1]Università degli Studi di Padova, Dip. TeSAF, Agripolis I-35020 Legnaro, Italy
[2]Instituto Pirenaico de Ecología (IPE-CSIC), Zaragoza 50059, Spain
[3]Institute of Botany and Landscape Ecology, University of Greifswald, 17487 Greifswald, Germany
[4]Institute of Plant and Animal Ecology UD RAS, Yekaterinburg 620144, Russia

*Corresponding author:
J. Julio Camarero
Instituto Pirenaico de Ecología, IPE-CSIC
Avda. Montañana 1005, 50080 Zaragoza, Spain.
Phone: +34 976 716031 / Fax: +34 976 716019
E-mail: jjcamarero@ipe.csic.es

Key words: climate warming, dendroecology, junipers, tree growth, thermal uncoupling, latitudinal transect

Paper Type: Primary Research Article

Global Change Biology: **in press**

Abstract

Climate warming is expected to enhance productivity and growth of woody plants, particularly in temperature-limited environments at the northernmost or uppermost limits of their distribution. However, this warming is spatially uneven and temporally variable, and the rise in temperatures differently affects biomes and growth forms. Here, applying a dendroecological approach with generalized additive mixed models, we analysed how the growth of shrubby junipers and coexisting trees (larch and pine species) responds to rising temperatures along a 5000-km latitudinal range including sites from the Polar, Alpine to the Mediterranean biomes. We hypothesize that, being more coupled to ground microclimate, junipers will be less influenced by atmospheric conditions and will less respond to the post-1950 climate warming than coexisting standing trees. Unexpectedly, shrub and tree growth forms revealed divergent growth trends in all the three biomes, with juniper performing better than trees at Mediterranean than at Polar and Alpine sites. The post-1980s decline of tree growth in Mediterranean sites might be induced by drought stress amplified by climate warming and did not affect junipers. We conclude that different but coexisting long-living growth forms can respond differently to the same climate factor and that, even in temperature-limited area, other drivers, like the duration of snow cover might locally play a fundamental role on woody plants growth across Europe.

Introduction

Climate warming is unequivocal and since the 1950s the rapid rise of air temperatures due to increasing atmospheric CO_2 concentrations is unprecedented over millennia in many regions (IPCC, 2014b). This is the case of Europe, where the average land temperature of the 2004–2013 period is 1.3 °C above the pre-industrial level, which makes it the warmest decade on record (Rohde *et al.*, 2013). Interestingly, this warming is seasonally heterogeneous and spatially variable with highest rates observed in peripheral European regions such as E. Spain (40º N) and NW. Russia (65º N) (Vautard *et al.*, 2014). Furthermore, European temperatures are projected to continue increasing by 2.4 to 4.1 ºC during the 21st century, i.e. more than global averages (Kjellström *et al.*, 2011). Here, we explore if different seasonal warming trends observed across European biomes (Polar, Alpine and Mediterranean biomes) translate into different growth patterns in prostrate vs. arborescent conifer growth-forms. We discuss how the shrub vs. tree dichotomy determines growth reactions to climate warming and could influence future changes in productivity of woody European biomes.

Rapid climate warming is expected to impact woody plants in the Polar biome more intensely and rapidly than elsewhere leading to enhanced growth in the species' northernmost limits of distribution, and promoting tree shifts and shrub encroachment northwards as has been already observed in boreal forests and the arctic tundra (Suarez *et al.*, 1999; Sturm *et al.*, 2001; Danby & Hik, 2007; MacDonald *et al.*, 2008; Harsch *et al.*, 2009; Hallinger *et al.*, 2010b; Myers-Smith *et al.*, 2011, 2015). Such treeline shifts and shrub encroachment phenomena are the result of warming-enhanced productivity success of these woody communities (Esper *et al.*, 2010; Forbes *et al.*, 2010; Hallinger & Wilmking, 2011), albeit warming-related drought stress has also been detected at some boreal forests (Barber *et al.*, 2000; Trahan & Schubert, 2016).

In the Alpine biome, where trees and shrubs reach their uppermost distribution limits, growth of woody plants is mainly constrained by decreasing temperatures upwards (Körner, 2012b), and for this reason, enhanced tree and shrub growth by climate warming is expected at high elevations in these mountain regions (Büntgen *et al.*, 2008a; Salzer *et al.*, 2009; Lu *et al.*, 2016). However, such environments illustrate at small spatial scales a fundamental dichotomy between arborescent (tree) and prostrate (shrub) growth forms and their expected responses to climate warming. Due to the erect growth and tall stature of trees, meristems are well coupled with free atmospheric conditions which enforce convective air exchange (Wilson *et al.*, 1987; Grace *et al.*, 1989). For this reason trees are usually more sensitive to

thermal air limitations than shrubs (Körner, 2012b). Contrastingly, in low-stature and prostrate shrubs meristems are more coupled to ground microclimate conditions, which are usually warmer with respect to free atmospheric conditions due to the reduction of heat exchange (Körner, 2012a). This more favorable microclimate allows shrub growth to be partially decoupled from atmospheric thermal states which explains their existence above the treeline (Körner, 2012a). In addition, during winter shrub meristems are often covered and protected by snow, limiting the risk of freezing and mechanical damages as compared to tree buds (Bokhorst *et al.*, 2009; Rixen *et al.*, 2010). However, the insulating benefits of snowpack to shrub meristems may also be detrimental if the snowpack is so thick or dense to induce a delayed snow melting and a shortening of the growing season (Pellizzari et al., 2014).

Lastly, in the Mediterranean biome shrub and tree growth is mainly constrained by seasonal drought (Gazol & Camarero, 2012), even at high-elevation sites (Garcia-Cervigón Morales *et al.*, 2012). Therefore, warmer conditions could amplify drought stress in this biome, and the aridification trend already observed in southern Europe (Vicente-Serrano *et al.*, 2014) may lead to slower growth of woody plants if precipitation is assumed not to change (Matías & Jump, 2015). Moreover, warmer growing-season conditions have already induced moisture limitation and reduced juniper growth in temperate mountains such as the Tibetan Plateau (Liang *et al.*, 2011); so warming-related drought constrains should be fully considered not just for the Mediterranean but also for similar dry biomes.

We aim to quantify the radial-growth responses to rising temperatures of junipers and co-occurring trees (larch and pine species) across a NE-SW European transect including sites located in Polar, Alpine and Mediterranean biomes. By assuming the decoupling between air temperature and shrubs growth, we hypothesize that erect trees will be more sensitive to recent climate warming than shrubby junipers, particularly in the case of the most cold-limited sites (Polar and Alpine biomes). We also expect to detect drought-related growth limitations in Mediterranean sites, chiefly affecting trees because they are more responsive to drought amplification by climate warming (Williams *et al.*, 2013)

Material and methods

Study species and sample collection

Common juniper (*Juniperus communis L.*) is a shrubby gymnosperm considered to be the most widespread conifer over the northern hemisphere (Farjon, 2005). We selected 10 sites

located in three contrasted biomes on the European continent going from the Russian Polar Urals to eastern Spain. In these biomes, Polar (Polar Urals), Alpine (Italian Alps) and Mediterranean (Spanish Iberian System, Apennines in S. Italy) the species grows at the northern, uppermost and southern limits of its distribution (Table 1, Fig. 1) .

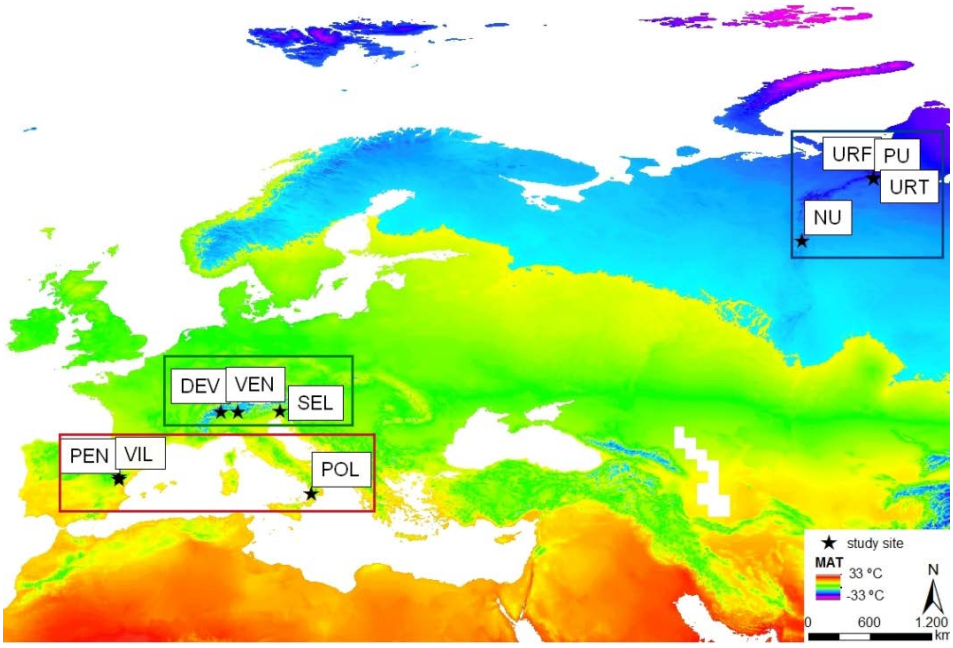

Figure 1. Juniper-tree sample sites. Colour boxes correspond to the three regions: blue for Polar sites (Russian Polar Urals), green for Alpine sites (N. Italy) and red for Mediterranean sites (E Spain, S. Italy). In the case of the NU site only junipers were sampled. See sites' characteristics in Table 1. Map colours correspond to the annual mean temperature (MAT).

Table 1. Description of the study sites and number of sampled junipers and trees.

Region	Site (code)	Latitude (N)	Longitude (W/E)	Elevation (m a.s.l.)	Tree species	No. junipers / trees
Polar	Polar Urals - treeline (URT)	66° 51'	65° 35' E	320	*Larix sibirica*	24 / 13
	Polar Urals - forest limit (URF)	66° 50'	65° 35' E	230	*Larix sibirica*	23 / 20
	Polar Urals (PU)	66° 48'	65° 33' E	220	*Larix sibirica*	20 / 24
	Northern Urals (NU)	61° 18'	59° 14' E	750	*Larix sibirica*	24 / –
Alpine	Devero (DEV)	46° 19'	8° 16' E	2100	*Larix decidua*	12 / 18
	Ventina (VEN)	46° 18'	9° 46' E	2300	*Larix decidua*	17 / 34
	Sella Nevea (SEL)	46° 22'	13° 27' E	1800	*Larix decidua*	24 / 17
Mediterranean	Pollino (POL)	39° 09'	16° 12' E	2100	*Pinus heldreichii*	16 / 14
	Peñarroya (PEN)	40º 23'	0º 40' W	2020	*Pinus uncinata*	13 / 41
	Villarroya de los Pinares (VIL)	40º 34'	0º 40' W	1350	*Pinus sylvestris*	12 / 20

In the Polar and northern Urals sites sampling took place near the undisturbed treeline ecotone which is situated between 270 m to 450 m a.s.l. and includes larch (*Larix sibirica* Ledeb.) and birch stands (*Betula tortuosa* Ledeb.), shrubs (junipers, *Salix* spp.), and alpine moss-grass-lichen communities. In these remote sites (URT, URF, PU; see Table 1), vegetation has not been heavily disturbed during the last centuries (Shiyatov *et al.*, 2005). Climatic data of the Salekhard meteorological station (66.5° N, 66.7° E, 137 m a.s.l., 55 km south-east of the URF and URT study sites) show a mean annual temperature of −6.4 ºC with January (−24.4 ºC) and July (+13.8 ºC) as the coldest and warmest months, respectively. According to climate-growth relationships and based on phenological field observations (needle and shoot elongation, stem wood formation) the growing season lasts from early June to mid August (J.J. Camarero *pers. observ.*; Devi *et al.*, 2008). Mean annual precipitation is 415 mm, with 50% falling as snow. Maximum snow depth is 200-250 cm (Hagedorn *et al.*, 2014). Soils develop on ultramafic rocks.

In the Italian Alps, the treeline is located between 1800 and 2200 m a.s.l., and vegetation is dominated by larch (*Larix deciduas* Mill.), spruce (*Picea abies* Karst) and stone pine (*Pinus cembra* L.) forests and shrubby (*Juniperus communis* L., *Rhododendron* spp., *Salix* spp.) communities (Pellizzari *et al.*, 2014). Climate is characterized by dry winters, with most of the precipitation occurring from late spring to early autumn; the mean annual temperature is 2.5 ºC (coldest and warmest months are usually January and July) and the total annual precipitation is ca. 1800 mm, while the growing period lasts from June to early September (Carrer & Urbinati, 2006a). Maximum snow depth is usually 250-600 cm. Soils are shallow rendzic leptosols formed over dolomite and limestone to spodosol over crystalline bedrocks. In this region, logging and livestock grazing decreased significantly during the past century and especially after World War II.

In the Mediterranean region, we selected a site (POL) located in southern Italy subjected to wetter conditions than the other two dryer sites (VIL, PEN) situated in eastern Spain (Camarero *et al.*, 2015a). In POL, forests are dominated by pine (*Pinus heldreichii*) accompanied by junipers and Mediterranean shrubs and grasslands (Todaro *et al.*, 2007). Climate is Mediterranean, humid type, with warm and fairly dry summers and the annual mean temperature is ca. 5.0 ºC whilst the precipitation is around 1570 mm mainly concentrated in autumn and winter. Snow cover lasts from November to late May and its maximum depth is 50-150 cm. Soils are shallow and formed over large outcropping rocks (limestome, dolomites). In the VIL and PEN sites located in Spain, forests are dominated by

Scots (*Pinus sylvestris* L.) and mountain pine (*Pinus uncinata* Ram.), whilst shrubby communities are formed by junipers (*J. communis*, *J. sabina* L.) and barberry (*Berberis vulgaris* L.) (Camarero *et al.*, 2015a). Climate is Mediterranean continental with a mean annual temperature of +4.0-9.0 ºC and annual precipitation of 510-900 mm. In the low-elevation VIL site, water deficit occurs in July and drought-induced dieback has been observed in some juniper stands (J.J. Camarero, *pers. observ.*). In the high-elevation PEN site snow cover lasts from November until March. Soils are shallow and derived from underlying limestone bedrock. The VIL and PEN sites have experienced low land-use pressures (logging, grazing) since the 1950s. Here the growing season usually starts from early May to early June and ends from late September to late October (Deslauriers *et al.*, 2008). Where the typical Mediterranean summer drought is present it is possible to observe a resting period within the growing season (Camarero *et al.*, 2010).

Juniper shrubs and trees were usually sampled near the treeline ecotone except at one Mediterranean site (VIL). We collected 350 junipers distributed over the ten study sites and 250 trees, from six different conifer species (Table 1), located at nine of these sites (there were no trees at the Polar NU site, while the PU tree-ring chronology was retrieved from the International Tree-Ring Data Bank (https://www.ncdc.noaa.gov/paleo/study/15341). In the field we measured the stem diameter of junipers (near the base as close as possible to the root collar) and trees (diameter at breast height measured at 1.3 m). We cut basal disks from the major juniper stems since most of the junipers were multi-stemmed and prostrate (height < 0.5 m) while for trees we collected two perpendicular cores at 1.3 m.

Dendrochronological methods

We sanded juniper disks and tree cores with progressively finer sandpapers to better analyse the annual rings. Junipers often present eccentric stems and a high number of wedging rings due to the irregular growth form (Supporting Information, Fig. S1). For this reason we measured 2 to 4 radii in each disk. The pronounced eccentricity prevented converting radial measurements to area increments (Buras & Wilmking, 2014; Myers-Smith *et al.*, 2014). In trees, 2 radii per individual were measured. Rings were measured to the nearest 0.01 mm using a LINTAB-TSAP (Rinn, Heidelberg, Germany) sliding stage micrometer system and then dated.

We used the COFECHA software (Holmes, 1983) to check the cross-dating. We successfully cross-dated 185 junipers (53% of the samples); in the other cases irregular

growth, wedging and missing rings, especially at the outer part of the cross-sections made the cross-dating of old individuals challenging (Supporting Information, Fig. S1). In junipers, the age was obtained by counting the rings from the bark to the pith, whilst in trees age was estimated (at 1.3 m) by fitting a geometric pith locator to the innermost rings in the case of cores without pith. Then, tree age was estimated by counting the rings in the oldest core of each tree and adding the estimate length of core missing up to the predicted pith.

To compare ring growth with climate variables, we standardized and detrended the juniper and tree ring-width series using the *dplR* (Bunn, 2010) package in the R statistical environment (R Core Team, 2015). In the case of junipers, we chose a spline function with a 50% frequency cut off at 100-years, in this way we removed the long-term biological growth trend, maintaining high- (annual) to mid-frequency (multidecadal) growth variability resulting in dimensionless ring-width indices (Helama *et al.*, 2004). Tree chronologies were similarly detrended to remove the typical age-related trend of declining ring-width (often absent in junipers; see Pellizzari et al. 2014) using firstly a negative exponential curve and then applying a 100-years long spline. Finally, with both growth forms, junipers and trees, the first-order autocorrelation of the standardized ring-width indices was removed through autoregressive modelling. The residual indices were averaged at the individual and site levels using a biweight robust mean to obtain residual individual and site chronologies. Statistical descriptive parameters (Fritts, 2001), including the mean, standard deviation, first-order autocorrelation of raw series, the mean sensitivity (a measure of the year to year variability) and the mean correlation between individual series of residual ring-width indices were also calculated for each site chronology considering the common 1950-2013 period.

Climate data

To analyse climate trends in the three regions we used the 0.5°-gridded CRU climate dataset considering monthly data (mean, maximum and minimum temperatures; total precipitation) for the 1901-2013 period (Harris *et al.*, 2014), and also the European-wide E-OBS v12 gridded dataset at 0.25º resolution for the 1950-2013 period (Haylock *et al.*, 2008; Van Den Besselaar *et al.*, 2011). We further investigated seasonal values (means in the case of temperatures, totals in the case of precipitation), considering previous year summer, autumn and winter (June to August, September to November and December to current February respectively) and current spring and summer (March to May and June to August respectively). Indeed we also analysed the sum of previous winter and current spring

precipitation, considering that snow is present during this period and could affect juniper growth in many sites (Pellizzari *et al.*, 2014). Linear trends of temperature anomalies with respect to the 1981-2010 period were calculated after 1950 considering either the CRU or the E-OBS climate datasets.

Due to a decreasing number of instrumental station records together with an increasing amount of uncertainty associated with climate data before the 1950s (Jones, 2016), and particularly across Mediterranean mountains (e.g. the greater Pyrenees region, cf. Büntgen *et al.*, 2008b), the statistical analyses (climate-growth correlations, models) were restricted to the 1950-2013 period.

Statistical analyses

Climatic drivers of the year-to-year growth variability

All statistical analyses were performed in R environment (R Core Team, 2015). First, to summarize the relationships among juniper and tree chronologies we calculated Pearson correlations and plotted them as a function of site-to-site distances. We also calculated a Principal Component Analysis (PCA) using the covariance matrices obtained by relating the residual chronologies. Second, we used Pearson correlations and Linear Mixed-Effects Models (LMEs; Pinheiro & Bates, 2000) to quantify the associations between climatic variables and ring-width indices at site and individual scales, respectively. In the correlation analyses, we considered monthly (from April to September) and seasonal climatic variables of the common 1950-2013 period. Moving correlations (25-year long intervals) were also calculated between growing-season mean temperatures (May to August) and juniper and tree site chronologies. Despite that growing-season length may differ between regions due to the broad latitudinal difference, parallel elevation variability can counteract this trend. Therefore, having in mind this consideration and looking at the results from the monthly climate/growth associations, we set the common May to August period as the time span expected to cover most of the potential growing season in all regions.

LMEs were fitted for all regions considering regions and individual trees or shrubs nested within sites as random factors, and also separately for each region considering again trees or shrubs as random factors. Seasonal and monthly climate variables were considered fixed factors (interactions between climate variables were also considered). The LMEs have the following form:

$$\mathrm{RW}_i = X_i\beta + Z_i b_i + \varepsilon_i \qquad (1),$$

where RW_i represents the shrubs' or trees' ring-width indices of any individual i, β is the vector of fixed effects (climate variables), b_i is the vector of random effects (site or tree/shrub identity), X_i and Z_i are, respectively, fixed and random effects regressor matrices, and ε_i is the within-group error vector. We ranked all the potential models that could be generated with the different explanatory variables according to the Akaike Information Criterion (AIC). We selected those most parsimonious models, i.e. the ones with the lowest AIC (Burnham & Anderson, 2002); these models were identified using the *MuMIn* package (Barton, 2013). In addition, we used the Akaike weights (*Wi*) of each model to measure the conditional probability of the candidate model assuming it was the best model. Finally, we evaluated the fit of the models by graphical examination of the residual and fitted values (Zuur *et al.*, 2009). The "lme" function of the *nlme* package was used to fit the LMEs (Pinheiro *et al.*, 2015).

Growth trends in junipers and trees

To analyse spatio-temporal patterns in juniper and tree ring-width data we used generalized additive mixed models (GAMMs; Wood, 2006). GAMM is a flexible semi-parametric method used to characterize nonlinear patterns observed between a 'response' variable as a function of 'explanatory' variables (Wood, 2006). The final GAMM we used was in the form:

$$RW_i = s\,(year_i * region_i) + s\,(age_i) + s\,(size_i) + Z_iB_i + \varepsilon_i \qquad (2)$$

In this model, the ring widths (RW) of tree i were modeled as a function of calendar year, age and stem basal area (size). An interaction term between year and region was included to account for different growth trends between regions. Thin plate regression splines (s) are used to represent all the smooth terms. The degree of smoothing is determined by internal cross validation (Wood, 2006). In addition, as RW represents multiple measurements performed on different trees from each site, tree identity (Z_iB_i) was regarded as a random effect. An error term (ε_i) with an AR1 (p = 1) correlation structure was also included in the model. GAMMs were fitted using the *mgcv* library (Wood, 2006).

Results

Climate trends

Unexpectedly, warming trends during the 1901-2013 and 1950-2013 periods were stronger in the Mediterranean and Alpine sites than in the Polar sites (Table S1; Supporting Information, Fig. S2). Seasonally, the warming was more intense in summer across Mediterranean sites, particularly in Spain, followed by spring minimum temperatures in the Polar and Alpine sites, particularly in the Polar Urals (Supporting Information, Table S1). Few significant trends were detected for seasonal precipitation.

Growth patterns and trends

Junipers were youngest at the Polar and grew more in Mediterranean sites, whereas the oldest individuals (ca. 400- and 1000-years old junipers and larches, respectively) were sampled in the Alpine sites (Supporting Information, Fig. S3). For junipers and trees younger than 200 years, the mean growth rate was always lowest at the Polar region, whilst growth was highest in the Alpine sites. The mean ring-widths of junipers (0.30 mm) was significantly lower (t = -4.41, P = 0.001) than that (0.90 mm) of trees (Table 2). However, neither the first-order autocorrelation nor the mean sensitivity differed between juniper and trees chronologies.

The mean correlation between individuals was also significantly lower (t = -5.56, P = 0.0002) in junipers (0.26) than in trees (0.54). This also explains why the correlation between trees' chronologies was much stronger than between junipers' chronologies within each biome (Supporting Information, Table S2, Fig. S4). Accordingly, the first axis of the PCA accounted for 45% and 32% of the total variance of ring-width indices in the case of tree and juniper sites, respectively (Supporting Information, Fig. S5). The PCA allowed grouping sites geographically, i.e. within each biome, but in the case of the Mediterranean sites, the humid Italian POL site clearly diverged from the dry Spanish PEN and VIL sites. Lastly, positive and significant ($P < 0.05$) correlations between juniper and tree chronologies within each site were found in the Polar and Mediterranean biomes, but not in the Alpine one (Table S2).

Table 2. Tree-ring series length and descriptive statistics for the juniper (J) and trees (T) computed over the common period 1950-2013. Values are means except for age data.

				Ring widths						Residual indices			
Region	Site	Age (years)		Mean (mm)		Standard deviation (mm)		First-order autocorrelation		Mean sensitivity		Correlation between individual series	
		J	T	J	T	J	T	J	T	J	T	J	T
Polar	URT	85	210	0.22	0.71	0.11	0.31	0.61	0.54	0.32	0.41	0.27	0.67
	URF	74	331	0.27	0.38	0.17	0.24	0.72	0.63	0.30	0.45	0.30	0.64
	PU	164	162	0.17	0.69	0.09	0.36	0.86	0.72	0.22	0.34	0.27	0.63
	NU	99	–	0.20	–	0.07	–	0.54	–	0.21	–	0.20	–
Alpine	DEV	103	564	0.27	0.77	0.14	0.42	0.59	0.35	0.36	0.32	0.16	0.59
	VEN	171	1000	0.25	0.66	0.11	0.39	0.68	0.72	0.27	0.33	0.23	0.56
	SEL	85	405	0.28	1.17	0.13	0.56	0.60	0.67	0.32	0.27	0.29	0.65
Mediterranean	POL	182	574	0.26	0.83	0.12	0.46	0.65	0.90	0.32	0.16	0.36	0.40
	PEN	95	256	0.57	1.59	0.30	0.70	0.49	0.81	0.38	0.23	0.21	0.33
	VIL	103	123	0.52	1.26	0.28	0.48	0.61	0.75	0.36	0.20	0.29	0.36

The GAMMs demonstrated a long-term growth increase of Polar junipers since the 1950s, which boosted after the 1980s when climate warming intensified (Supporting Information, Fig. S2), closely followed by Mediterranean junipers (Fig. 2). In contrast, Mediterranean trees showed a rapid declining in growth since the 1980s, whereas Alpine trees followed by Polar ones featured growth acceleration.

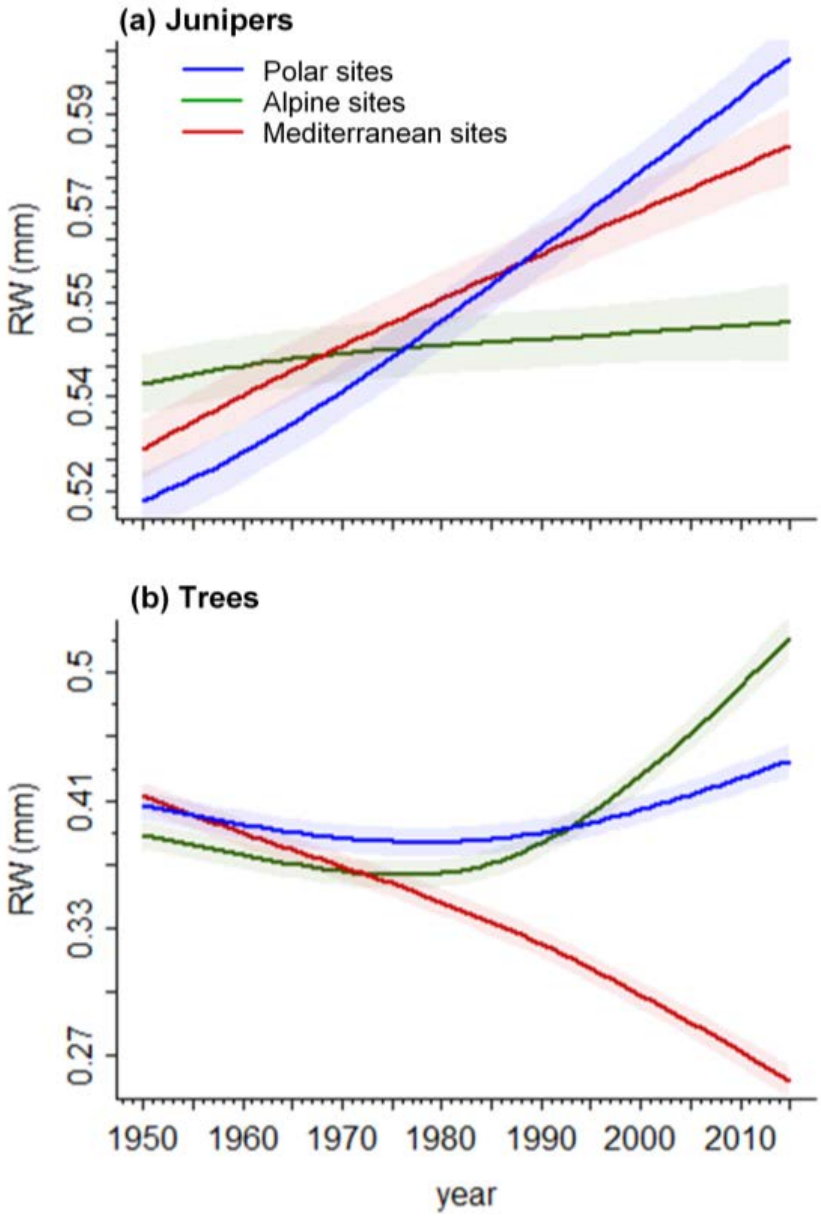

Figure 2. Ring-width growth (RW, ring-width; values are means ± SE) based on the generalized additive mixed models (GAMM) for (a) junipers and (b) trees in each region (blue, green and red lines refer to the Polar, Alpine and Mediterranean sites, respectively). Trends were assumed for a theoretical individual with mean age and basal area across all the study sites.

Growth associations with climate

Warm summer conditions enhanced growth in cold regions (Polar and Alpine biomes) with stronger temperature-growth correlations in trees than in junipers (Fig. 3).

Specifically, higher June to July maximum temperatures were related to wider ring widths, particularly in treeline trees at the Polar sites. Wet September conditions enhanced juniper and tree growth at several Polar sites. Winter-to-spring wet conditions were negatively associated to Alpine juniper growth. In contrast, cool and wet spring and early-summer

conditions favoured growth of junipers and trees in the PEN and VIL dry Mediterranean sites, whereas warm spring and summer conditions enhanced tree and juniper growth in the wet POL Mediterranean site (Fig. 3). In the two dry Mediterranean sites the growth of junipers and trees was enhanced by wet conditions in May-June and June-July, respectively. Previous summer temperatures influence positively juniper growth at Polar Urals and tree growth at some Polar and Alpine sites. These associations at the site level were also reflected by the LMEs fitted at individual level which showed: i) the dominant role played by summer maximum temperatures for Polar juniper and tree growth; ii) the negative influence of high winter-to-spring precipitation for Alpine juniper growth and iii) the relevance of cool and wet spring and summer conditions to Mediterranean growth (Table 3; see also Supporting Information, Table S3).

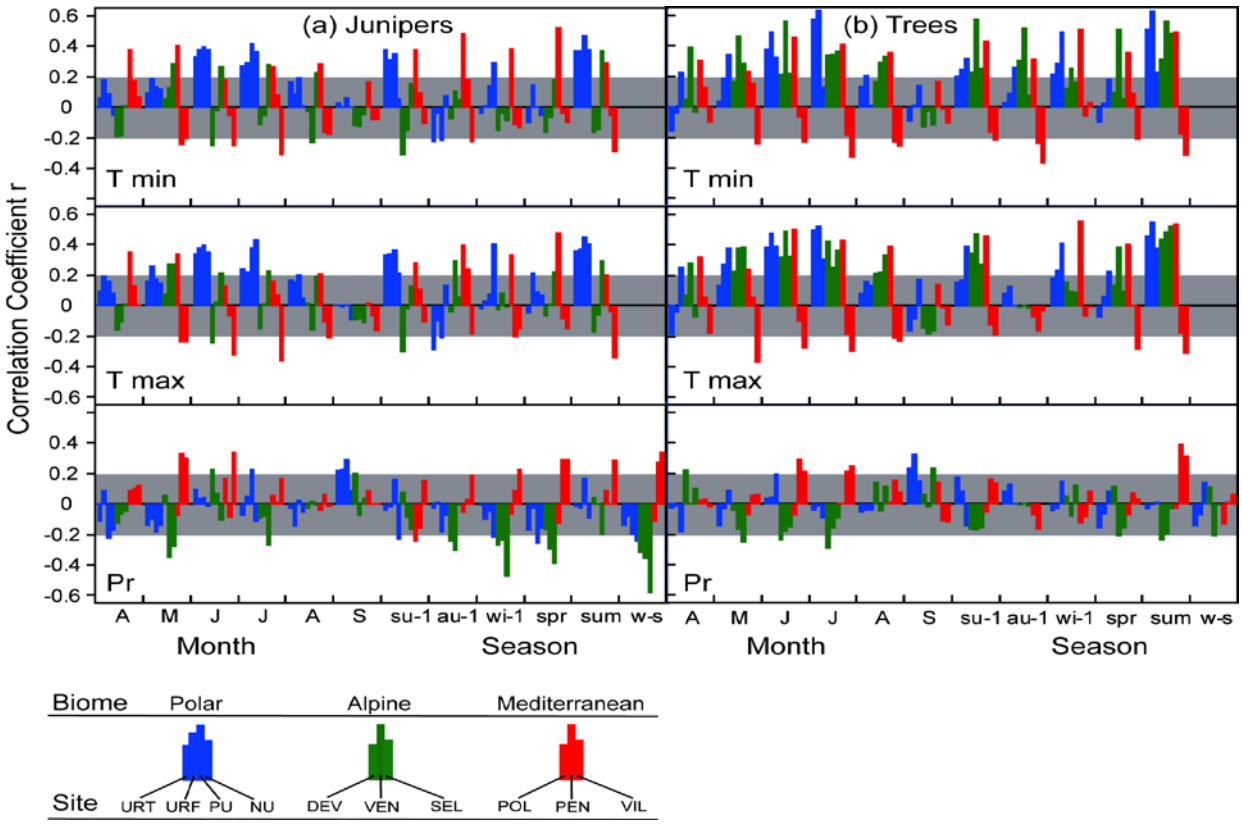

Figure 3. Site-level climate-growth relationships for the juniper and trees. Bars are Pearson correlation coefficients obtained by relating seasonal or monthly mean minimum (Tmin) or maximum (Tmax) temperatures and precipitation (Pr) with site chronologies of ring-width indices for the common period 1950-2013. Grey boxes indicate non-significant values. The temporal window includes monthly climate values from April to September and seasons are indicated by three-letter codes (w-s is the previous winter to spring season). Previous year summer (su-1), autumn (au-1) and winter (wi-1) have also been considered.

Table 3. Summary of the linear mixed-effects models of juniper and tree growth (ring-width indices) as a function of region and climate variables (mean temperatures, total precipitation). Note that the models' intercepts are not presented for simplicity. Abbreviations: aut, autumn; Pr, precipitation; spr, spring; sum, summer; Tn, mean minimum temperatures; Tx, mean maximum temperatures; win, winter; *Wi*, Akaike weights; WS, winter to spring. Numbers after climate variables indicate months, whereas the subscript "t-1" indicates the previous year.

Dataset or region	Junipers		Trees	
	Parameters	*Wi*	Parameters	*Wi*
All regions	+0.022 $Txaut_{t-1}$ +0.012Txsum + 0.001Tnspr − 0.002 $PrWS_{t-1}$	0.88	+0.072 Txsum + 0.014 $Txaut_{t-1}$ + 0.001 $Prwin_{t-1}$	0.86
Polar	+ 0.048 Tm67 − 0.001 $PrWS_{t-1}$	0.97	+ 0.077 Tx7 + 0.041 Tm6	0.89
Alpine	+ 0.013 Tm5 − 0.003 $PrWS_{t-1}$	0.56	+ 0.118 Txsum + 0.021 Tx5	0.97
Mediterranean	− 0.020 Txsum + 0.001 Pr5	0.77	− 0.029 Txsum + 0.001 Pspr	0.83

Growing-season temperatures were significantly ($P < 0.05$) and positively related to Polar tree growth during most of the 1950-2013 period, but in the case of Polar junipers such association decreased to not significant values after the 1990s (Fig. 4). In the case of Alpine trees, temperatures were playing a more important role by enhancing growth since 1970 and turning significant after 1982. In Alpine junipers, positive and significant temperature-growth relationships occurred only during the mid 1960s, following afterwards a reverse trend to that described for coexisting trees. Growth of Mediterranean trees and shrubs did not show significant correlations with temperature.

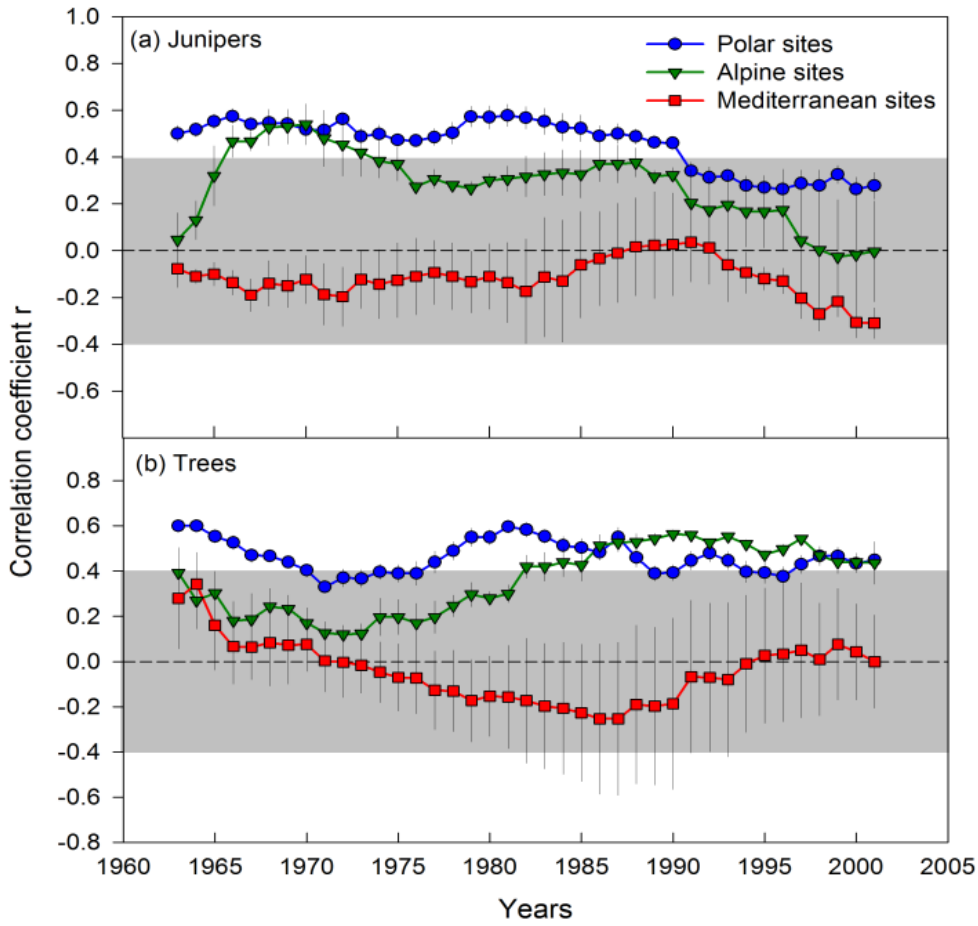

Figure 4. Moving Pearson's correlations (25-year long intervals, 1950-2013 period) calculated between growing-season mean temperatures (May to August) and the mean (± SE) site chronologies of ring-width indices for (a) junipers and (b) trees. The symbols correspond to the mid year of each 25-year long interval of . Values located outside the grey boxes are significant at the 0.05 level.

Discussion

The growth of the two plant forms (shrub and tree), despite featuring even opposite trends, clearly diverges in all the three biomes. This outcome is also corroborated by the climate/growth associations which highlight general higher tree sensitivity to temperature. As assumed, shrubby junipers were less coupled to air temperature and related atmospheric patterns than coexisting tree species across the three biomes in Europe. Unexpectedly, juniper showed enhanced growth at the extreme latitudinal Polar and Mediterranean sites, whereas trees increased their growth rates in Alpine and Polar regions (Fig. 2) and mostly declined in Mediterranean sites. We discuss how this tree-shrub dichotomy could explain these findings by analysing, in space and time, the contrasting macro- and micro-climatic influences to which these two growth forms are exposed in different biomes.

The Arctic is rapidly warming because of the climate-albedo feedbacks related to snow dynamics (IPCC, 2014b). The effect on plants life is a stronger warming-triggered boosting of growth and productivity at the Polar biome with a widespread shrub expansion and a rapid shift from low to tall shrubs (Arctic "greening") observed in many tundra ecosystems (Tape *et al.*, 2006; Devi *et al.*, 2008; Macias-Fauria *et al.*, 2012; Myers-Smith *et al.*, 2015). Our results are in line with this picture with tree-ring growth of Polar junipers and trees (Fig. 2) mainly constrained by the short growing season and cold summer conditions (Fig. 3). However, at the study sites warming trends after 1950 were more pronounced in the Mediterranean and Alpine biomes due to the contribution of increasingly warmer summer conditions (Table S1). This highlights that the typical representation featuring a straight northward or upward growth enhancement and a growth reduction at the southernmost species' distribution limit (as e.g. in Matías & Jump (2015) for juniper and Scots pine), is more complex, with the role of precipitation that should not be overlooked.

In our case, the significant positive correlations at Polar treeline sites recorded on both the growth forms for September precipitation (Fig. 3), even though in the region according to current knowledge the vegetative period is almost if not fully ended, could indicate a positive effect of wet conditions in late summer and early autumn. This would suggest a longer growing season than that previously described (Devi *et al.*, 2008) or even a potential late-summer drought stress induced by warmer conditions, since many junipers establish on rocky substrates and shallow sandy soils, which intensify water deficit. In addition, at the Polar biome, beside the key role of summer temperature, the expansion of shrubs and trees might be also related to the snow amount and cover (Frost & Epstein, 2014). Previous investigations across the Siberian subarctic, including some of our Polar study sites, detected a post-1960s divergence between tree growth and summer temperatures which was explained by a delayed snow melt due to increasing winter precipitation (Vaganov *et al.*, 1999). Late snow melting could have postponed the onset of cambial activity, thus leading to slower growth and a loss of growth sensitivity to summer temperatures (Kirdyanov *et al.*, 2003). Similar detrimental effect of snowpack duration on growth has been described for prostrate junipers in the Alps (Pellizzari *et al.*, 2014). In this mountain region, the amount of winter precipitation is at least double compared to the other biomes and could lead to a short growing season due to late snow melt (Fig. 3, Table 3). However, in most northern Russia, consistently with the trend observed across the Northern hemisphere (Kunkel *et al.*, 2016), the extent and duration of snow cover tends to be shorter

because the first snowfall occurs later and spring snowmelt arrives earlier due to rising temperatures (Table S1) even if the amount of fallen snow increases (Bulygina *et al.*, 2009). Such widespread reduction in snow cover could lead to a longer growing season through an earlier snow melt together with the abovementioned relaxation of September conditions and this can explain the rise of Polar juniper growth.

Unsurprisingly, tree growth at cold sites from the Polar and Alpine biomes responded more to temperature than coexisting junipers, and this response has been stable (Polar sites) or got stronger (Alpine sites) after the 1980s when temperatures started rising rapidly (Figs. 3 and 4). Juniper growth at these temperature-limited sites is getting uncoupled from warmer conditions even though temperatures have kept rising. This suggests an overwhelming role played by local factors or other indirect effects of climate warming rather than the temperature rise *per se*, such as, as mentioned, a reduced snow cover period or a longer growing season. Other drivers such as changes in light availability (Stine & Huybers, 2013), nitrogen deposition and rising CO_2, biotic interactions, disturbance regime and local adaptations could also affect Polar juniper and tree growth but their roles have to be further explored (Matías & Jump, 2015).

Our findings, supporting the hypothesis that trees were more coupled with atmospheric conditions and better responded to climate warming than junipers, could also explain why Mediterranean trees showed a decreasing growth trend in the dry Spanish sites (Fig. 2). Here, the warming-induced drought stress (Galván *et al.*, 2015; Gazol *et al.*, 2015) may drive trees to be more responsive to wet spring conditions than junipers (Fig. 3) which, being less exposed to extreme warm temperatures, likely experience lower evapotranspiration rates. In drought-prone areas as the SW of USA and the Mediterranean Basin warming-induced aridification has been predicted to trigger forest die-off and the replacement of drought-sensitive pine species by junipers (Williams *et al.*, 2013; Camarero *et al.*, 2015b). Nevertheless, cold spells could also cause the die-off of junipers in dry and continental areas (Soulé & Knapp, 2007). It should also be noted the strong differences in climate conditions between POL and the other two more dry and continental Mediterranean PEN and VIL sites which causes a variable growth response to temperature in the case of trees (Fig. 4). This confirms that warming would mainly amplify drought stress in continental Mediterranean sites whilst wetter sites may buffer this aridification trend (Macias *et al.*, 2006). Note also that the climate-growth associations in the dry sites from the Mediterranean biome indicated an earlier onset of xylogenesis in junipers than in trees (see

also Garcia-Cervigón Morales *et al.*, 2012), which suggests that drier summer conditions would be less detrimental to early-growing junipers than to late-growing trees. These results not agreeing with other studies that predicted a reduced performance of common juniper in the southernmost distribution limit (Matías & Jump, 2015), highlight the importance of considering multiple proxies of performance and long-term perspectives to understand species range shifts in response to climate warming.

To conclude, tree growth seems more coupled to temperature than juniper growth in cold-limited regions such as the Polar and Alpine biomes. In the Polar and Mediterranean biomes junipers grow more since the 1950s, and this growth enhancement accelerated in the 1980s. Contrastingly, in the Mediterranean biome, tree growth was negatively associated to climate warming suggesting an increasing importance of drought stress which would explain the observed long-term growth decline. The increased growth observed in cold-limited sites (Polar junipers and Alpine trees) is coherent with an influence of climate warming, but local factors such an extended snow-free period or wetter conditions could also explain the acceleration of growth rates in other places (e.g. Mediterranean junipers).

This contrasting behaviour and sensitivity to climate between different growth forms should be also considered when forecasting current and future vegetation responses to climate change. This study can contribute to improved understanding of carbon sink dynamics of woody communities and improve dynamic global vegetation models which currently do not fully account for the different responses of the shrub and tree growth forms to projected climates.

Acknowledgments

This work was support by the “TreeClim” ERA.Net RUS Pilot Joint Call for Collaborative S&T Projects, European Union. A. Gazol and E. Granda are supported by Postdoctoral grants form MINECO (FPDI 2013-16600 and FJCI-2014-19615, respectively). We also thank the support of the projects CGL2011-26654 and CGL2015-69186-C2-1-R (Spanish Ministry of Economy, FEDER funds). We thank the FPS COST Action FP1304 PROFOUND for facilitating collaborative work.

References

Barber VA, Juday GP, Finney BP (2000) Reduced growth of Alaskan white spruce in the twentieth century from temperature-induced drought stress. *Nature*, **405**, 668–673.

Barton K (2013) MuMI: Multi-Model Inference.

Van Den Besselaar EJM, Haylock MR, Van Der Schrier G, Klein Tank AMG (2011) A European daily high-resolution observational gridded data set of sea level pressure. *Journal of Geophysical Research Atmospheres*, **116**.

Bokhorst SF, Bjerke JW, Tømmervik H, Callaghan T V, Phoenix GK (2009) Winter warming events damage sub-Arctic vegetation: consistent evidence from an experimental manipulation and a natural event. *Journal of Ecology*, **97**, 1408–1415.

Bulygina ON, Razuvaev VN, Korshunova NN (2009) Changes in snow cover over Northern Eurasia in the last few decades. *Environmental Research Letters*, **4**, 45026.

Bunn AG (2010) Statistical and visual crossdating in R using the dplR library. *Dendrochronologia*, **28**, 251–258.

Büntgen U, Frank D, Wilson R, Carrer M, Urbinati C, Esper J (2008a) Testing for tree-ring divergence in the European Alps. *Global Change Biology*, **14**, 2443–2453.

Büntgen U, Frank D, Grudd H, Esper J (2008b) Long-term summer temperature variations in the Pyrenees. *Climate Dynamics*, **31**, 615–631.

Buras A, Wilmking M (2014) Straight lines or eccentric eggs? A comparison of radial and spatial ring width measurements and its implications for climate transfer functions. *Dendrochronologia*, **32**, 313–326.

Burnham KP, Anderson DR (2002) *Model selection and multimodel inference: a practical information-theoretic approach*, Vol. 172. 488 pp.

Camarero JJ, Olano JM, Parras A (2010) Plastic bimodal xylogenesis in conifers from continental Mediterranean climates. *New Phytologist*, **185**, 471–480.

Camarero JJ, Gazol A, Tardif JC, Conciatori F (2015a) Attributing forest responses to global-change drivers: Limited evidence of a CO2-fertilization effect in Iberian pine growth. *Journal of Biogeography*, **42**, 2220–2233.

Camarero JJ, Gazol A, Sangüesa-Barreda G, Oliva J, Vicente-Serrano SM (2015b) To die or not to die: early warnings of tree dieback in response to a severe drought. *Journal of Ecology*, **103**, 44–57.

Carrer M, Urbinati C (2006) Long-term change in the sensitivity of tree-ring growth to climate forcing in Larix decidua. *New Phytologist*, **170**, 861–871.

Danby RK, Hik DS (2007) Variability, contingency and rapid change in recent subarctic alpine tree line dynamics. *Journal of Ecology*, **95**, 352–363.

Deslauriers A, Rossi S, Anfodillo T, Saracino A (2008) Cambial phenology, wood formation and temperature thresholds in two contrasting years at high altitude in southern Italy. *Tree physiology*, **28**, 863–871.

Devi N, Hagedorn F, Moiseev P, Bugmann H, Shiyatov S, Mazepa V, Rigling A (2008) Expanding forests and changing growth forms of Siberian larch at the Polar Urals treeline during the 20th century. *Global Change Biology*, **14**, 1581–1591.

Esper J, Frank D, Büntgen U, Verstege A, Hantemirov R, Kirdyanov A V. (2010) Trends and uncertainties in Siberian indicators of 20th century warming. *Global Change Biology*, **16**, 386–398.

Farjon A (2005) *A monograph of Cupressaceae and Sciadopitys*. Royal Botanic Gardens, Kew.

Forbes BC, Fauria MM, Zetterberg P (2010) Russian Arctic warming and "greening" are closely tracked by tundra shrub willows. *Global Change Biology*, **16**, 1542–1554.

Fritts HC (2001) *Tree Rings and Climate.* Cladwell, NJ.

Frost G V., Epstein HE (2014) Tall shrub and tree expansion in Siberian tundra ecotones since the 1960s. *Global Change Biology*, **20**, 1264–1277.

Galván DJ, Büntgen U, Ginzler C, Grudd H, Gutiérrez E, Labuhn I, Julio Camarero J (2015) Drought-induced weakening of growth-temperature associations in high-elevation Iberian pines. *Global and Planetary Change*, **124**, 95–106.

Garcia-Cervigón Morales AI, Olano Mendoza JM, Eugenio Gozalbo M, Camarero Martínez JJ (2012) Arboreal and prostrate conifers coexisting in Mediterranean high mountains differ in their climatic responses. *Dendrochronologia*, **30**, 279–286.

Gazol A, Camarero JJ (2012) Mediterranean dwarf shrubs and coexisting trees present different radial-growth synchronies and responses to climate. *Plant Ecology*, **213**, 1687–1698.

Gazol A, Julio Camarero J, Gutierrez E et al. (2015) Distinct effects of climate warming on populations of silver fir (Abies alba) across Europe. *Journal of Biogeography*, **42**, 1150–1162.

Grace J, Allen SJ, Wilson C (1989) Climate and the meristem temperatures of plant communities near the tree-line. *Oecologia*, **79**, 198–204.

Hagedorn F, Shiyatov SG, Mazepa VS et al. (2014) Treeline advances along the Urals

mountain range - driven by improved winter conditions? *Global Change Biology*, **20**, 3530–3543.

Hallinger M, Wilmking M (2011) No change without a cause – why climate change remains the most plausible reason for shrub growth dynamics in Scandinavia. *New Phytologist*, **189**, 902–908.

Hallinger M, Manthey M, Wilmking M (2010) Establishing a missing link: warm summers and winter snow cover promote shrub expansion into alpine tundra in Scandinavia. *New Phytologist*, **186**, 890–899.

Harris I, Jones PD, Osborn TJ, Lister DH (2014) Updated high-resolution grids of monthly climatic observations - the CRU TS3.10 Dataset. *International Journal of Climatology*, **34**, 623–642.

Harsch MA, Hulme PE, McGlone MS, Duncan RP (2009) Are treelines advancing? A global meta-analysis of treeline response to climate warming. *Ecology Letters*, **12**, 1040–1049.

Haylock MR, Hofstra N, Klein Tank AMG, Klok EJ, Jones PD, New M (2008) A European daily high-resolution gridded data set of surface temperature and precipitation for 1950-2006. *Journal of Geophysical Research Atmospheres*, **113**.

Helama S, Lindholm M, Timonen M, Eronen M (2004) Detection of climate signal in dendrochronological data analysis: A comparison of tree-ring standardization methods. *Theoretical and Applied Climatology*, **79**, 239–254.

Holmes RL (1983) Computer-assisted quality control in tree-ring dating and measurement. *Tree Ring Bulletin*, **43**, 69–78.

IPCC (2014) *Climate Change 2014: Impacts, Adaptation, and Vulnerability. Part B: Regional Aspects. Contribution of Working Group II to the Fifth Assessment Report of the Intergovernmental Panel on Climate Change [Barros, V.R., C.B. Field, D.J. Dokken, M.D. Mastrandre*. Cambridge University Press, Cambridge, United Kingdom and New York, NY, USA, 688 pp.

Jones P (2016) The reliability of global and hemispheric surface temperature records. *Advances in Atmospheric Sciences*, **33**, 269–282.

Kirdyanov A, Hughes M, Vaganov E, Schweingruber F, Silkin P (2003) The importance of early summer temperature and date of snow melt for tree growth in the Siberian Subarctic. *Trees-Structure and Function*, **17**, 61–69.

Kjellström E, Nikulin G, Hansson U, Strandberg G, Ullerstig A (2011) 21st century changes in the European climate: Uncertainties derived from an ensemble of regional climate

model simulations. *Tellus, Series A: Dynamic Meteorology and Oceanography*, **63**, 24–40.

Körner C (2012a) *Alpine Treelines: Functional Ecology of the Global High Elevation Tree Limits*. Springer Basel.

Körner C (2012b) Treelines will be understood once the functional difference between a tree and a shrub is. *Ambio*, **41**, 197–206.

Kunkel KE, Robinson DA, Champion S, Yin X, Estilow T, Frankson RM (2016) Trends and Extremes in Northern Hemisphere Snow Characteristics. *Current Climate Change Reports*, **2**, 65–73.

Liang E, Lu X, Ren P, Li X, Zhu L, Eckstein D (2011) Annual increments of juniper dwarf shrubs above the tree line on the central Tibetan Plateau: A useful climatic proxy. *Annals of Botany*, **109**, 721–728.

Lu X, Huang R, Wang Y, Sigdel S., Dawadi B, Liang E, Camarero JJ (2016) Summer temperature drives radial growth of alpine shrub willows on the northeastern Tibetan Plateau. *Arctic, Antarctic and Alpine Research*.

MacDonald GM, Kremenetski K V, Beilman DW (2008) Climate change and the northern Russian treeline zone. *Philosophical transactions of the Royal Society of London. Series B, Biological sciences*, **363**, 2285–2299.

Macias M, Andreu L, Bosch O, Camarero JJ, Guti??rrez E (2006) Increasing aridity is enhancing silver fir (Abies alba Mill.) water stress in its south-western distribution limit. *Climatic Change*, **79**, 289–313.

Macias-Fauria M, Forbes BC, Zetterberg P, Kumpula T (2012) Eurasian Arctic greening reveals teleconnections and the potential for structurally novel ecosystems. *Nature Climate Change*, **2**, 613–618.

Matías L, Jump AS (2015) Asymmetric changes of growth and reproductive investment herald altitudinal and latitudinal range shifts of two woody species. *Global Change Biology*, **21**, 882–896.

Myers-Smith IH, Forbes BC, Wilmking M et al. (2011) Shrub expansion in tundra ecosystems: dynamics, impacts and research priorities. *Environmental Research Letters*, **6**, 45509.

Myers-Smith IH, Hallinger M, Blok D et al. (2014) Methods for measuring arctic and alpine shrub growth: A review. *Earth-Science Reviews*, **140**, 1–13.

Myers-Smith IH, Elmendorf SC, Beck PS a et al. (2015) Climate sensitivity of shrub growth

across the tundra biome. *Nature Clim. Change*, **advance on**, 1–44.

Pellizzari E, Pividori M, Carrer M (2014) Winter precipitation effect in a mid-latitude temperature-limited environment: the case of common juniper at high elevation in the Alps. *Environmental Research Letters*, **9**, 104021.

Pinheiro JC, Bates DM (2000) Mixed effects models in S and S-Plus. *Springer VerlagNewYork*, 528.

Pinheiro J, Bates D, DebRoy S, Sarkar D, R Development Core Team R (2015) nlme: linear and nonlinear mixed effects models. *R package version 3.1-122*, **R package**, 1–3.

R Core Team (2015) R: A Language and Environment for Statistical Computing. *R Foundation for Statistical Computing Vienna Austria*, **0**, {ISBN} 3-900051-07-0.

Rixen C, Schwoerer C, Wipf S (2010) Winter climate change at different temporal scales in Vaccinium myrtillus, an Arctic and alpine dwarf shrub. *Polar Research*, **29**, 85–94.

Rohde R, Muller R, Jacobsen R, Muller E, Groom D, Wickham C (2013) A New Estimate of the Average Earth Surface Land Temperature Spanning 1753 to 2011. *Geoinformatic & Geostatistics: An Overview*, **1**, 1–7.

Salzer MW, Hughes MK, Bunn AG, Kipfmueller KF (2009) Recent unprecedented tree-ring growth in bristlecone pine at the highest elevations and possible causes. *Proceedings of the National Academy of Sciences of the United States of America*, **106**, 20348–53.

Shiyatov SG, Terent'ev MM, Fomin V V. (2005) Spatiotemporal dynamics of forest-tundra communities in the Polar Urals. *Russian Journal of Ecology*, **36**, 69–75.

Soulé PT, Knapp PA (2007) Topoedaphic and morphological complexity of foliar damage and mortality within western juniper (Juniperus occidentalis var. occidentalis) woodlands following an extreme meteorological event. *Journal of Biogeography*, **34**, 1927–1937.

Stine AR, Huybers P (2013) Arctic tree rings as recorders of variations in light availability. *Nature Communications*, **5**, 3836.

Sturm M, Racine C, Tape K (2001) Climate change. Increasing shrub abundance in the Arctic. *Nature*, **411**, 546–547.

Suarez F, Binkley D, Kaye MW, Stottlemyer R (1999) Expansion of forest stands into tundra in the Noatak National Preserve, northwest Alaska. *Ecoscience*, **6**, 465–470.

Tape K, Sturm M, Racine C (2006) The evidence for shrub expansion in Northern Alaska and the Pan-Arctic. *Global Change Biology*, **12**, 686–702.

Todaro L, Andreu L, D'Alessandro CM, Gutiérrez E, Cherubini P, Saracino A (2007)

Response of Pinus leucodermis to climate and anthropogenic activity in the National Park of Pollino (Basilicata, Southern Italy). *Biological Conservation*, **137**, 507–519.

Trahan MW, Schubert BA (2016) Temperature-induced water stress in high-latitude forests in response to natural and anthropogenic warming. *Global Change Biology*, **22**, 782–791.

Vaganov EA, Hughes MK, Kirdyanov A V, Schweingruber FH, Silkin PP (1999) Influence of snowfall and melt timing on tree growth in subarctic Eurasia. *Nature*, **400**, 149–151.

Vautard R, Gobiet A, Sobolowski S et al. (2014) The European climate under a 2 °C global warming. *Environmental Research Letters*, **9**, 34006.

Vicente-Serrano SM, Lopez-Moreno J-I, Beguería S et al. (2014) Evidence of increasing drought severity caused by temperature rise in southern Europe. *Environmental Research Letters*, **9**, 44001.

Williams AP., Allen CD, Macalady AK et al. (2013) Temperature as a potent driver of regional forest drought stress and tree mortality. *Nature Climate Change*, **3**, 292–297.

Wilson C, Grace J, Allen S, Slack F (1987) Temperature and Stature: A Study of Temperatures in Montane Vegetation. *Functional Ecology*, **1**, 405–413.

Wood SN (2006) Generalized additive models: an introduction with R (ed R. Chapman & Hall U). *Texts in statistical science*, **16**, xvii, 392 .

Zuur AF, Ieno EN, Walker NJ, Saveliev A a, Smith GM, Ebooks Corporation. (2009) Mixed Effects Models and Extensions in Ecology with R. *Statistics for Biology and Health*, 579 p.

Supporting Information

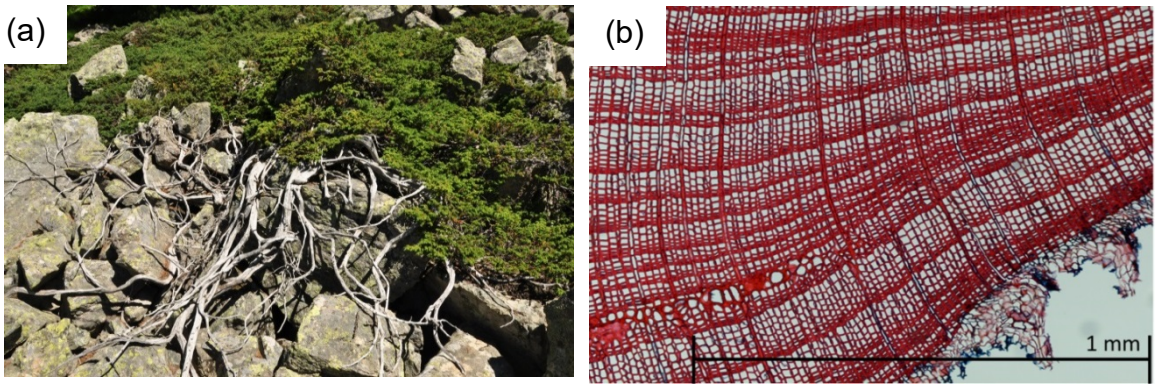

Figure S1. (a) Shrubby juniper sampled at a mountain site located in the Italian Alps and (b) typical wedging rings in a juniper cross-section.

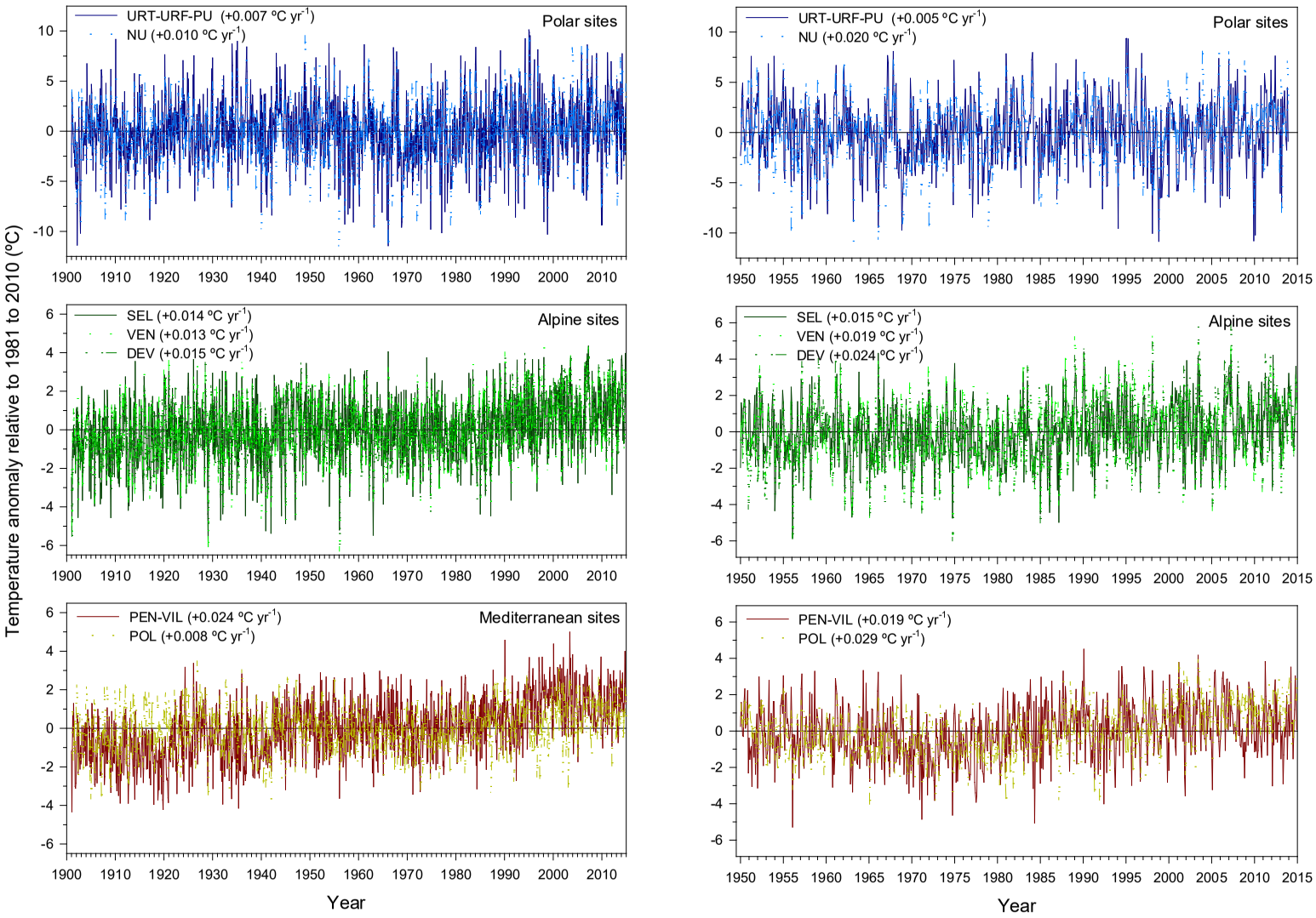

Figure S2. Trends in mean annual temperatures in the study sites for the (a) 1901-2013 and (b) 1950-2013 periods quantified as temperature anomalies with respect to the 1981-2010 average annual cycle for each 0.5º (a, CRU climate dataset) or 0.25º grid (b, E-OBS climate dataset) including each site. See sites' codes in Table 1. Numbers between brackets indicate the annual trends which were significant at the 0.01 level in all cases.

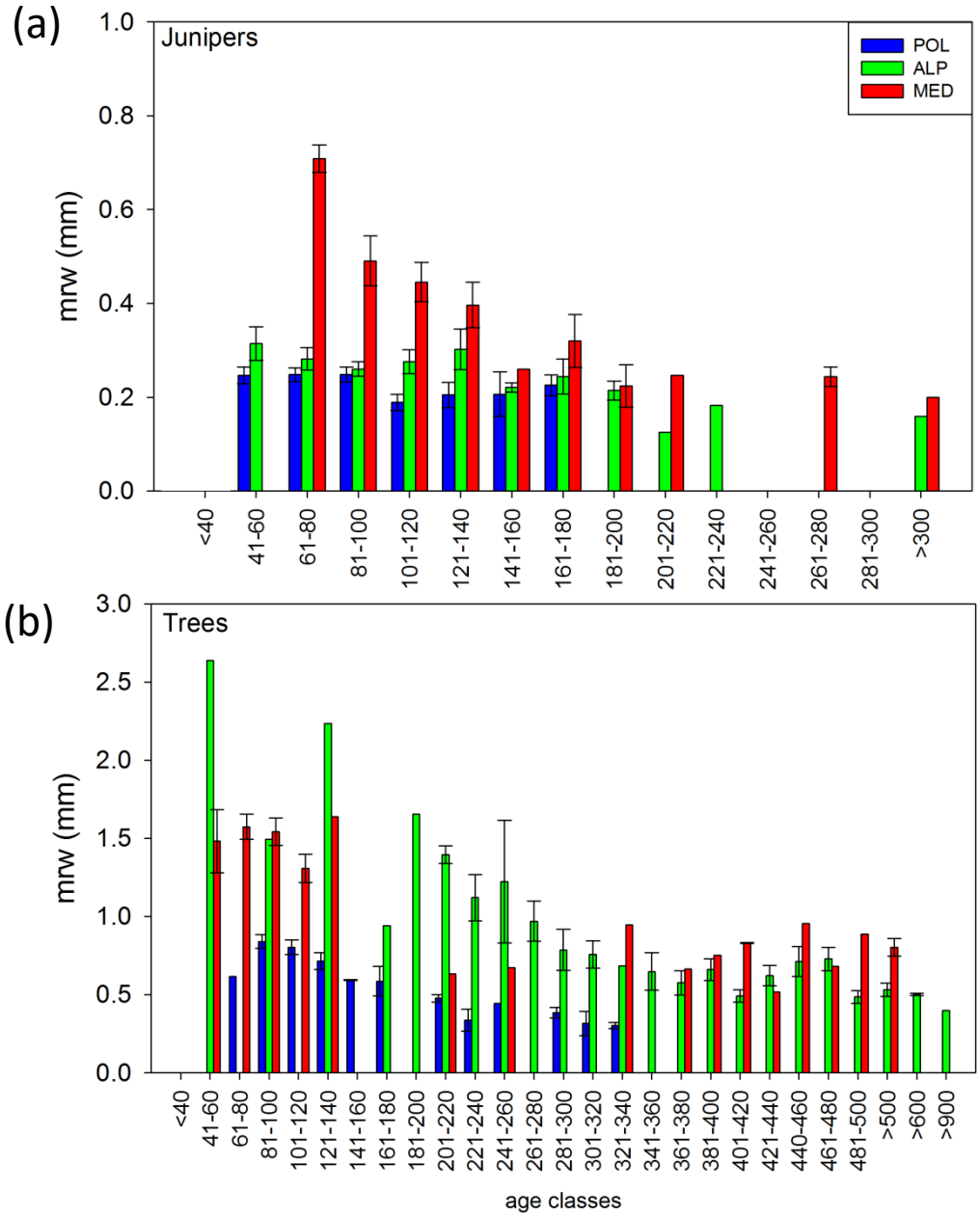

Figure S3. Mean ring-width (mrw) of (a) junipers and (b) tree species averaged for 20-years age classes. Data are plotted considering the three regions: Mediterranean (MED), Alpine (ALP) and Polar (POL). In the case of trees older than 500 years, age classes are presented using wider intervals.

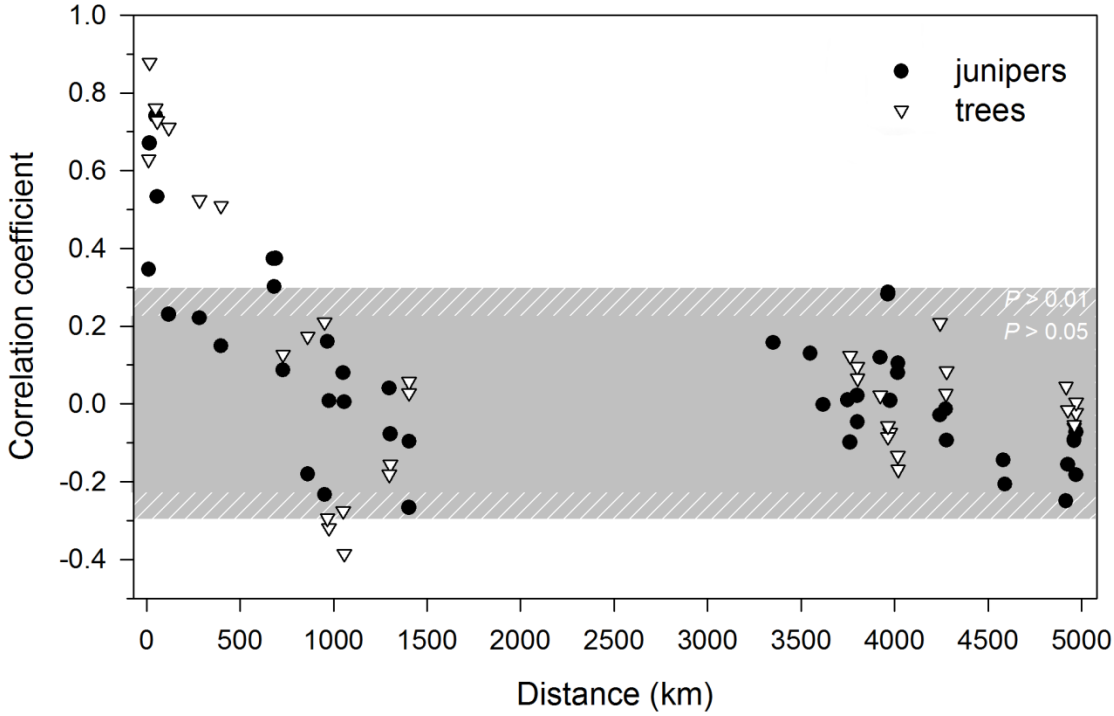

Figure S4. Changes in correlation coefficients (Pearson *r*) calculated between site ring-width residual chronologies for junipers (filled circles) and trees (empty triangles) as a function of the distance between sites. Two significance thresholds ($P > 0.05$, $P > 0.01$) are displayed with different fills. Correlations have been calculated between samples of the same growth form (junipers with junipers and trees with trees).

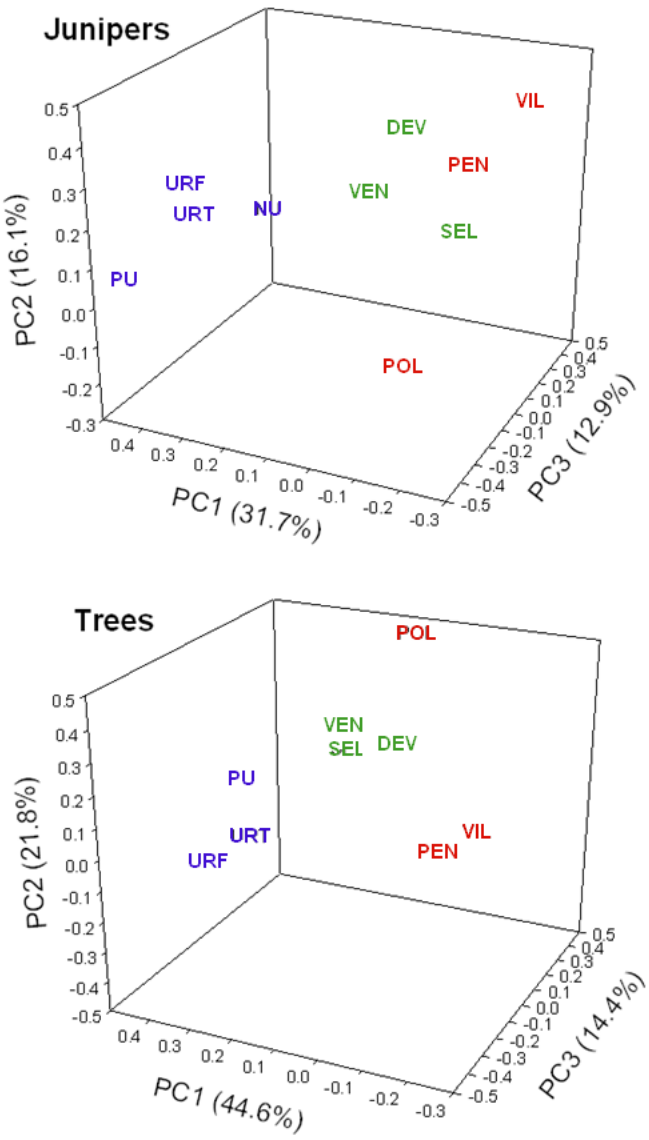

Figure S5. Triplots showing the first three axes (PC1, PC2 and PC3) of a Principal Component Analysis calculated on the variance-covariance matrix of the juniper and trees ring-width site chronologies.

Table S1. Seasonal climatic values (means for temperatures and totals for precipitation) and trends calculated for the study sites considering the three study biomes. Climatic means and trends were calculated for the 1950-2013 period considering the 0.5°-gridded CRU climate dataset. Seasons' abbreviations: Sp, spring; Su, summer; Au, autumn; Wi, winter. Significant ($P < 0.05$) trends are indicated with bold values.

Mean values (ºC or mm)													
Region	Site	Mean maximum temperature				Mean minimum temperature				Precipitation			
		Sp	Su	Au	Wi	Sp	Su	Au	Wi	Sp	Su	Au	Wi
Polar	Urt	-2.8	16.6	-0.7	-16.5	-8.7	11.6	-4.7	-22.6	85	182	127	69
	Urf												
	PU	-4.2	14.0	-2.5	-4.8	-12.0	6.6	-7.9	-25.7	82	179	128	65
	NU	2.9	18.0	0.4	-14.7	-8.8	5.8	-7.3	-24.6	133	243	166	88
Alpine	Dev	5.1	13.8	6.8	-1.2	-1.7	6.6	1.0	-6.9	486	628	465	423
	Ven	8.6	18.2	10.4	1.4	2.4	10.9	4.6	-3.5	371	485	442	196
	Sel	14.7	24.5	15.2	4.7	7.6	16.8	9.2	-0.4	470	471	577	363
Mediterranean	Pol	4.4	15.0	7.9	-0.7	0.9	10.7	4.6	-3.5	347	212	523	481
	Pen	17.3	26.3	19.8	12.0	5.7	16.2	8.5	0.5	175	114	158	116
	Vil												
Trends (ºC yr^{-1} or mm yr^{-1})													
Region	Site	Sp	Su	Au	Wi	Sp	Su	Au	Wi	Sp	Su	Au	Wi
Polar	Urt	***0.04***	0.02	***0.04***	0.02	***0.05***	0.01	***0.04***	0.04	0.48	0.86	-0.24	1.32
	Urf												
	PU	0.03	0.01	0.02	0.01	***0.04***	***0.02***	***0.03***	0.01	-0.04	-0.12	-0.38	-0.20
	NU	0.02	0.00	0.02	0.01	***0.03***	***0.02***	***0.04***	0.02	***0.62***	0.09	0.26	0.04
Alpine	Dev	***0.02***	***0.03***	***0.02***	***0.02***	***0.04***	***0.04***	***0.04***	***0.03***	0.80	0.08	-0.35	-0.51
	Ven	0.01	0.01	0.00	0.02	***0.02***	***0.02***	***0.01***	0.01	0.36	0.49	0.05	0.97
	Sel	***0.03***	0.02	0.01	0.02	0.01	0.01	0.01	0.01	-0.77	-0.76	-0.82	-0.60
Mediterranean	Pol	***0.02***	***0.02***	***0.02***	***0.01***	***0.02***	***0.02***	***0.02***	***0.01***	***1.14***	1.22	1.18	***2.11***
	Pen	***0.02***	***0.04***	0.01	0.00	***0.02***	***0.03***	***0.02***	***0.02***	0.94	0.81	-0.11	1.56
	Vil												

Table S2. Correlation values (Pearson correlation coefficients) calculated of the residual ring-width chronologies (a) between the study sites and (b) between junipers and trees within each site considering the common 1950-2013 period. Significant ($P < 0.05$) correlations are indicated with bold values.

(a)		**Polar sites**				**Alpine sites**			**Mediterranean sites**	
		Urt	Pu	Nu		Ven	Sel		Pen	Vil
Junipers	Urf	**0.685**	**0.251**	**0.618**	Dev	**0.242**	0.178	Pol	**0.222**	0.018
	Urt		**0.293**	**0.767**	Ven		**0.219**	Pen		**0.338**
	Pu			**0.485**						
Trees	Urf	**0.889**	**0.766**	---	Dev	**0.692**	**0.568**	Pol	0.064	-0.05
	Urt		**0.845**	---	Ven		**0.607**	Pen		**0.592**

(b)	**Polar sites**				**Alpine sites**			**Mediterranean sites**		
Junipers-trees	Urt	Urf	Pu	Nu	Dev	Ven	Sel	Pen	Vil	Pol
	0.254	**0.352**	**0.532**	---	-0.182	0.079	0.115	0.119	**0.417**	**0.293**

Table S3. Summary of the statistics of the most parsimonious linear mixed-effects models fitted to ring-width indices of junipers and trees as a function of monthly and seasonal climate variables for the 1950-2013 period. Abbreviations: AIC, Akaike Information Criterion; Pr, precipitation; spr, spring; sum, summer; Tn, mean minimum temperatures; Tx, mean maximum temperatures; win, winter; *Wi*, Akaike weights; WS, winter to spring. Numbers after climate variables indicate months and the symbol ":" indicates interactions between climate variables. See sites' codes in Table 1.

Region	Site	**Junipers**			**Trees**		
		Model parameters	AIC	*Wi*	Model parameters	AIC	*Wi*
POLAR	URF	0.449 +0.049Tm67−0.001PWS	1173	0.42	−1.146 +0.146 Tm67 −0.048Tnspr	519	0.72
		0.384+0.049Tm67+0.001Pspr	1174	0.31	−1.163 +0.147Tm67 −0.049Tnspr+0.001P5	521	0.28
	URT	−0.165−0.021Tnspr+0.068Tnsum−0.010Tnwin+ 0.008Tnaut	893	0.69	−0.460 + 0.112 Tm67 + 0.002 P9	451	0.89
		0.170+0.055Tm67−0.021Tnspr	895	0.31	−0.832 +0.133 Tm67−0.029Tnspr	455	0.11
	PU	0.675+0.068 Tm67−0.002Pspr	1316	0.75	−0.460 + 0.112 Tm67 + 0.002 P9	1529	0.66
		0.672 + 0.068Tnsum − 0.002P9	1319	0.20	−0.135−0.001Tnspr:PWS+0.143Tm67+0.002P9	1530	0.34
	NU	0.441 +0.002Txspr +0.54Txsum +0.029Txwin	1918	0.98	–––		
		1.075 −0.015Tnspr +0.074Tnsum +0.026Tnwin	1926	0.01			
ALPINE	DEV	1.052 −0.001Pwin:Tm6+ 0.001 P5:Tm5	633	0.71	−0.33 + 0.139 Txsum −0.035Txspr−0.039Tx9	89	0.65
		1.18−0.001PWS:Tx6 + 0.001 PWS:Tx5	636	0.15	−0.103 + 0.112 Txsum−0.001P6 − 0.034Tx9	91	0.34
	VEN	1.131 −0.001PWS:Tx6 + 0.001PWS:Tx5	836	0.55	−0.653+0.129Txsum −0.001 P5 −0.039Tx9	1686	0.91
		1.069 −0.001PWS − 0.011Tx6 + 0.019Tx5	839	0.17	−0.993+0.117 Txsum+ 0.029Tx5 −0.035Tx9	1691	0.08
	SEL	1.576−0.001Pspr−0.001Psum−0.001Pwin	924	0.84	−1.317 +0.150Txsum −0.045Txspr−0.032 Tx9	593	0.92
		1.367− 0.001PWS:Tm6	928	0.15	−3.11+0.159Txsum+0.001Psum	599	0.05
MEDITERRANEAN	POL	0.770+0.032Tnsum−0.001PWS+0.002Psum	869	0.56	−0.952 + 0.147Txsum + H150.001Txwin:PWS	681	0.83
		1.029 −0.001Pspr:Txspr + 0.001Psum:Txsum + 0.001Pwin:Txwin	870	0.26	−1.011+0.006Txspr+0.133Txsum +0.130Txwin	684	0.17
	PEN	1.346 −0.016Txsum −0.001 P5:Tx5 + 0.001P6	830	0.48	1.409 −0.024Txsum +0.001Pspr+0.002Psum	584	0.50
		1.270 −0.013Txsum + 0.001P5:Tx5 −0.001 P6:Tx6	831	0.34	1.412−0.024Txsum+0.001P5:Tx5 +0.002Psum	585	0.47
	VIL	2.116 −0.052Txsum +0.001PWS:Tnspr+ 0.001Psum	503	0.83	1.741 − 0.031Txsum−0.001P5:Tx5+0.001 Psum	1118	0.51
		1.956 −0.041Txsum + 0.002P5:Tx5 + 0.001P6	507	0.14	1.746−0.031Txsum−0.001Pspr+0.001Psum	1119	0.49

CHAPTER III

Global Change Biology

Global Change Biology (2016) **22**, 2125–2137, doi: 10.1111/gcb.13227

Wood anatomy and carbon-isotope discrimination support long-term hydraulic deterioration as a major cause of drought-induced dieback

ELENA PELLIZZARI[1], J. JULIO CAMARERO[2], ANTONIO GAZOL[2], GABRIEL SANGÜESA-BARREDA[2] and MARCO CARRER[1]

[1]*Dip. TeSAF, Universitá degli Studi di Padova, Agripolis I-35020, Legnaro, Italy,* [2]*Instituto Pirenaico de Ecología (IPE-CSIC), Avda Montañana 1005, Zaragoza 50059, Spain*

Abstract

Hydraulic impairment due to xylem embolism and carbon starvation are the two proposed mechanisms explaining drought-induced forest dieback and tree death. Here, we evaluate the relative role played by these two mechanisms in the long-term by quantifying wood-anatomical traits (tracheid size and area of parenchyma rays) and estimating the intrinsic water-use efficiency (iWUE) from carbon isotopic discrimination. We selected silver fir and Scots pine stands in NE Spain with ongoing dieback processes and compared trees showing contrasting vigour (declining vs nondeclining trees). In both species earlywood tracheids in declining trees showed smaller lumen area with thicker cell wall, inducing a lower theoretical hydraulic conductivity. Parenchyma ray area was similar between the two vigour classes. Wet spring and summer conditions promoted the formation of larger lumen areas, particularly in the case of nondeclining trees. Declining silver firs presented a lower iWUE than conspecific nondeclining trees, but the reverse pattern was observed in Scots pine. The described patterns in wood anatomical traits and iWUE are coherent with a long-lasting deterioration of the hydraulic system in declining trees prior to their dieback. Retrospective quantifications of lumen area permit to forecast dieback in declining trees 2–5 decades before growth decline started. Wood anatomical traits provide a robust tool to reconstruct the long-term capacity of trees to withstand drought-induced dieback.

Keywords: Abies alba, dendrochronology, dieoff, hydraulic conductivity, parenchyma, *Pinus sylvestris*, quantitative wood anatomy, water-use efficiency, xylem

Received 10 September 2015; revised version received 23 December 2015 and accepted 30 December 2015

Introduction

Forests store almost half of the terrestrial carbon (Bonan, 2008), and most of this sink corresponds to lasting woody pools that contribute to mitigate the ongoing rise of atmospheric CO_2 (Pan *et al.*, 2011). However, there is growing concern about the fate of some forests in drought-prone areas because increasing frequency and intensity of climate extremes, such as heat waves and prolonged droughts, can make some stands particularly vulnerable to water deficit (Bréda *et al.*, 2006; Allen *et al.*, 2010; Allen *et al.* 2015). Global forest die-off in response to drought illustrates how rapidly some forest ecosystem services may be partially lost, such as the ability to sequester carbon due to fast vigour loss, growth decline, and increasing mortality rates (Anderegg 2015).

The physiology of drought-induced dieback and tree mortality likely involves failures of the coupled hydraulic system and carbon dynamics (McDowell, 2011; Sala *et al.*, 2012). Drought stress acts on several tree processes that are usually interrelated. For instance, stomatal closure prevents xylem embolism but reduces carbon uptake, which impairs phloem functioning and decreases the availability of sugar osmolytes (Sevanto *et al.*, 2014). Drought stress constrains and also uncouples growth and photosynthesis (Hsiao, 1973), and such decoupling could increase the concentrations of nonstructural carbohydrates in tissues of drought-stressed trees (Körner, 2003; but see Galiano *et al.*, 2011). Traits such as wood density and anatomy, often linked to hydraulic conductivity, also determine how vulnerable species and trees are to die-off by affecting xylem embolism, growth and carbon use (Hoffmann *et al.*, 2011; Anderegg, 2015).

Wood formation reflects changes in forest productivity and carbon sequestration (Babst *et al.*, 2014), but it also captures changes in tree vigour since water shortage usually induces the formation of narrow tree rings (Dobbertin, 2005). Wood anatomical features such as lumen area (a proxy for the theoretical hydraulic conductivity provided by each tracheid (von Wilpert, 1991;

Correspondence: J. Julio Camarero, tel. +34 976 369393, fax+34 976 716019, e-mail: jjcamarero@ipe.csic.es

Cuny *et al.*, 2014)) or cell-wall thickness (closely related to xylem carbon costs) are useful proxies to quantify the long-term tree responses to drought stress (Fonti *et al.*, 2010). Nonetheless, quantitative wood anatomy has been little exploited to infer the relative importance played by the physiological mechanisms proposed to explain drought-triggered die-off (but see Levanič *et al.*, 2011; Hereş *et al.*, 2014) and often with contrasting findings. For instance, some authors reported a drought-reduced lumen area leading to a decline in stem hydraulic conductivity (Bryukhanova & Fonti, 2013; Liang *et al.*, 2013), whilst others found the opposite (Eilmann *et al.*, 2009, 2011; Martin-Benito *et al.*, 2013). This evidences that growth responses to drought are complex due to contingency on tree features such as age, size and species-specific traits. We hypothesize that quantitative wood anatomy, a loosely explored field, may help to advance our knowledge in this topic.

Most mechanistic approaches investigating drought-induced forest dieback focus mainly on the short-term processes such as altered hydraulic functions or loss in carbon uptake (McDowell *et al.*, 2008). For instance, tree hydraulic performance in conifers is usually restricted to the last 10–20 rings which encompass the most active sapwood (Sperry & Love, 2015), even if in some species the number of sapwood rings can be up to 50 (Knapic & Pereira, 2005). But trees are long-lived organisms whose susceptibility to extreme droughts can change in parallel with the corresponding long-term variability in climate or stand features (e.g. rising temperature, increase evapotranspiration, increasing competition, etc.). Within this context, time series of wood-anatomical features combined with carbon isotopes can provide a long-term record suitable to assess how trees are predisposed to drought-induced die-off.

Long-term variability in xylem anatomical traits can be related not only to ontogeny (Carrer *et al.*, 2015), but also to carbon fixation and water exchange by analyzing the corresponding changes in intrinsic water-use efficiency (iWUE) derived from carbon-isotope discrimination of tree-ring wood (Saurer *et al.*, 2004). The iWUE is a proxy of the amount of water loss at the leaf level due to stomatal conductance per unit of assimilated carbon (Seibt *et al.*, 2008). Increases in iWUE may respond to greater photosynthetic efficiency due to reduced rates of photorespiration at high leaf-internal CO_2 concentration, reduced water loss due to stomata closure, or both (Lévesque *et al.*, 2013). Rising CO_2 reduces stomatal conductance and decreases water loss, and in some cases leads to larger lumen areas or increases latewood density (Yazaki *et al.*, 2005). However, fertilization effects on growth due to rising CO_2, postulated to be stronger on forests located in dry areas, have not been documented in drought-prone areas (McDowell, 2011; Linares & Camarero, 2012). Hence, the long-term characterization of iWUE can help to disentangle the photosynthetic and hydraulic responses in trees experiencing drought-induced dieback.

Here, we aim to investigate the trees hydraulic performances at the same time scale of their lifespan. Our target is to gain knowledge on the different responses of tree species to drought-triggered die-off by analysing and comparing the long-term changes in some wood anatomical traits and carbon-isotope discrimination of declining and nondeclining Scots pine and silver fir trees. As successive droughts may lead to accumulated hydraulic conductance loss in declining trees (Anderegg *et al.*, 2013), we hypothesize that these trees are characterized by a lower hydraulic conductivity than nondeclining ones. Specifically, we expect that declining trees will produce earlywood tracheids, which account for most of the ring conductivity, with smaller lumen area than nondeclining trees. We also expect that nondeclining trees will show an improved iWUE due to reduced water loss per unit carbon gain as compared to declining trees. Investigating how trees react to drought will help to forecast which forests will be the most vulnerable in coupled carbon-climate-vegetation models (Bréda *et al.*, 2006). This will be particularly useful in the Mediterranean Basin and other areas subjected to season water shortage where future climate scenarios predict an increased frequency of extreme droughts (IPCC, 2014).

Materials and methods

Study sites and tree species

In early 2012, we selected two sites in NE Spain (Aragón) dominated by silver fir (*Abies alba*) and Scots pine (*Pinus sylvestris*) and significantly affected by the 2012 drought with abundant defoliated and dying trees (Camarero *et al.*, 2015). The selection of two species allowed comparison of their different wood-anatomical and growth responses to the severe drought. The climate at both sites is continental Mediterranean, however, the silver fir site is mesic (mean annual temperature 9.9 °C, total precipitation 1066 mm and annual water balance 531 mm), whereas the Scots pine site is xeric (mean annual temperature 11.8 °C, total precipitation 375 mm and annual water balance −210 mm). Regarding the regulation of water status, the species' stomatal strategy is relatively isohydric, even if isohydry and anisohydry strategies are likely a continuum (Klein, 2014).

Field sampling

The two stands presented many defoliated and dying trees of the two dominant species after the 2012 drought, which was

the most severe (<mean -SD if expressed as drought indices) in NE Spain since 1950 (Trigo *et al.*, 2013; Camarero *et al.*, 2015). We measured size variables (dbh, diameter at breast height measured at 1.3 m; height) and defoliation status in 38 trees per species to characterize the die-off pattern. To describe tree vigour we estimated the percentage of crown defoliation using binoculars (Dobbertin, 2005). Trees showing <50% postdrought defoliation were considered to be nondeclining, whereas trees with ≥50% postdrought defoliation were considered as declining. This represented a more robust criterion to differentiate declining from nondeclining trees than those based on radial-growth data (Camarero *et al.*, 2015). We randomly selected five trees per vigour class in each species. We then estimated the current competition-intensity index (Camarero *et al.*, 2011) of each tree by measuring the neighbourhood basal area of all woody species with height ≥1.3 m. The neighbourhood was defined as a circular area located within an 8-m wide circle centred on each focal tree (see Sangüesa-Barreda *et al.*, 2015). We obtained monthly and seasonal climatic variables for the 1950–2012 period [mean maximum and minimum temperatures, precipitation (P), estimated potential evapotranspiration (PET) and water balance (P-PET)] from meteorological stations located near the sampling sites (*cf.* Camarero *et al.*, 2015 for further details on site characteristics, sampling design and climate data).

Processing of wood samples

Trees were cored at 1.3 m using a 10-mm Pressler increment borer. First, we divided the cores in 3–5 cm long blocks, which were boiled in water to soften them and remove resins. We then used a rotary microtome (Leica RM 2255; Leica Microsystems, Germany) to cut transverse and tangential wood sections (15–20 μm thick) for the respective measurements of the tracheid (dimensions) and parenchyma (area) variables. Wood sections were stained by mixing safranin (1%) and astra blue (0.5%) solutions. They were then fixed and permanently mounted onto glass microscope slides using a synthetic resin (Eukitt™; Merck, Darmstadt, Germany). Digital images were captured at 100× with a digital camera attached to a light microscope. We created panoramas stitching together multiple overlapping images using the PtGui software. Finally, images were processed using the ROXAS software (von Arx & Carrer, 2014), specifically developed for the analysis of long series of wood-anatomical features.

In the analyses of wood-anatomical traits we avoided tissue anomalies such as compression wood or callus tissue. Furthermore, the selected cores contained the innermost rings located close to the pith to ensure the measurement of the whole ontogenetic sequence of wood formation. We considered 10 trees per species for the transverse measures, while six trees (three declining plus three nondeclining trees) were processed in the tangential measures.

Wood anatomy data

All tracheids forming a ring were measured across transverse sections, but the resulting variables were quantified at the whole ring level or separately for the earlywood and latewood. Sections were ca. 10-μm thick. The identification of earlywood, transition wood and latewood was based on the ring division in five sectors according to the position of each cell within the ring, and based on a Principal Component Analysis calculated on the sectors' time series (Figs S1 and S2). This separation was preferred over the delineation based on the Mork index (Denne, 1988) for its higher efficiency in defining earlywood and latewood in conifers within the Mediterranean region (e.g. Pacheco *et al.*, 2015). Variables measured included ring width, number of tracheids forming a ring, their mean lumen area and cell-wall thickness (henceforth CWT), computed as the average between the tangential and radial thicknesses. Using these variables, we calculated the annual theoretical hydraulic conductivity (K_h) according to the Hagen-Poiseuille law, which states that the capillary flow rate is proportional to the square of the conduit area (Tyree & Zimmermann, 2002). We also calculated the cell-wall thickness-to-span ratio [$(CWT/LD)^2$] where LD is the mean lumen diameter calculated as the average between radial and tangential internal cell diameter. This ratio is assumed to be a surrogate of the xylem resistance against embolism, since it considers both cell wall thickness (mechanical properties) and lumen diameter (hydraulic properties), and it is usually linked to wood density (Hacke *et al.*, 2001). Finally, we estimated the carbon cost investment of tracheid formation (C_{cost}) by multiplying the number of tracheids by CWT for each tree ring (*cf.* Hereş *et al.*, 2014). To assign the correct calendar year to all these variables, the tree-ring series were visually cross-dated among trees and compared with published site ring-width chronologies (Camarero *et al.*, 2015). In total, 475 673 and 976 510 tracheids were measured in Scots pine and silver fir, respectively, considering the 1950–2012 period (1 214 725 and 1 409 018 tracheids considering the whole chronologies).

The parenchyma rays were measured across tangential sections in six trees per species to obtain a proxy for potential storage of nonstructural carbohydrates in the wood (*cf.* Olano *et al.*, 2013; von Arx *et al.*, 2015). We summed the area covered by parenchyma cells across a 4-mm^2 tangential surface, paying attention to not consider the area of resin canals. Since parenchyma rays generally extend through several tree rings (3 on average), we cut tangential sections every five rings and computed the mean parenchyma area every 10 years.

Water-use efficiency inferred from carbon isotope discrimination

To compare the changes in iWUE of nondeclining and declining trees we measured $^{13}C/^{12}C$ isotope ratios in the stem wood. We used the same trees selected for wood-anatomical analyses and with a razor blade under a binocular microscope we carefully separated decadal wood segments for the period 1900–2010. We preferred this time resolution to account for a sufficient number of trees while keeping the low-frequency variability as for the parenchyma rays measurements.

Wood samples were homogenized and milled using an ultra-centrifugation mill (Retsch ZM1). An aliquot of 0.5 mg of each wood sample was weighed on a balance (Mettler

Toledo AX205) and placed into a tin capsule for isotopic analyses. Cellulose was not extracted, since both whole wood and cellulose isotope time-series showed similar long-term trends related to atmospheric CO_2 concentration and climate (Saurer *et al.*, 2004). Furthermore, a carryover effect from year to year can be regarded as negligible, given that we analysed decades. The isotope ratio $^{13}C/^{12}C$ ($\delta^{13}C$) was determined on an isotope ratio mass spectrometer (ThermoFinnigan MAT 251) at the Stable Isotope Facility (University of California, Davis, USA). The results were expressed as relative differences in the $^{13}C/^{12}C$ ratio of tree material with respect to the Vienna Pee-Dee Belemnite (V-PDB) standard. The accuracy and precision of analyses were 0.07‰ and ±0.1‰, respectively.

Isotopic discrimination between the carbon of atmospheric CO_2 and wood carbon (Δ; see Farquhar & Richards, 1984) was defined as:

$$\Delta = (\delta^{13}C_{air} - \delta^{13}C_{plant})/(1 + \delta^{13}C_{plant}/1000), \quad (1)$$

where $\delta^{13}C_{air}$ and $\delta^{13}C_{plant}$ are the isotope ratios of carbon ($^{13}C/^{12}C$) in atmospheric CO_2 and tree-ring wood, respectively, expressed in parts per thousand (‰) relative to the standard V-PDB; Δ is linearly related to the ratio of intercellular (c_i) to atmospheric (c_a) CO_2 mole fractions, by:

$$\Delta = a + (b - a)c_i/c_a, \quad (2)$$

where a is the fractionation during CO_2 diffusion through the stomata (4.4‰), and b is the fractionation associated to Rubisco and other enzymes (Farquhar & Richards, 1984). The values of c_a and $\delta^{13}C_{air}$ were obtained from McCarroll & Loader (2004) and from Mauna Loa (Hawaii) records.

The c_i/c_a ratio reflects the balance between net assimilation (A) and stomatal conductance for CO_2 (g_c) according to Fick's law: $A = g_c(c_a - c_i)$. Stomatal conductances for CO_2 and water vapour (g_w) are related by a constant factor ($g_w = 1.6g_c$), and hence these last two variables allow linking the leaf-gas exchange of carbon and water. The linear relationship between c_i/c_a and Δ may be used to calculate the iWUE (μmol mol^{-1}) as:

$$\text{iWUE} = (c_a/1.6)[(b - \Delta)/(b - a)] \quad (3)$$

Statistical analyses

We used Generalized Additive Models (GAM; Wood, 2006) to study within- and between year variability in lumen area of declining and nondeclining trees. GAMs are a semiparametric case of generalized linear models in which the response variable depends on a collection of smooth functions of the explanatory variable (Hastie & Tibshirani, 1990). Thus, they represent a flexible method to characterize nonlinear trends in time-series that vary at different temporal scales, such as wood-anatomical data. Since tree rings reflect the variability of lumen area anatomy between (long-term) and within (short-term) years we proposed a GAM that includes two different smooth terms: one reflecting between-years variability and another corresponding to the within-year variability in lumen area summarized as a continuous variable that ranges from 0 (early earlywood, beginning of the ring) to 100 (late latewood, end of the ring) indicating how lumen area changes along the relative position within each ring (*cf.* Cuny *et al.*, 2014). For each species (silver fir and Scots pine) and vigour class (declining vs nondeclining trees), we obtained the mean lumen areas along the first 60% of each ring, that is the three earlywood sectors which account for most (around 90%) of the K_h of the whole ring. These series were obtained for the 1950–2012 period and they were used as response variables in the subsequent analyses.

The GAM proposed had the form:

$$\text{Lumen area}_i = s(\text{within year trend}_i) + s(\text{between years trend}_i) + e_i \quad (4)$$

In which the lumen area of a ring i of declining and nondeclining trees is modelled as smooth functions (s) of the within- and between-years trends. The smooth terms were represented using default settings of the function *gamm* in the *mgcv* package (Wood, 2006) of the R environment (R Development Core Team, 2014).

To study the influence of vigour class and climate on cell size formation we used a multi-model inference approach based on information theory (Burnham & Anderson, 2002). This approach relies on the use of information theory to calculate the probability that a given model is more appropriate than other competing models to explain the response variable. We proposed 10 models including vigour class and selected climatic variables and their interactions with the two smooth terms (see Table S1). Climatic variables were first of all analysed through Pearson's correlation with the response variables (tracheid features) and we then selected the strongest correlations. We ranked all the potential models that could be generated with the different explanatory variables according to the second-order Akaike Information Criterion (AICc). For each model, we calculated its ΔAICc, i.e. the difference between AICc of each model and the minimum AICc found for the set of fitted models. The ΔAICc can be used to select those models that best explain the response variable since values of ΔAICc lower than two indicate that the considered model is as good a candidate as the best model. Carbon-isotope data were analysed using linear mixed-effects models considering tree vigour (declining vs nondeclining trees) and time (decades) as fixed factors. The MuMIn package (Barton, 2012) of the R environment (R Development Core Team, 2014) was used to perform the multimodel selection. Finally, to compare declining vs nondeclining trees without considering the time dimension, we adopted the Mann–Whitney test, a nonparametric method used to contrast two groups without considering any distribution information on the population (Sokal & Rohlf, 2012).

Results

Declining and nondeclining trees did not differ significantly in terms of diameter, height, age or neighbourhood basal area (one-way ANOVAs, F = 2.80–0.51, P = 0.12–0.49; Table 1).

However, declining trees of both species had narrower rings formed by fewer tracheids than nondeclining trees.

Table 1 Structural variables describing nondeclining and declining Scots pine and silver fir trees. Data are means ± SE

	Scots pine		Silver fir	
	Nondeclining trees	Declining trees	Nondeclining trees	Declining trees
No. trees	5	5	5	5
Diameter at 1.3 m (cm)	25.1 ± 3.2	26.7 ± 2.0	38.5 ± 3.7	32.0 ± 3.0
Tree height (m)	8.7 ± 1.2	8.4 ± 1.0	25.4 ± 1.8	22.5 ± 1.8
Age (years)	136 ± 17	137 ± 9	98 ± 8	90 ± 10
Neighbourhood basal area (m^2 ha^{-1})	10.8 ± 2.0	7.8 ± 1.0	20.4 ± 5.3	14.3 ± 2.8
Crown cover (%)	75 ± 6 b	15 ± 5 a	96 ± 2 b	35 ± 4 a

Different letters indicate significantly different values ($P < 0.05$) based on Mann–Whitney test.

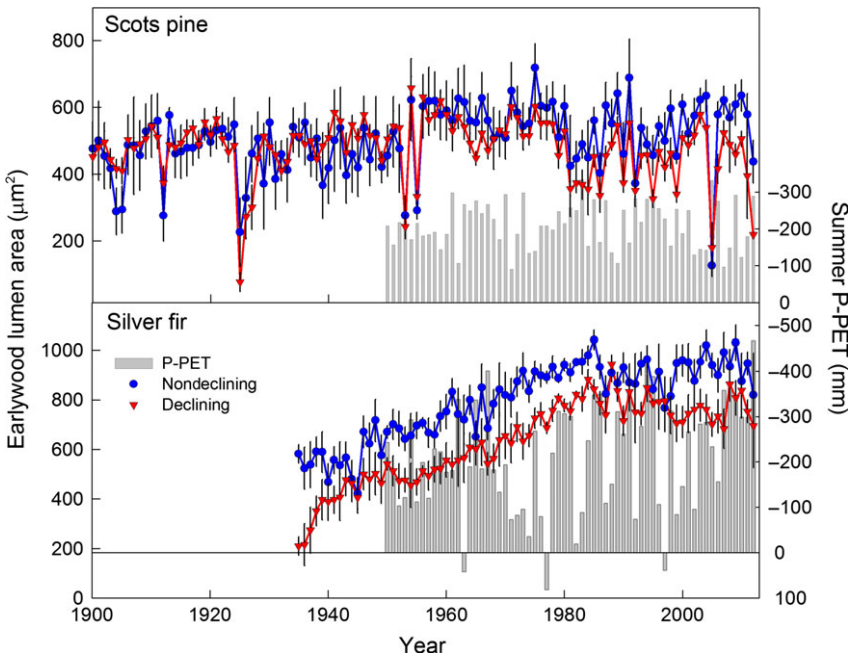

Fig. 1 Annual values of earlywood lumen area in nondeclining and declining trees of Scots pine and silver fir as related to spring or summer water balance (P-PET), respectively (the bars and right y-axis correspond to the water balance; note the reverse scales). Wood anatomy data are means ± SE.

In addition, earlywood tracheids in nondeclining trees had larger lumen areas and thinner cell walls. Consequently, the theoretical earlywood K_h of declining trees decreased while their $(CWT/LD)^2$ increased (Fig. 1 and Table 2; see also Fig. S3).

Wet conditions during the growing season promoted larger lumen in earlywood tracheids while lumen area sharply dropped during dry years (2005, 2012) in the case of Scots pine (Fig. 1). In this species we also noticed reductions in earlywood lumen area, more pronounced in declining trees, during years without dry springs such as 1953 and 1955 and during years without available climate data such as 1925. In silver fir, earlywood lumen area increased steadily from the 1930s to about 1985 at a mean rate of 9.5 μm^2 yr^{-1}. These significant and positive trends did not significantly differ between nondeclining and declining trees ($F = 1.90$, $P = 0.17$). Lumen area in both tree groups was then abruptly reduced after the dry summer in 1985, reaching similar values (ca. 900 μm^2) in 1988. Instead, declining Scots pine trees presented a significant ($P = 0.003$) reduction in lumen area since 1950 at a mean rate of -2.0 μm^2 yr^{-1}, whereas nondeclining trees did not, i.e. there was a long-term divergence between the two vigour classes (significant time x vigour interaction, $F = 7.86$, $P = 0.005$).

Overall, wood anatomy traits responded more to yearly climate variability among Scots pines than in silver firs, with minor differences being observed between the vigour classes. The spring and summer

Table 2 Statistics describing the mean values of measured and derived wood-anatomical variables of nondeclining (ND) and declining (D) Scots pine and silver fir trees

	Scots pine				Silver fir			
	Earlywood		Latewood		Earlywood		Latewood	
	ND	D	ND	D	ND	D	ND	D
Lumen area (μm^2)	542.6 ± 17.2 b	471.8 ± 17.8 a	141.5 ± 8.8	126.3 ± 7.5	850.3 ± 20.2 b	684.9 ± 20.0 a	128.0 ± 6.3	100.54 ± 5.95
Cell-wall thickness (μm)	3.86 ± 0.04 a	4.08 ± 0.06 b	4.98 ± 0.10	5.11 ± 0.11	3.71 ± 0.06 a	3.93 ± 0.06 b	6.60 ± 0.07	6.73 ± 0.06
K_h (kg m MPa^{-1} s^{-1}) 10^{-15}	1.22 ± 0.05 b	0.97 ± 0.04 a	0.18 ± 0.02	0.15 ± 0.01	2.30 ± 0.08 b	1.69 ± 0.07 a	0.14 ± 0.02	0.11 ± 0.01
C_{cost} (μm)	1458.8 ± 100.8	1753.6 ± 236.0	1040.9 ± 77.0	1108.0 ± 90.8	3244.7 ± 239.1	3485.8 ± 243.1	3138.7 ± 225.5	2907.0 ± 185.8
$(CWT/LD)^2$	0.11 ± 0.01 a	0.14 ± 0.01 b	0.71 ± 0.06	0.82 ± 0.08	0.06 ± 0.01 a	0.09 ± 0.01 b	1.19 ± 0.06	1.25 ± 0.08

	Tree ring			
	ND (n = 193 661 tracheids)	D (n = 282 012 tracheids)	ND (n = 544 015 tracheids)	D (n = 43 2495 tracheids)
No. tracheids	655 ± 20 b	525 ± 21 a	1508 ± 51 b	1168 ± 40 a
Width (μm)	645.9 ± 47.1 b	539.2 ± 51.3 a	2109.1 ± 115.0 b	1583.3 ± 111.5 a
Ray parenchyma area (μm^2)	94.6 ± 4.7	90.0 ± 6.6	61.8 ± 2.5	58.9 ± 1.9

Values are presented separately for earlywood and latewood or for the whole tree-ring (last two lines; n is the number of measured tracheids). Data are means ± SE and correspond to the 1950–2012 period. Different letters indicate significant ($P < 0.05$) differences based on Mann–Whitney tests. Abbreviations of variables are: K_h, theoretical hydraulic conductivity; C_{cost}, carbon cost of tracheid formation; CWT/LD, cell-wall thickness-to-span ratio.

water balances were the major climatic drivers of Scots pine and silver fir earlywood lumen areas, respectively (Fig. S4). Differences in lumen area were more evident during wet than dry years (Fig. S5). A previous wet winter and cold and wet summer conditions enhanced the formation of thicker latewood tracheids in Scots pine, whereas warm summer conditions did in silver fir.

We found no significant differences in parenchyma area between tree vigour classes (Table 2, Fig. 2). Only in the last decade (2000s) nondeclining trees tended to produce more parenchyma area than declining ones (Fig. 2), but differences were not significant (Scots pine, $P = 0.35$; silver fir, $P = 0.42$).

According to the fitted GAMs, the climatic signal of lumen area was stronger in Scots pine, whereas the interaction between climate and tree vigour was stronger in silver fir (Table 3, Fig. 3). The GAMs accounted for 79% and 95% of the lumen area variation in Scots pine and silver fir, respectively (Table 3; see also Table S1). These models confirmed that the lumen areas in declining and nondeclining trees had diverged at least since the 1950s with a slight trend to convergence in the late 1980s only in the case of silver fir. The within-ring pattern of lumen area variability was very similar between vigour classes, with differences magnified just in the early to mid earlywood where tracheids reached the largest size.

In Scots pine, declining trees presented significantly ($F = 81.6$, $P < 0.001$) higher $\delta^{13}C$ values (mean ± SD = −23.5 ± 0.2 ‰) than nondeclining trees (−24.3 ± 0.3 ‰) (Fig. 4). However, in silver fir we found the opposite pattern (declining trees, −25.6 ± 0.4 ‰; nondeclining trees, −24.9 ± 0.7 ‰) and differences were again significant albeit less marked ($F = 7.8$, $P = 0.01$). In both species $\delta^{13}C$ values significantly decreased along time (Scots pine, $F = 5.6$, $P = 0.03$; silver fir, $F = 6.9$, $P = 0.02$). No significant decline x time interactions were detected, but declining and nondeclining Silver firs presented similar $\delta^{13}C$ values from the 1990s onwards, whereas a significant negative trend in $\delta^{13}C$ was only detected in nondeclining Scots pine trees (slope = −0.006, $P = 0.015$). Accordingly, only nondeclining Scots pine trees presented a sustained increase in iWUE, particularly since the 1980s (Fig. 4). In agreement with $\delta^{13}C$ values, declining silver firs presented a lower mean iWUE (73 μmol mol^{-1}) than nondeclining trees (81 μmol mol^{-1}), but this difference disappeared in the 1990s. However, a reverse pattern was observed in Scots pine with declining trees showing higher iWUE (92 μmol mol^{-1}) than nondeclining ones (84 μmol mol^{-1}) and this divergence was more marked since the 1960s.

Discussion

Our findings confirm that declining trees were prone to drought-induced dieback because they produced smaller lumen areas which potentially provide less hydraulic conductivity to trees and constrain their ability to grow. Such anatomic and hydraulic divergence with respect to the nondeclining trees could be considered a predisposing factor (*sensu* Manion, 1991) since it was detected several decades (1950s in Scots pine, at least since the 1980s in silver fir) before the droughts

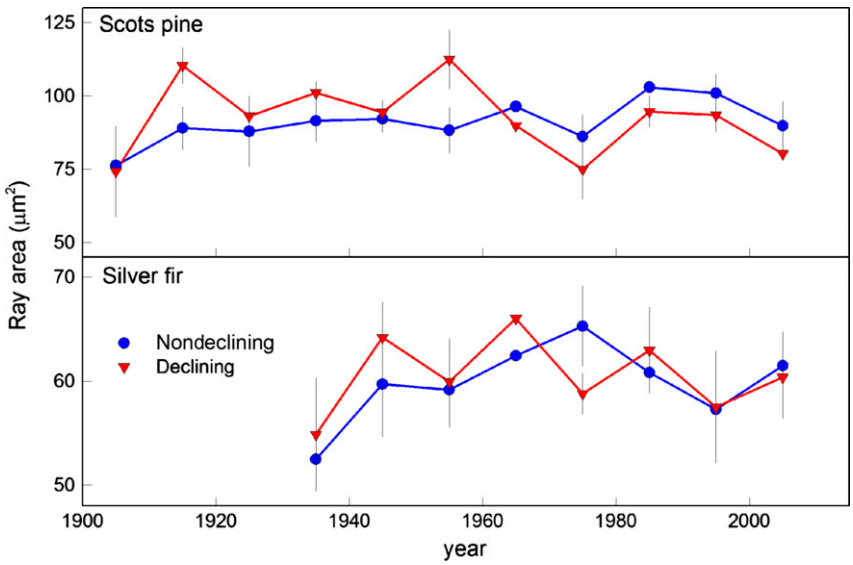

Fig. 2 Decadal variability in the parenchyma ray area of nondeclining and declining trees of Scots pine and silver fir. Values are means ± SE.

Table 3 Statistics corresponding to generalized additive models of earlywood lumen area (*edf*, degrees of freedom; *F* value; *P*, probability level)

Species	Factors	*edf*	*F*	*P*
Scots pine	Long-term trend			
	*vigour: nondeclining	8.88	76.5	<0.001
	*vigour: declining	8.88	71.8	<0.001
	Short-term trend			
	*vigour: nondeclining	8.89	2556.2	<0.001
	*vigour: declining	8.86	2358.3	<0.001
	Climate (P-ETP)	1	930.2	<0.001
	*vigour	1	4.1	0.042
	vigour	1	17.2	<0.001
Silver fir	Long-term trend			
	*vigour: nondeclining	8.79	199.8	<0.001
	*vigour: declining	8.43	632.0	<0.001
	Short-term trend			
	*vigour: nondeclining	8.91	12423	<0.001
	*vigour: declining	8.94	12407	<0.001
	Climate (P-ETP)	1	4.07	0.003
	*vigour	1	24.16	<0.001
	vigour	1	1461.02	<0.001

These models described the long-term and short-term trends of lumen area, i.e. the interannual and intra-annual variability, respectively, as related to tree vigour (declining vs nondeclining trees) and seasonal water balance (P-PET; spring and summer water balances were considered for Scots pine and silver fir, respectively). We created a model containing a continuous variable representing the long-term trend (between rings) in wood anatomy and a variable ranging from 0 to 100 (relative tree-ring width) showing the short-term (within rings) lumen area trend for each species (Scots pine, silver fir). The short-term and long-term terms of lumen area were modelled as thin plate regression splines, whereas the effect of climate was regarded as linear.

triggered die-off and induced mortality (Figs 1 and 3). Short-term investigations have shown that the reduction in hydraulic conductivity can be counterbalanced by concurrent changes in sapwood and leaf area allowing a similar capacity to supply leaves with water (Hereş *et al.*, 2014). However, tuning the leaf-to-sapwood area ratio does not seem an adequate and valid strategy to fully offset the long-term reduction of lumen area detected in declining trees. Yet, the reconstruction of wood-anatomical variables supports die-off mechanisms related to enduring hydraulic deterioration, and it is much less consistent with those concerning carbon starvation. Although the process of tree death is complex and involves a suite of parallel declines throughout multiple tissues (Anderegg *et al.*, 2014), we have contributed solid evidence confirming that long-term and plastic adaptations in xylem traits such as lumen area do allow identifying trees vulnerable to drought stress in terms of growth decline and vigour loss.

This long-term predisposing factor is also confirmed at functional level with the clear separation in iWUE between trees of different vigour. Here, the reverse pattern observed between the species could be explained by the idiosyncratic drought sensitivity of the species with silver fir being much more drought-sensitive respect to the 'drought-avoiding' Scots pine (Irvine *et al.*, 1998; Aussenac, 2002). In addition, the higher iWUE of declining Scots pine trees could indicate that they experience long-term drier local conditions due to particular soil characteristics (lower soil water holding capacity), or because they form shallow root systems. Nevertheless, the lower iWUE of declining silver firs as compared with nondeclining conspecifics and the convergence from the 1990s onwards suggest that both tree vigour classes are becoming less able to regulate their water loss in response to warming-induced evapotranspiration deficits (Vicente-Serrano *et al.*, 2015). Overall, carbon-isotope data produced opposite patterns in two tree species experiencing dieback which indicate that iWUE reconstructions should be always supported by additional long-term datasets of tree functioning such as growth, changes in leaf and sapwood area, and wood-anatomical data.

Wet conditions during the growing season promoted the formation of larger lumen areas and thus increased the theoretical hydraulic conductivity of tracheids. However, nondeclining trees seemed more prompt than declining ones to enlarge lumen area in response to higher water availability, particularly in the case of Scots pine. The divergence in this species can be traced back to the 1950s, suggesting a long-term deterioration in hydraulic conductivity. Drought stress, i.e. evaporative demand that is not met by available water (*cf.* Stephenson, 1998), is mainly controlled by air temperatures at the Scots pine site, which is drier than the silver fir one. Wood-anatomical data, echoed by growth data (Camarero *et al.*, 2015), together with the higher responsiveness to climate detected in the Scots pine site as compared with the silver fir site confirmed this. We must also emphasize that the Scots pine stand constitutes one of the southernmost and drought-exposed limits of distribution of the species.

The two conifers also presented seasonal differences in the wood anatomical responses to climate with spring or summer water balance controlling earlywood lumen area and conductivity in Scots pine, whilst in silver fir previous summer water balance was the most relevant driver of lumen area (Table 3) and also of radial growth (Camarero *et al.*, 2011). The different climatic drivers of wood formation are further illustrated by the contrasting conditions enhancing latewood cell-wall thickening which, during late xylogenesis (summer growing season), was more related to water

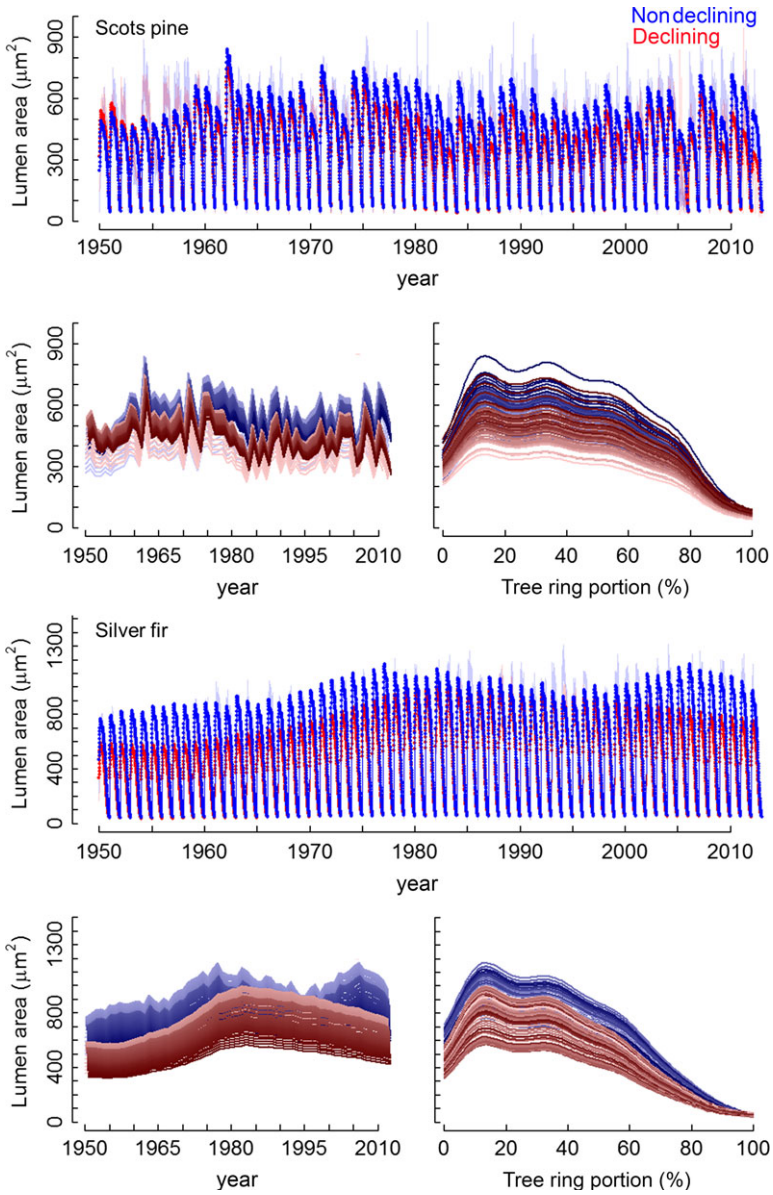

Fig. 3 Observed (thin lines) and modelled long- (between annual ring) and short-term (within a ring) fitted trends in lumen area of nondeclining and declining in Scots pine and silver fir. Generalized additive models were used to characterize the changes in lumen area. These changes are plotted (i) by comparing between years (first 60% portion of the ring; lines of darker and lighter colours corresponding to firstly and lastly formed tracheids, respectively, lower plots to the left); and (ii) by describing lumen area within a ring (darker and lighter colours corresponding to wetter and drier conditions, respectively; note that the differences are more marked in the Scots pine than in the silver fir).

availability in Scots pine and to temperature in silver fir.

The wood-anatomical traits considered did not indicate that declining and nondeclining trees presented different xylem resistances against embolism, although the $(CWT/LD)^2$ ratio may not fully reflect the actual xylem vulnerability to embolism (Domec *et al.*, 2006; Choat *et al.*, 2008; Hacke & Jansen, 2009), More importantly, none of the measured (parenchyma area) or calculated (C_{cost}) variables support the hypothesis that declining trees were presenting previous or concurrent symptoms of carbon starvation as evaluated in the stem wood. Carbon starvation is a highly complex process and the anatomical proxies we considered may not permit to fully assess the processes involved in carbon fixation and use within a tree. However, our findings are consistent with the slight predrought decreases in the concentrations of sapwood soluble sugars in the

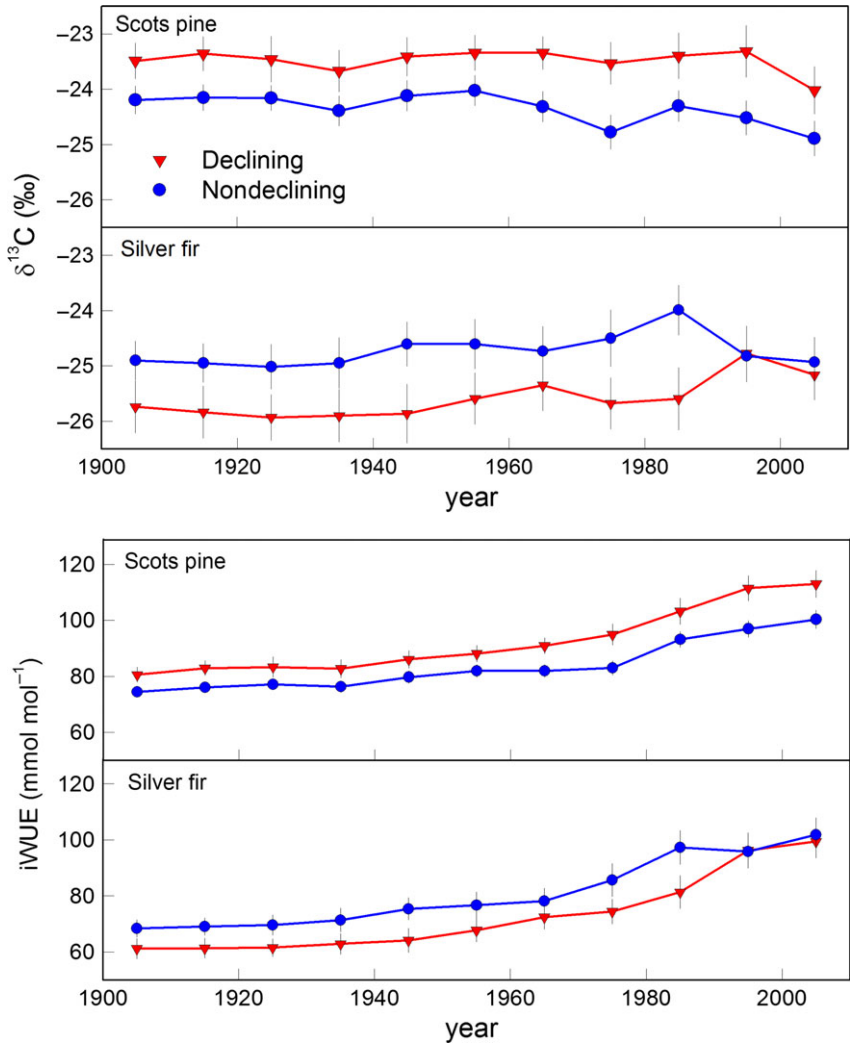

Fig. 4 Trends of wood carbon-isotope discrimination ($\delta^{13}C$) and intrinsic water-use efficiency (iWUE) of declining and nondeclining silver firs and Scots pines. Values are means ± SE.

declining and most defoliated trees of both species during 2012, which were followed by postdrought increases in the case of silver fir (Camarero *et al.*, 2015). We interpret these changes as responses to drought-induced declines in sink activity such as wood formation or to the formation of mobile sugars refilling embolized tracheids (Dietze *et al.*, 2014). Furthermore, declining silver firs presented a lower physiological performance than nondeclining trees confirming that late-summer drought (elevated vapour pressure deficit due to high evapotranspiration rates) caused die-off in the mesic silver-fir site (Peguero-Pina *et al.*, 2007).

In the case of silver fir the increase in earlywood lumen area from the 1930s to the mid-1980s agrees with the typical ontogenetic trend, manifested regardless of the vigour status, and linked to height growth (Carrer *et al.*, 2015). This suggests that silver firs were steadily increasing their hydraulic conductivity and growth capacity until the late-summer 1985 drought caused a sharp decline in earlywood area of all trees, preceding the die-off observed in the 2010s (Fig. 1). It was during the 1980s when lumen areas of declining and nondeclining trees almost converged (Figs 1 and 3), as in fact occurred with iWUE in sites showing high and low dieback intensity (Linares & Camarero, 2012). From the 1980s onwards, these authors reported a progressive drought-induced growth decline and a reduced iWUE improvement in declining silver firs, which they interpreted as reflecting a constant ratio between intercellular and atmospheric CO_2 concentrations. This study confirms that declining silver firs consistently produced smaller lumens and thus always showed lower hydraulic conductivity than nondeclining trees. In other words, declining silver firs were more prone to

drought-induced dieback due to their inferior hydraulic and radial-growth performances as compared with nondeclining trees. The loss in hydraulic performance translated into growth decline (Camarero *et al.*, 2015), and possibly reduced photosynthetic rates, could be linked to the low stomatal control of leaf gas exchange in silver fir in response to warming-induced vapour pressure deficits (Aussenac, 2002). Furthermore, our findings confirm that the rise in atmospheric CO_2, aligned with the corresponding increase in iWUE, did not counterbalance the negative effects of droughts on growth and conductivity, whose decreases were the final drivers of the die-off. For both Scots pine and silver fir, the hydraulic deterioration prior to the die-off could be considered a chronic process since the water balance has been steadily decreasing from the 1950s onwards in both study areas. In addition, the declining trees showed similar diameter respect to nondeclining trees, but lower cells dimension, and this suggests that declining trees were larger than nondeclining before the dieback process started. This assumption may be explained by the fact that big trees are differently coupled with the environment than smaller trees.

It is evident that this study raises many questions related to the ultimate causes making trees more susceptible to decline in hydraulic terms. Ongoing research will investigate if soils or microtopographic features determine the different susceptibility of neighbouring trees to drought stress, particularly in the case of Scots pine. Genetic predisposition to drought-induced die-off within a tree population is also an unknown driver, albeit it has been proved that genetic variability between populations is related to their susceptibility to dieback in the case of silver fir (Sancho-Knapik *et al.*, 2014). Lastly, environmental and genetic drivers could also interact determining tree vigour and vulnerability to drought.

To conclude, this research evidences that long-lasting wood-anatomical differences prior to the onset of water shortage predispose trees to selective drought-induced dieback. Declining trees of both Scots pine and silver fir were those least fit from the hydraulic point of view. In Scots pine the divergence between declining and nondeclining trees can be traced back to fifty years prior to the die-off, whilst in silver fir the tracheid-lumen areas of declining trees were consistently and significantly smaller during the whole ontogeny, and therefore they presented a lower hydraulic performance. None of the analysed wood-anatomical variables supported carbon starvation as a major mechanism of the present die-off phenomena. Retrospective analyses of lumen-area time series could be used as prognosis tools to predict which trees are more prone to drought-induced die-off. Improving these forecasts by increasing the number of trees, sites and species under investigation is urgent since many conifer stands will be more widely affected by drought-induced die-offs in the Anthropocene (Allen *et al.* 2015; Anderegg *et al.*, 2015).

Acknowledgements

This study was supported by projects 387/2011 (OAPN, Spanish Ministry of Environment) and CGL2011-26654 (Spanish Ministry of Economy). We thank the FPS COST Action FP1106 STReESS for facilitating collaborative work. We acknowledge AEMET for providing climatic data. A. Gazol is supported by a Postdoctoral grant from MINECO (Contrato Formacion Postdoctoral MINECO - FPDI 2013-16600, FEDER funds).

References

Allen CD, Macalady AK, Chenchouni H *et al.* (2010) A global overview of drought and heat-induced tree mortality reveals emerging climate change risks for forests. *Forest Ecology and Management*, **259**, 660–684.

Anderegg WRL (2015) Spatial and temporal variation in plant hydraulic traits and their relevance for climate change impacts on vegetation. *New Phytologist*, **205**, 1008–1014.

Anderegg WRL, Plavcová L, Anderegg LDL, Hacke UG, Berry JA, Field CB (2013) Drought's legacy: multiyear hydraulic deterioration underlies widespread aspen forest die-off and portends increased future risk. *Global Change Biology*, **19**, 1188–1196.

Anderegg WRL, Anderegg LDL, Berry JA, Field CB (2014) Loss of whole-tree hydraulic conductance during severe drought and multi-year forest die-off. *Oecologia*, **175**, 11–23.

Anderegg WRL, Schwalm C, Biondi F *et al.* (2015) Pervasive drought legacies in forest ecosystems and their implications for carbon cycle models. *Science*, **349**, 528–532.

von Arx G, Carrer M (2014) ROXAS – A new tool to build centuries-long tracheid-lumen chronologies in conifers. *Dendrochronologia*, **32**, 290–293.

von Arx G, Arzac A, Olano JM, Fonti P (2015) Assessing conifer ray parenchyma for ecological studies: pitfalls and guidelines. *Frontiers in Plant Science*, **6**, 1016.

Aussenac G (2002) Ecology and ecophysiology of circum-Mediterranean firs in the context of climate change. *Annals of Forest Science*, **59**, 823–832.

Babst F, Bouriaud O, Papale D *et al.* (2014) Above-ground woody carbon sequestration measured from tree rings is coherent with net ecosystem productivity at five eddy-covariance sites. *New Phytologist*, **201**, 1289–1303.

Barton K (2012) MuMIn: multi-model inference. R package, version 0.12.2.

Bonan GB (2008) Forests and climate change: forcings, feedbacks, and the climate benefits of forests. *Science (New York, N.Y.)*, **320**, 1444–1449.

Bréda N, Huc R, Granier A, Dreyer E (2006) Temperate forest trees and stands under severe drought: a review of ecophysiological responses, adaptation processes and long-term consequences. *Annals of Forest Science*, **63**, 625–644.

Bryukhanova M, Fonti P (2013) Xylem plasticity allows rapid hydraulic adjustment to annual climatic variability. *Trees - Structure and Function*, **27**, 485–496.

Burnham KP, Anderson DR (2002) *Model Selection and Multimodel Inference: a Practical Information-theoretic Approach*, 2nd edn, Vol. 60. Springer-Verlag, New York, NY.

Camarero JJ, Bigler C, Linares JC, Gil-Pelegrín E (2011) Synergistic effects of past historical logging and drought on the decline of Pyrenean silver fir forests. *Forest Ecology and Management*, **262**, 759–769.

Camarero JJ, Gazol A, Sangüesa-Barreda G, Oliva J, Vicente-Serrano SM (2015) To die or not to die: early warnings of tree dieback in response to a severe drought. *Journal of Ecology*, **103**, 44–57.

Carrer M, Von ArxG, Castagneri D, Petit G (2015) Distilling allometric and environmental information from time series of conduit size: the standardization issue and its relationship to tree hydraulic architecture. *Tree Physiology*, **35**, 27–33.

Choat B, Cobb AR, Jansen S (2008) Structure and function of bordered pits: new discoveries and impacts on whole-plant hydraulic function. *New Phytologist*, **177**, 608–626.

Cuny HE, Rathgeber CBK, Frank D, Fonti P, Fournier M (2014) Kinetics of tracheid development explain conifer tree-ring structure. *New Phytologist*, **203**, 1231–1241.

Denne M (1988) Definition of latewood according to Mork. *Iawa Bull*, **10**, 59–62.

Dietze MC, Sala A, Carbone MS, Czimczik CI, Mantooth JA, Richardson AD, Vargas R (2014) Nonstructural carbon in woody plants. *Annual Review of Plant Biology*, **65**, 667–687.

Dobbertin M (2005) Tree growth as indicator of tree vitality and of tree reaction to environmental stress: a review. *European Journal of Forest Research*, **124**, 319–333.

Domec JC, Lachenbruch B, Meinzer FC (2006) Bordered pit structure and function determine spatial patterns of air-seeding thresholds in xylem of douglas-fir (*Pseudotsuga menziesii*; Pinaceae) trees. *American Journal of Botany*, **93**, 1588–1600.

Eilmann B, Zweifel R, Buchmann N, Fonti P, Rigling A (2009) Drought-induced adaptation of the xylem in Scots pine and pubescent oak. *Tree Physiology*, **29**, 1011–1020.

Eilmann B, Zweifel R, Buchmann N, Graf Pannatier E, Rigling A (2011) Drought alters timing, quantity, and quality of wood formation in Scots pine. *Journal of Experimental Botany*, **62**, 2763–2771.

Farquhar GD, Richards RA (1984) Isotopic composition of plant carbon correlates with water-use efficiency of wheat genotypes. *Australian Journal of Plant Physiology*, **11**, 539–552.

Fonti P, Von Arx G, García-González I, Eilmann B, Sass-Klaassen U, Gärtner H, Eckstein D (2010) Studying global change through investigation of the plastic responses of xylem anatomy in tree rings. *New Phytologist*, **185**, 42–53.

Galiano L, Martínez-Vilalta J, Lloret F (2011) Carbon reserves and canopy defoliation determine the recovery of Scots pine 4 yr after a drought episode. *New Phytologist*, **190**, 750–759.

Gutschick VP, BassiriRad H (2003) Extreme events as shaping physiology, ecology, and evolution of plants: toward a unified definition and evaluation of their consequences. *New Phytologist*, **160**, 21–42.

Hacke UG, Jansen S (2009) Embolism resistance of three boreal conifer species varies with pit structure. *New Phytologist*, **182**, 675–686.

Hacke UG, Sperry JS, Pockman WT, Davis SD, McCulloh KA (2001) Trends in wood density and structure are linked to prevention of xylem implosion by negative pressure. *Oecologia*, **126**, 457–461.

Hastie TJ, Tibshirani R (1990) *Generalized Additive Models*, vol. 1, pp. 297–318. Chapman & Hall, New york, NY, USA.

Hereş A-M, Camarero J, López B, Martínez-Vilalta J (2014) Declining hydraulic performances and low carbon investments in tree rings predate Scots pine drought-induced mortality. *Trees*, **28**, 1737–1750.

Hoffmann WA, Marchin RM, Abit P, Lau OL (2011) Hydraulic failure and tree dieback are associated with high wood density in a temperate forest under extreme drought. *Global Change Biology*, **17**, 2731–2742.

Hsiao T (1973) Plant responses to water stress. *Annual review of Plant Physiology*, **24**, 519–570.

Irvine J, Perks MP, Magnani F, Grace J (1998) The response of Pinus sylvestris to drought: stomatal control of transpiration and hydraulic conductance. *Tree Physiology*, **18**, 393–402.

IPCC (2014) Climate change 2014: impacts, adaptation, and vulnerability. In: *Part B: Regional Aspects. Contribution of Working Group II to the Fifth Assessment Report of the Intergovernmental Panel on Climate Change*, (eds Barros VR, Field CB, Dokken DJ, Mastrandre MD, Mach KJ, Bilir TE, Chatterjee M, Ebi KL, Estrada YO, Genova RC, Girma B, Kissel ES, Levy AN, MacCracken S, Mastrandrea PR, White LL), Cambridge University Press, Cambridge.

Klein T (2014) The variability of stomatal sensitivity to leaf water potential across tree species indicates a continuum between isohydric and anisohydric behaviours. *Functional Ecology*, **28**, 1313–1320.

Knapic S, Pereira H (2005) Within-tree variation of heartwood and ring width in maritime pine (*Pinus pinaster* Ait.). *Forest Ecology and Management*, **210**, 81–89.

Körner C (2003) Carbon limitation in trees. *Journal of Ecology*, **91**, 4–17.

Levanič T, Čater M, McDowell NG (2011) Associations between growth, wood anatomy, carbon isotope discrimination and mortality in a Quercus robur forest. *Tree Physiology*, **31**, 298–308.

Lévesque M, Saurer M, Siegwolf R, Eilmann B, Brang P, Bugmann H, Rigling A (2013) Drought response of five conifer species under contrasting water availability suggests high vulnerability of Norway spruce and European larch. *Global Change Biology*, **19**, 3184–3199.

Liang W, Heinrich I, Simard S, Helle G, Liñán ID, Heinken T (2013) Climate signals derived from cell anatomy of scots pine in NE Germany. *Tree Physiology*, **33**, 833–844.

Linares JC, Camarero JJ (2012) From pattern to process: linking intrinsic water-use efficiency to drought-induced forest decline. *Global Change Biology*, **18**, 1000–1015.

Manion PD (1991) *Tree Disease Concepts*. Prentice Hall, Englewood Cliffs, NJ, USA.

Martin-Benito D, Beeckman H, Cañellas I (2013) Influence of drought on tree rings and tracheid features of *Pinus nigra* and *Pinus sylvestris* in a mesic Mediterranean forest. *European Journal of Forest Research*, **132**, 33–45.

McCarroll D, Loader NJ (2004) Stable isotopes in tree rings. *Quaternary Science Reviews*, **23**, 771–801.

McDowell NG (2011) Mechanisms linking drought, hydraulics, carbon metabolism, and vegetation mortality. *Plant Physiology*, **155**, 1051–1059.

McDowell N, Pockman WT, Allen CD *et al.* (2008) Mechanisms of plant survival and mortality during drought: why do some plants survive while others succumb to drought? *New Phytologist*, **178**, 719–739.

Olano JM, Arzac A, Garcia-Cervigon AI, Von Arx G, Rozas V (2013) New star on the stage: amount of ray parenchyma in tree rings shows a link to climate. *New Phytologist*, **198**, 486–495.

Pacheco A, Camarero J, Carrer M (2015) Linking wood anatomy and xylogenesis allows pinpointing climate and drought influences on growth of coexisting conifers in continental Mediterranean climate. *Tree Physiology*. doi:10.1093/treephys/tpv125

Pan Y, Birdsey RA, Fang J *et al.* (2011) A large and persistent carbon sink in the world's forests. *Science (New York, N.Y.)*, **333**, 988–993.

Peguero-Pina JJ, Camarero JJ, Abadía A, Martín E, González-Cascón R, Morales F, Gil-Pelegrín E (2007) Physiological performance of silver-fir (*Abies alba* Mill.) populations under contrasting climates near the south-western distribution limit of the species. *Flora: Morphology, Distribution, Functional Ecology of Plants*, **202**, 226–236.

R Development Core Team (2014) *R: A Language and Environment for Statistical Computing*. R Foundation for Statistical Computing, Vienna, 409.

Sala A, Woodruff DR, Meinzer FC (2012) Carbon dynamics in trees: feast or famine? *Tree Physiology*, **32**, 764–775.

Sancho-Knapik D, Peguero-Pina J, Cremer E *et al.* (2014) Genetic and environmental characterization of *Abies alba* Mill. populations at its western rear edge. *Pirineos*, **169**, e007.

Sangüesa-Barreda G, Camarero JJ, Oliva J, Montes F, Gazol A (2015) Past logging, drought and pathogens interact and contribute to forest dieback. *Agricultural and Forest Meteorology*, **208**, 85–94.

Saurer M, Siegwolf RTW, Schweingruber FH (2004) Carbon isotope discrimination indicates improving water-use efficiency of trees in northern Eurasia over the last 100 years. *Global Change Biology*, **10**, 2109–2120.

Seibt U, Rajabi A, Griffiths H, Berry JA (2008) Carbon isotopes and water use efficiency: sense and sensitivity. *Oecologia*, **155**, 441–454.

Sevanto S, Mcdowell NG, Dickman LT, Pangle R, Pockman WT (2014) How do trees die? A test of the hydraulic failure and carbon starvation hypotheses. *Plant, Cell and Environment*, **37**, 153–161.

Sokal RR, Rohlf FJ (2012) *Biometry: the Principles and Practice of Statistics in Biological Research*, 4th edn. Freeman, New York, NY, USA.

Sperry JS, Love DM (2015) What plant hydraulics can tell us about responses to climate-change droughts. *New Phytologist*, **207**, 14–27.

Stephenson NL (1998) Actual evapotranspiration and deficit: biologically meaningful correlates of vegetation distribution across spatial scales. *Journal of Biogeography*, **25**, 855–870.

Trigo RM, Añel J, Barriopedro D *et al.* (2013) The record winter drought of 2011-12 in the Iberian Peninsula, in explaining extreme events of 2012 from a climate perspective. *Bulletin of the American Meteorological Society*, **94**, S41–S45.

Tyree MT, Zimmermann MH (2002) *Xylem Structure and the Ascent of Sap*, 2nd edn. Springer-Verlag, Berlin, Germany.

Vicente-Serrano SM, Camarero JJ, Zabalza J, Sangüesa-Barreda G, López-Moreno JI, Tague CL (2015) Evapotranspiration deficit controls net primary production and growth of silver fir: implications for circum-mediterranean forests under forecasted warmer and drier conditions. *Agricultural and Forest Meteorology*, **206**, 45–54.

von Wilpert K (1991) Intraannual variation of radial tracheid diameters as monitor of site specific water stress. *Dendrochronologia*, **9**, 95–113.

Wood SN (2006) *Generalized Additive Models: An Introduction With R*. Chapman and Hall/CRC. CRC, Boca Raton, FL.

Yazaki K, Maruyama Y, Mori S, Koike T, Funada R (2005) Effects of elevated carbon dioxide concentration on wood structure and formation in trees. In: *Plant Responses to Air Pollution and Global Change SE - 11* (eds Omasa K, Nouchi I, De Kok L), pp. 89–97. Springer Japan, Tokyo.

Supporting Information

Additional Supporting Information may be found in the online version of this article:

Figure S1. Changes in lumen area along the five tree-ring sectors.
Figure S2. Application of a Principal Componet Analysis to define earlywood and latewood from tree-ring sectors.
Figure S3. Observed changes in earlywood cell-wall thickness.
Figure S4. Nondeclining and declining Scots pine and silver fir correlations profiles.
Figure S5. Differences in earlywood lumen area of declining and nondeclining trees during years with contrasting water availability.
Table S1. Selection of best-fitted generalized additive models of earlywood lumen area for the two tree species.

Supporting Information

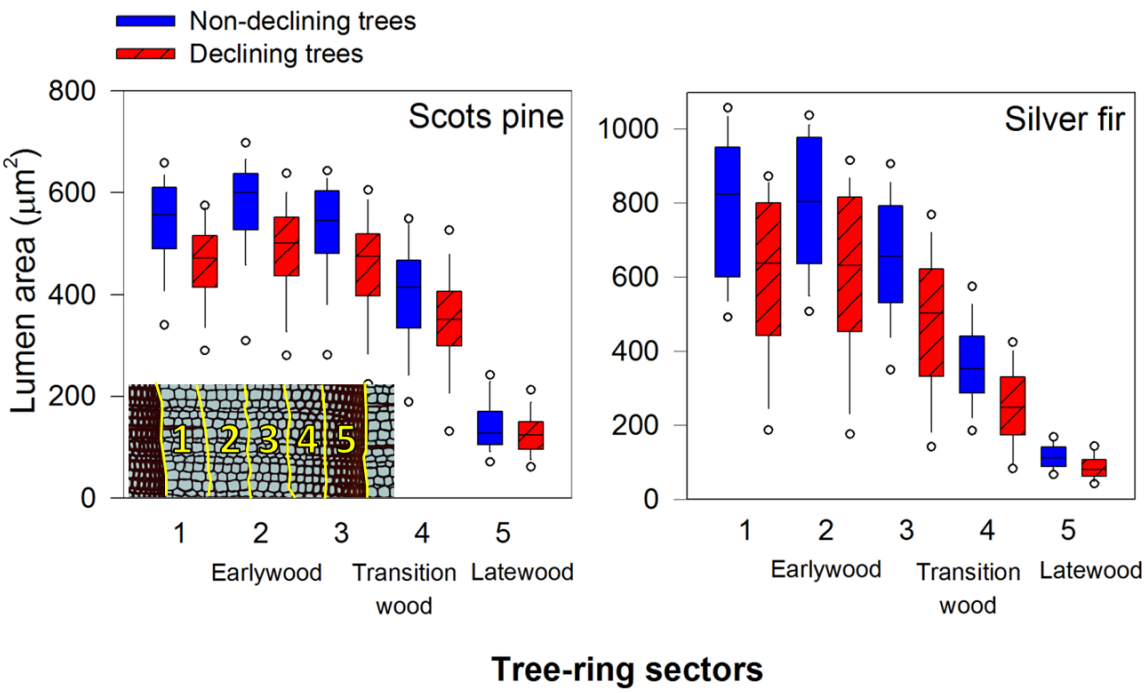

Fig. S1. Changes in lumen area along the five sectors forming a tree ring and used to differentiate, according to the PCA results presented in Fig. S2, earlywood (sectors 1, 2 and 3), transition wood (sectors 4) and latewood (sector 5) in Scots pine and silver fir. Data are separately shown for non-declining and declining trees. Note that lumen area was consistently smaller in declining than in non-declining trees in the three first sectors where lumen areas were big, i.e. those tracheids accounting for most of the tree-ring hydraulic conductivity. Data correspond to the 1950-2012 period.

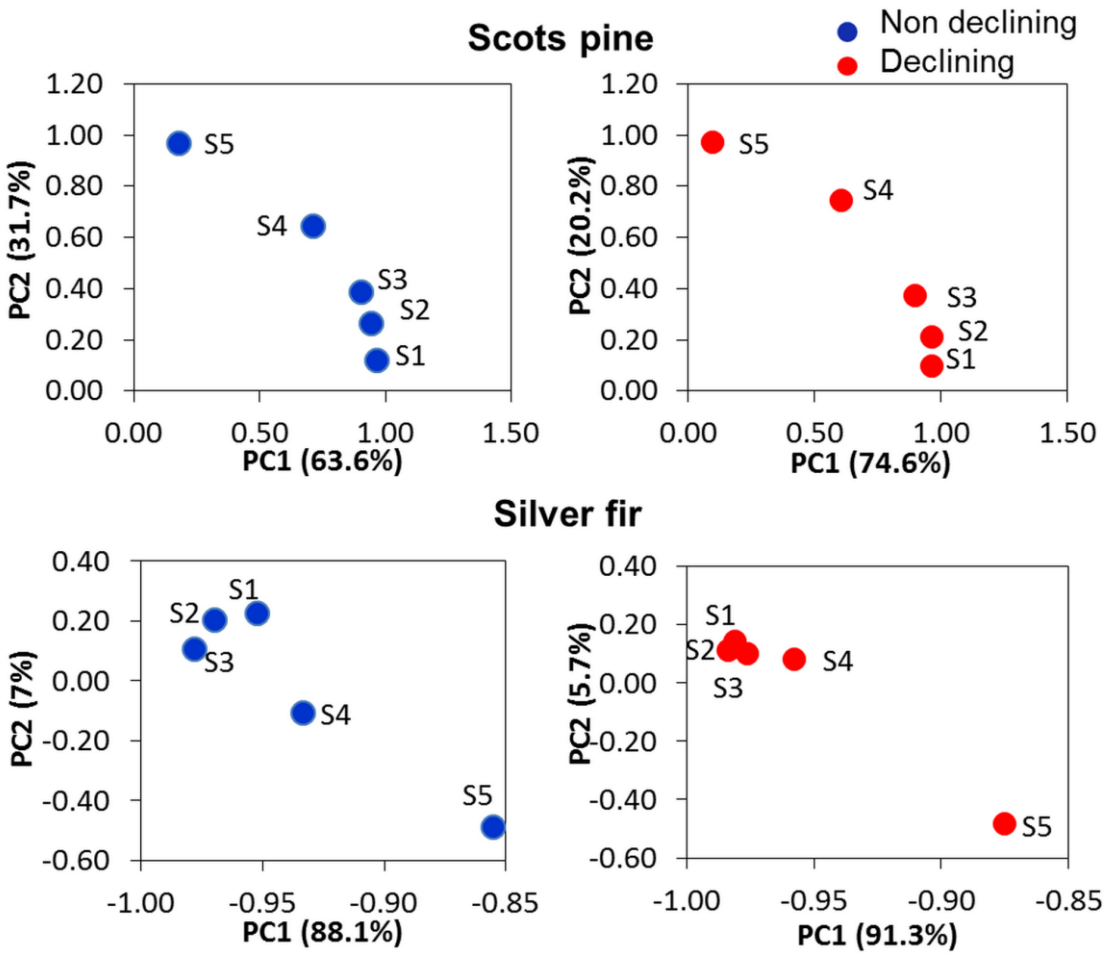

Fig. S2. Scatter plots of the weighting coefficients for the first (PC1) and second (PC2) components of the Principal Component Analysis computed with the lumen-area time series (1950-2012 period.) separated in five sectors (see Fig. S1). The variance percentage accounted for by each component is indicated.

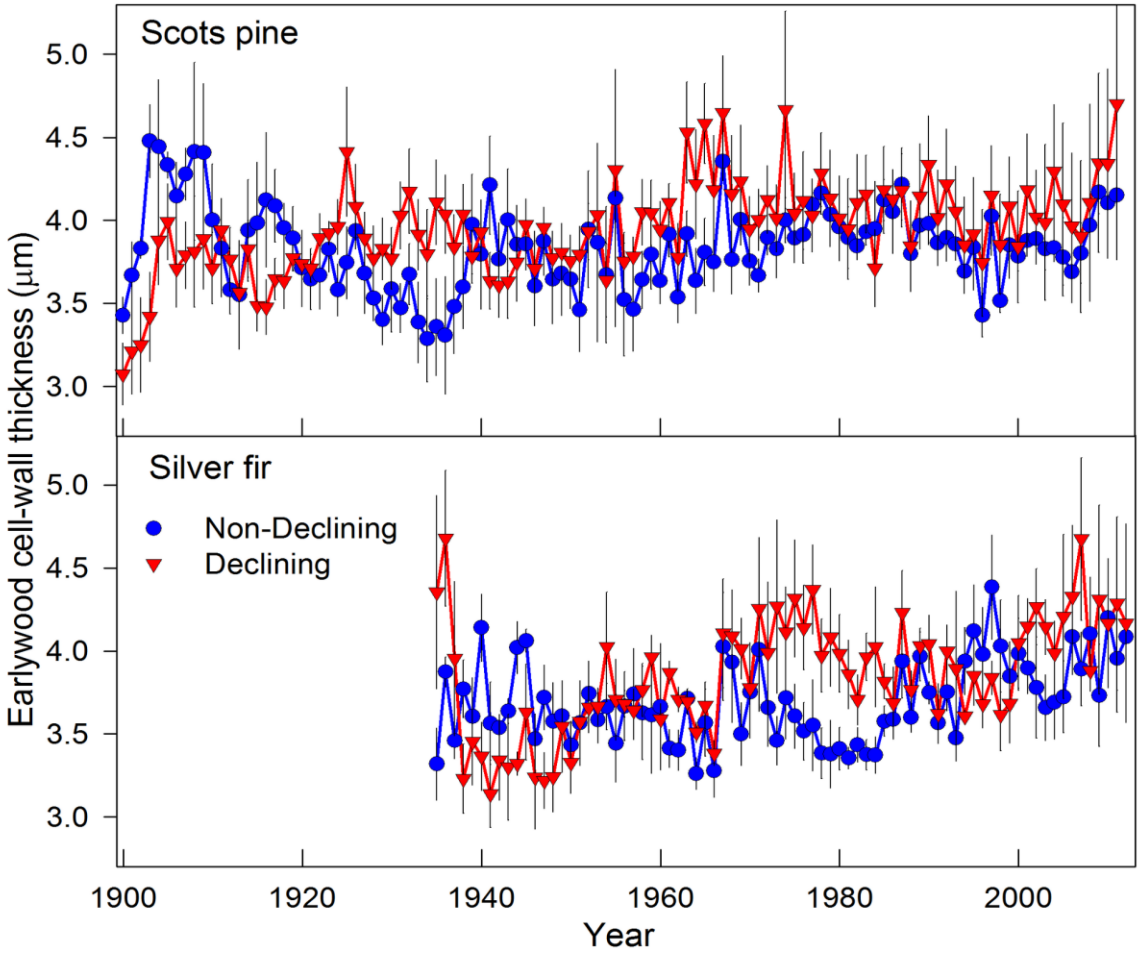

Fig. S3. Changes in earlywood cell-wall thickness observed in non-declining (ND) and declining (D) Scots pine and silver fir trees. Values are means ± SE.

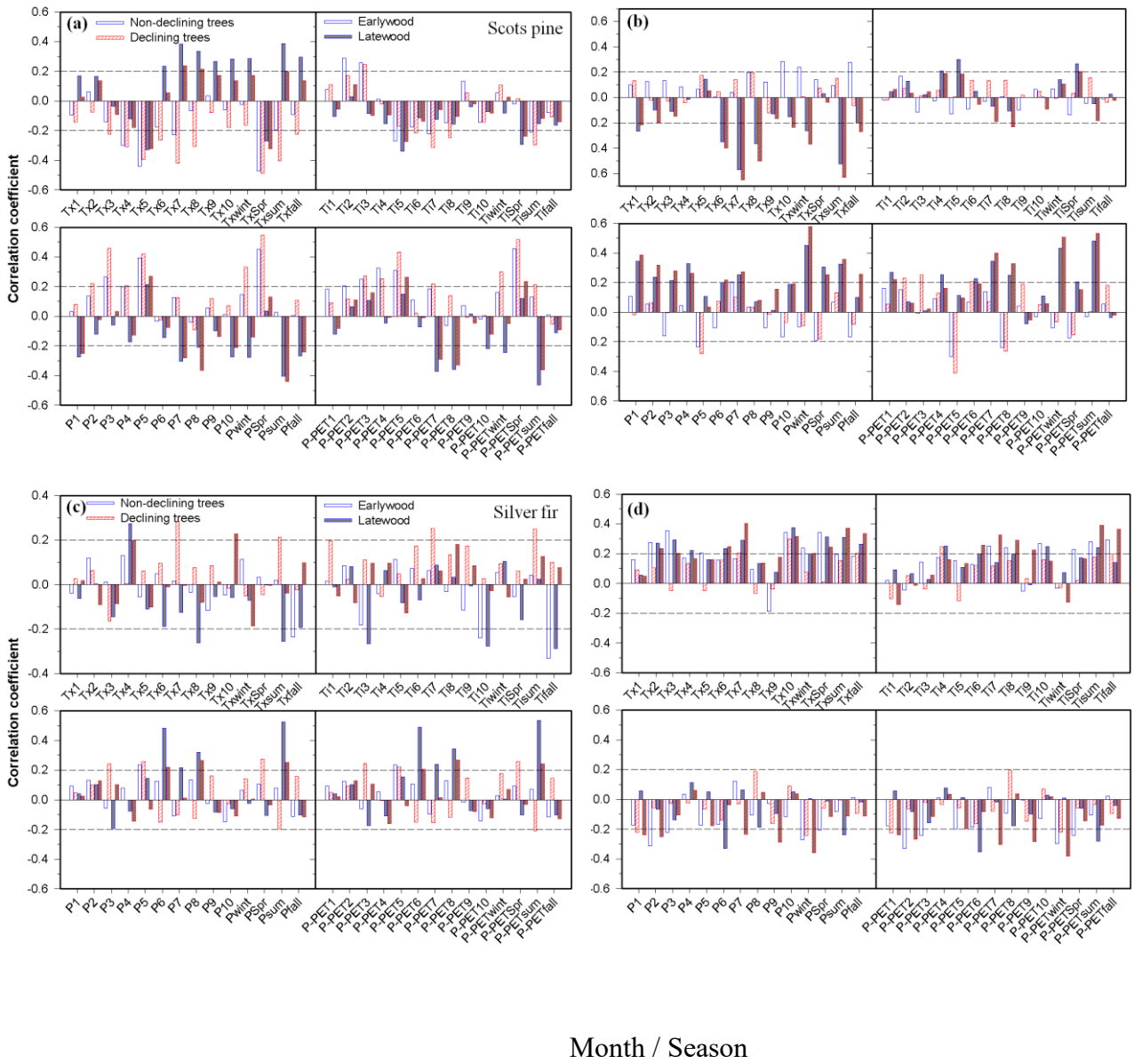

Fig. S4. Non-declining and declining Scots pine (a, b) and silver fir (c, d) correlations profiles calculated separately for earlywood and latewood, relating mean annual values of lumen area (a, c) or cell-wall thickness (b, d) to monthly or seasonal climatic variables (Tx and Ti, mean maximum and minimum temperatures, respectively; P, precipitation; and P-PET, water balance or difference between P and potential evapotranspiration, PET). Months are indicated with numbers, whilst seasons are abbreviated with letter codes. The dashed lines indicate the significance level ($P < 0.05$).

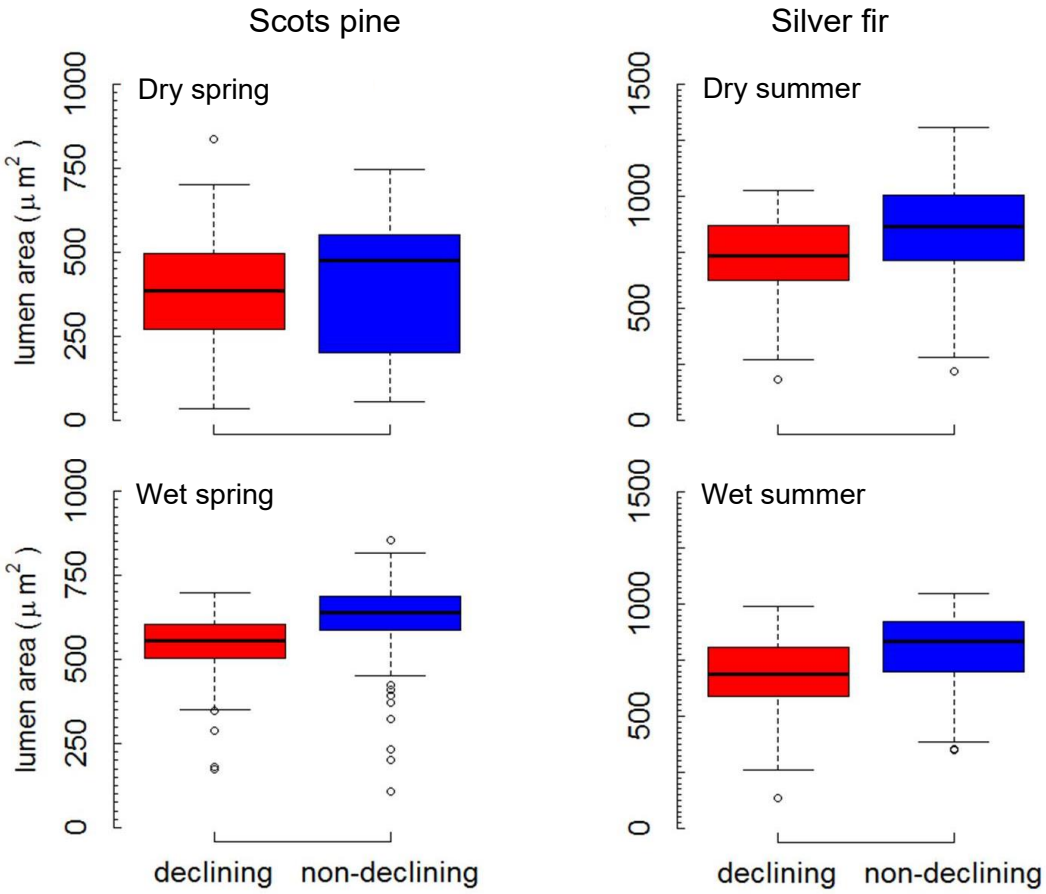

Fig. S5. Box plots showing the differences in earlywood (the first three sectors of each tree ring; see Fig. S1) lumen area of declining and non-declining Scots pine and silver fir trees during years with contrasting water availability. We plotted the three years with lowest or highest spring and summer water balances in the case of Scots pine and silver fir, respectively. In the Scots pine site the driest (wettest) springs were recorded in 1961, 1983 and 2005 (1962, 1971 and 2007). In the silver fir site the driest (wettest) summers were recorded in 1967, 1986 and 2012 (1963, 1977 and 1997).

Table S1. Selection of best-fitted generalized additive models of earlywood lumen area considering long- (between years) and short-term (within years) trends of this variable as related to tree vigour (declining *vs*. non-declining trees) and spring (Scots pine) or summer (Silver fir) water balance for the two tree species.

Short-term trend	Long-term trend	Vigour	Water balance	Long-term trend * vigour	Short-term trend * vigour	Water balance * vigour	*edf*	ΔAICc	Relative weight
Scots pine									
		+	+	+	+	+	40.83	0.1	1.00
+		+	+	+		+	31.92	26	0.00
	+	+	+		+	+	31.87	290	0.00
+	+	+	+			+	22.96	315	0.00
+	+	+	+				21.96	337	0.00
			+	+	+		38.82	521	0.00
+			+	+			29.91	545	0.00
	+		+		+		29.86	817	0.00
+	+		+				20.95	839	0.00
+	+	+					20.95	1850	0.00
+	+						19.93	147208	0.00
Silver fir									
		+	+	+	+	+	40.45	0.1	1.00
+		+	+	+		+	31.50	394	0.00
	+	+	+		+	+	31.75	1084	0.00
+	+	+	+			+	22.81	1445	0.00
+	+	+	+				21.81	1475	0.00
+	+	+					20.79	1526	0.00
			+	+	+		38.22	4754	0.00
+			+	+			29.31	5021	0.00
	+		+		+		29.63	5512	0.00
+	+		+				20.72	5763	0.00
+	+						19.64	162586	0.00

Note: For each species, the variables included in each of the models selected and associated degrees of freedom (*edf*), increase in the second-order Akaike Information Criterion (ΔAICc), and the relative weight of the model are shown. The symbols "+" indicate variables entering each evaluated model.

CHAPTER IV

Comparing millennium-long chronologies of wood maximum density and anatomical traits in northern Finland.

Elena Pellizzari[1], Jan Esper[2], Marco Carrer[1]

[1]Università degli Studi di Padova, Dip. TeSAF, Agripolis I-35020 Legnaro, Italy

[2] Department of Geography, Johannes Gutenberg University, DE-55099 Mainz, Germany

Introduction

Tree-rings are by far one of the most accurate and valuable proxy indicator of pre-instrumental climate variability (Fritts, 1976; Carrer & Urbinati, 2006). In particular, boreal forests in Fennoscandia, being at their limits of distribution are highly sensitive to climate variation, especially temperature. For this reason they have attracted an increasing number of dendrochronological studies aimed to reconstruct centuries- or even millennia- climate conditions (Lindholm & Eronen, 2000; Hughes, 2002; Esper *et al.*, 2004; Jones *et al.*, 2009; Linderholm *et al.*, 2014).

Tree ring-width represents only one and the easiest of the multiple parameters that can be extracted out of a wood sample for dendrochronological analysis indeed, other techniques in paleoclimatology have been proved to be very efficient to obtain high resolution data. Maximum latewood density (MXD), extracted from tree rings through high precision densitometry (Schweingruber *et al.*, 1978), for example, allows the analysis of detailed information retained in the latewood, the part of the ring formed at the end of the growing season (Fonti *et al.*, 2013). Being latewood cells influenced by the climatic conditions throughout the whole growing season, MXD has been proved to be a better proxy of summer temperatures respect to TRW (tree-ring width) at temperature-limited environments (Grudd, 2008; Esper *et al.*, 2012; McCarroll *et al.*, 2013). In northern Finland recent investigations on this parameter were directed to build multi-millennia MXD-chronologies, by combining both relict preserved sub-fossil material (Eronen *et al.*, 2002) and living trees. To date, the most well-replicated MXD chronology is the N-Scan (Esper *et al.*, 2012) which has been used to investigate on orbital forcing and to reconstruct over 2000 years of summer temperature variability in northern Europe (N-Eur, see Esper *et al.*, 2014). However, despite the great potential of this parameter to extract high resolution paleoclimate data, the procedure for the measurements are still challenging, time consuming (Schweingruber *et al.*, 1978; Sheppard *et al.*, 1996), and not always comparable among different laboratories.

Taking into account those limitations, in this work we considered other tree-ring parameters, able to provide even higher resolution information at intra-annual level. Dendroanatomy analyses cell features to extract valuable/climatic information, starting from the assumption that variation in anatomical structures is strongly linked to climate during their formation (Panyushkina *et al.*, 2003; Eilmann *et al.*, 2006; Schweingruber, 2007; Fonti *et al.*, 2010; Seo *et al.*, 2011; Gurskaya *et al.*, 2012; Bryukhanova & Fonti, 2013; Liang *et al.*, 2013). The latest improved techniques in dendroanatomy (von Arx *et al.*, 2016) allow to extract huge amount of data from a single measurement and thus reducing significantly the time needed for sample preparation and analysis. These new improvements are permitting to really consider dendroanatomy as a valid alternative to the classical approaches in building long chronologies of cell-related features to study long-term climatic fluctuations.

In detail in this research we aim to i) build a millennium-long cell-chronology using multiple cell parameters; ii) test whether anatomical features, as cell wall thickness can be a valuable surrogate of maximum latewood density measurements and iii) test the quality of the climatic imprint in cell-chronology.

Materials and methods

Data collection

Sub-fossil wood material used for the anatomical analysis are part of the samples considered for the N-Scan TRW (tree-ring width) and MXD chronologies (Esper *et al.*, 2012, 2014). Scots pine (*Pinus sylvestris L.)* disks of relict material have been collected from lakes (Eronen *et al.*, 2002), whereas living trees have been cored at dbh next to the lakeshores (Düthorn *et al.*, 2013). Sampling area was in northern Finland at 68.45°-69.52° N, 27.30°-28.55°E (Fig. 1); here the mean annual temperature is -0.9°C and the coldest and warmest months are January (-13.7°C) and July (+14.6°C) respectively, and annual precipitation is around 530 mm, with the highest amount occurring mainly during summer.

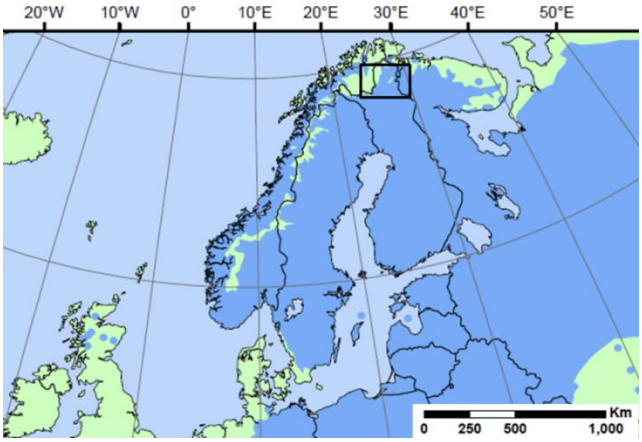

Figure 1: Study area (black rectangle) and Scots pine distribution map (EUFORGEN Networks).

Tree-ring anatomy

We extracted 0.5-1 cm wide sections from the sub-fossil disks and divided both, the cores from living tree and the disk sections in 3-5 cm long blocks which were boiled in water to soften them and remove resin. From each piece, using a rotary microtome (Leica RM 2255; Leica Microsystems, Germany), we cut transverse 15 µm thick slices that we prepared following the standard protocol (von Arx *et al.*, 2016) staining the samples with saphranine at 1% and astra blue 0.5% and permanently fixing the slices with Eukitt®. Digital images at 100x of magnification have been captured using a microscope with a mounted digital camera with a green filter to better visualize also the smallest cells of the latewood. Panoramas were created using PTGui software stitching together the pictures collected in order to obtain high resolution image of the entire section. Tracheid anatomy was measured for each sample using ROXAS (von Arx & Carrer, 2014), a software developed to measure long time-series of wood anatomical traits, considering not just few cell rows, but all the cells in a section (Fig. 2). For each cell we analysed several anatomical features, including lumen area (as the internal tracheid size), the tangential and radial cell wall thickness (Vysotskaya & Vaganov, 1989), and the Mork's index (Denne, 1988).

TRW chronology has been used to check the cross-dating of tree rings for the anatomical analysis.

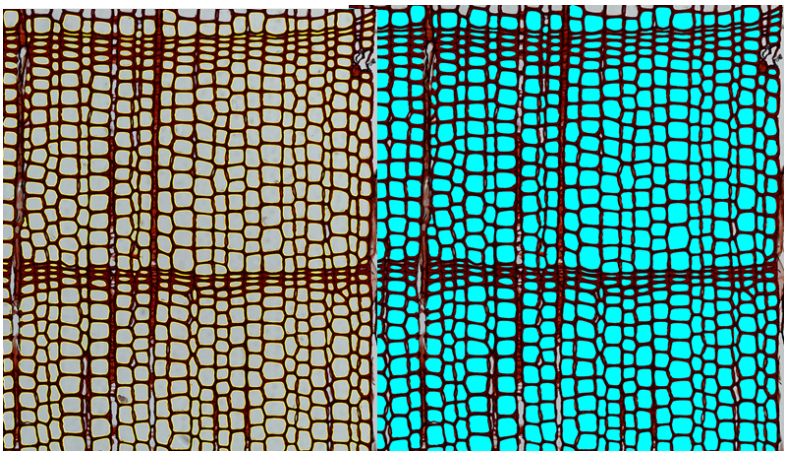

Figure 2 : Cell analysis with ROXAS allow to measure all the cells in a section.

Once obtained the yearly measurements of anatomical traits, intra-annual profiles at 10µm step have been also calculated using R (R Core Team, 2015). This resolution could permit to directly compare different anatomical parameters, and in particular minimum Lumen area (mLA), maximum value of Mork's index and radial and tangential cell wall thickness (MXW), with MXD data which are usually collected at this step. Descriptive descriptive statistics as the Mean sensitivity (MS), autocorrelation (AC), rbar and Expressed Population Signal (EPS) have been calculated for different anatomical and tree ring parameter for the whole period considered (900-2011).

Standardization and comparison with MXD reconstruction

Previous researches detected an age-related trend in cell chronologies, especially for what concerns vessel size (Carrer *et al.*, 2015), but also in MXD chronologies in Fennoscandia (Konter *et al.*, 2016). In this latter work significant trends characterized by increasing values for the first 30 years, followed by a decreasing trend during the maturation has been detected For this reason, all the time series have been standardized to remove this non climatic signal. We opted for the Regional curve standardization (RCS), which has been proved to be the most efficient and most suitable method to remove the non-climatic noise in boreal environments (Esper *et al.*, 2003, 2009; Helama *et al.*, 2004) being able to preserve climatic information also in the low-frequencies domain. TRW chronology, however, considering the different age-related trend, has been standardized using negative exponential curves. N-Scan MXD data has been compared and correlated with different anatomical parameters, both at annual (Lumen area and Cell wall thickness) and intra-annual resolution. We focused in particular to the latewood part considering mLA, MXWtan, Mork's index and MXWrad, to

find within these wood anatomical traits any parameter that could perform as a surrogate of maximum latewood density.

Climate data

Climate-growth associations have been computed to verify the quality of the climatic signal encoded in the wood-anatomical chronologies. Regional temperature anomalies, spanning from 1875 to 2011, from the CRUTEM4 (Jones *et al.*, 2012) gridded dataset have been considered. Mean monthly and summer temperature anomalies (the mean of June, July and August (JJA)) have been correlated (Pearson's correlation) with latewood anatomical parameters: mLA, Mork's index, and maximum radial cell wall thickness (MXWrad). We selected these latewood parameters since this is the same ring portion considered in the MXD measurements.

Results

Chronologies of anatomical features

We were able to build a millennium-long chronology using cell features (Fig. 3). We measured a total of 45 samples, 8 living and 37 relic trees and more than 8 million cells. Adopting as reference the crossdated tree-ring width series, we dated each ring and cell feature. The final chronologies span over 1000 years (900-2011), with a sample replication of at least 5 measurements per year. To date this represents the longest chronologies assemblage built with anatomical traits.

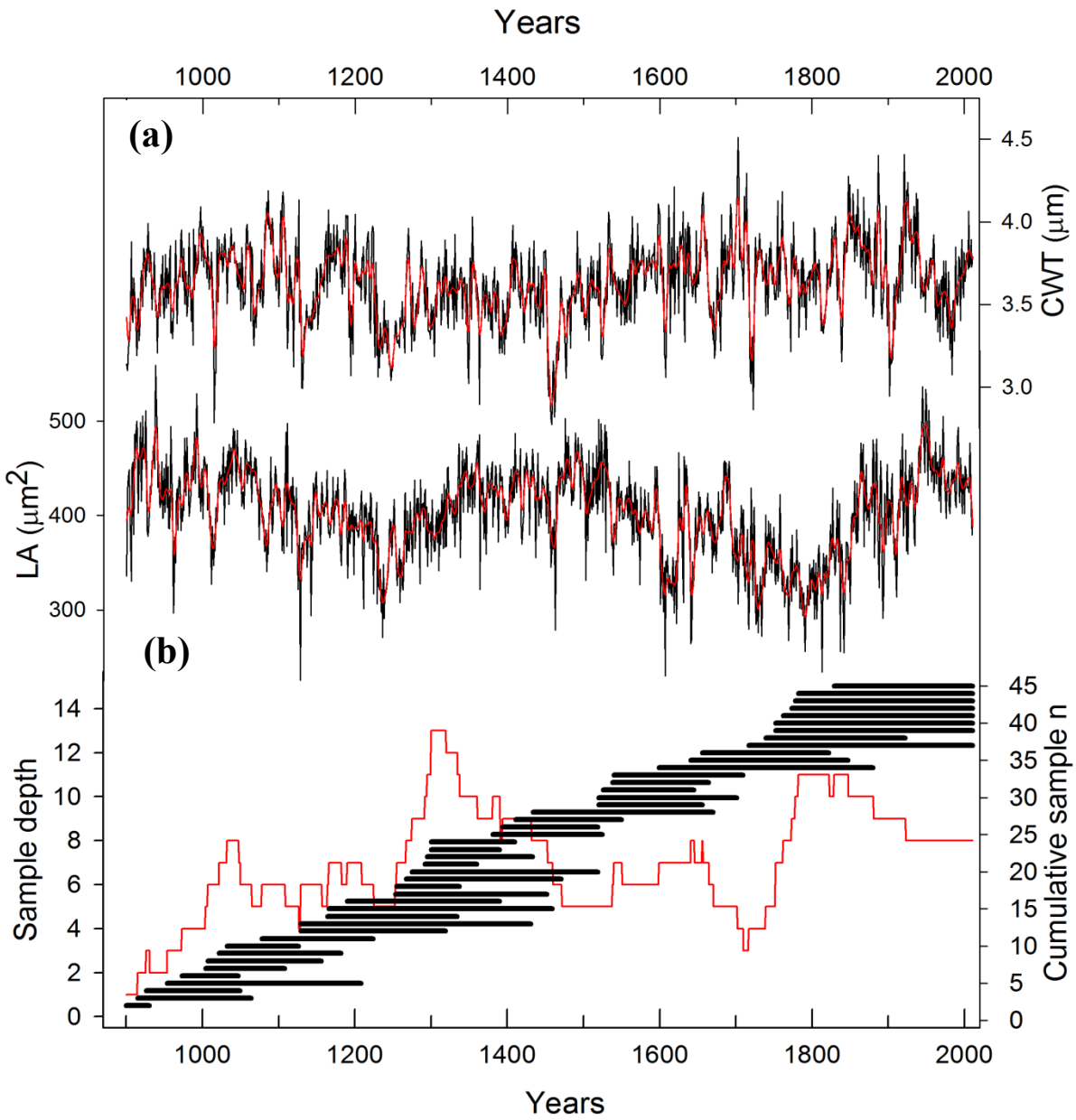

Figure 3: a) Raw lumen area and cell wall thickness chronologies. **b)** Sample depth (red line) and distribution over time (black segments).

Comparison with MXD chronology

Considering all the anatomical features, the highest correlation value is between detrended N-Scan MXD and MXWrad chronologies: r = 0.70 over 1106 years (900-2006) (Table 1). In general, annual resolution parameters as Lumen area (LA), tree ring width (TRW) and cell wall thickness (CWT) were the less correlated with the others or with the MXD chronology. On the other side intra-annual resolution parameters, related to the latewood and considering the 10 µm step, have been proved to be highly correlated with d N-Scan MXD chronology. N-Scan is negatively correlated with latewood minimum lumen area (mLA) and positively

with Mork's index while MXWtan strongly affect the mean CWT. In addition, considering the same samples, the correlations slightly increased respect when consider the whole N-Scan chornology (Tab. 1).

Table 1 : Correlation values (Pearson's) among various tree-ring parameters detrended over the period 900-2006. N-Scan is the complete chronology for maximum cell wall thickness, whereas MXD (900-1900) is related only to the same samples used for the anatomical analysis. Anatomical parameters are: mean lumen area (LA) and cell wall thickness (CWT) of the whole ring, maximum Mork's index, minimum lumen area (mLA), and maximum radial and tangential cell wall thickness (MXWrad and MXWtan).

		N-Scan	MXD	LA	CWT	TRW	Mork's index	mLA	MXWrad
Annual resolution	**LA**	-0.076	-0.10						
	CWT	0.585	0.63	-0.107					
	TRW	0.446	0.407	0.276	0.466				
Intra-annual resoultion	**Mork's index**	0.568	0.570	-0.020	0.577	0.320			
	mLA	-0.531	-0.54	0.112	-0.466	-0.243	-0.763		
	MXWrad	**0.700**	0.747	-0.011	0.726	0.504	0.690	-0.579	
	MXWtan	0.646	0.65	0.062	0.796	0.568	0.542	-0.417	0.705

Anatomical descriptive statistics (Table 2) show an EPS value under the fixed threshold (0.85) for all cell features and even for tree-ring width. Mean sensitivity is also very low, indicating that series are complacent, however this is consistent to other studies at high latitudes (Pritzkow *et al.*, 2014)..

Table 2: Descriptive statistics of the anatomical features and TRW at annual and intra-annual resolution. Sd, MS, AC and EPS correspond to standard deviation, mean sensitivity and Expressed Population Signal, respectively. The period considered is 900-2011.

		mean	sd	MS	AC	rbar	EPS
Annual resolution	**TRW (mm)**	0.473	0.211	0.186	0.861	0.312	0.808
	LA (μm^2)	399.17	52.69	0.091	0.605	0.225	0.705
	CWT (µm)	3.683	0.316	0.051	0.684	0.249	0.738
Intra-annual resoultion	**mLA(μm^2)**	45.09	11.271	0.204	0.413	0.103	0.730
	Mork's index (µm)	3.614	0.791	0.146	0.579	0.130	0.721
	MXWtan(µm)	4.424	0.712	0.094	0.685	0.216	0.752
	MXWrad(µm)	5.781	0.749	0.088	0.630	0.304	0.766

The most well correlated anatomical feature with N-Scan MXD chronology is MXWrad, henceforward MXW. It shows even a stronger correlation (r = 0.84) over the period 1875 to 2006 therefore, it could be considered a valuable surrogate for maximum density in this region.

Comparing N-Scan MXD and MXW chronologies (Fig. 4) in the low-frequencies, we detected similar long-term fluctuations that are connected to long-term climatic variation, as the Medieval warm period or the Little ice age. For what concern the high frequency, and the year-to-year variability, we were able to detect several pointer years for both MXD and MXW in 1363, 1453, 1757, 1607 and in 1902.

To better assess the consistency of the connection between MXD and MXW over the whole millennium we performed the 100-years running correlation (Fig. 4) . These correlation values are relatively strong (r > 0.8) especially in correspondence of higher sample depth, e.g. from 1250 to 1450, however are weaker (r < 0.6), but still highly significant (p<0.01) for period with less sample replication (1700-1800) or when most of the living trees entered in the chronology (1720-2011).

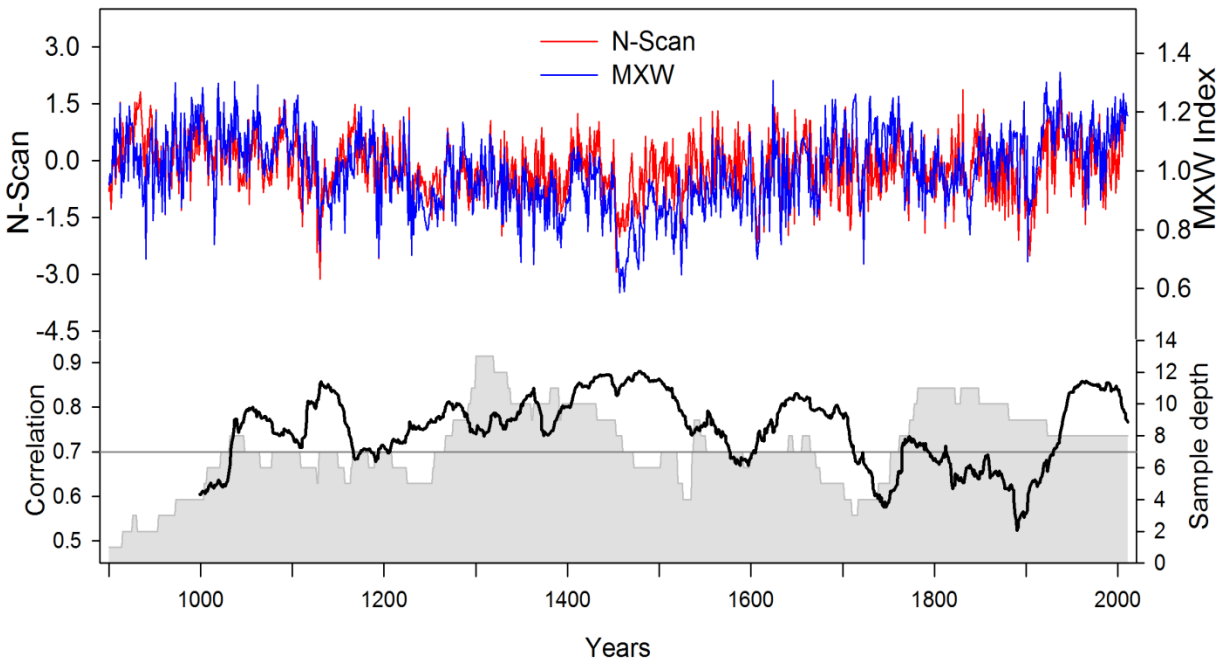

Figure 4: Comparison between detrended N-Scan (blue line) and MXWrad chronologies (red line). Black line corresponds to the 100-years running correlation between the two chronologies while the straight line refers to the mean correlation value over the entire period 900-2006. Grey area plot correspond to the sample depth.

Climate correlation

Monthly climate data have been correlated with intra-annual resolution cell parameters connected to latewood: mLA, Mork's index and MXW (Fig. 5). Mork's index shows higher monthly temperatures correlation during the early growing season, in May-June, respect to MXW. The highest correlations, however are related to the summer temperatures, in particular July and August and are positive for MXW and Mork's index, and negative for mLA. JJA seasonal temperature shows the highest correlation, with cell-wall thickness (r = 0.72), having a value similar to that obtained with MXD measurements (around r = 0.77) (Esper *et al.*, 2012). The comparison of JJA temperature with this anatomical parameter show a consistence of the signal, both at high and medium frequency, throughout the whole period (1875-2011). In addition, the spatial correlation map between MXW and JJA temperatures over the same period (Fig. 6) indicates a weaker but still significant ($p<0.01$) correlation respect to N-Scan MXD measurements with similar spatial coherence of the signal extended throughout the whole northern Fennoscandia region.

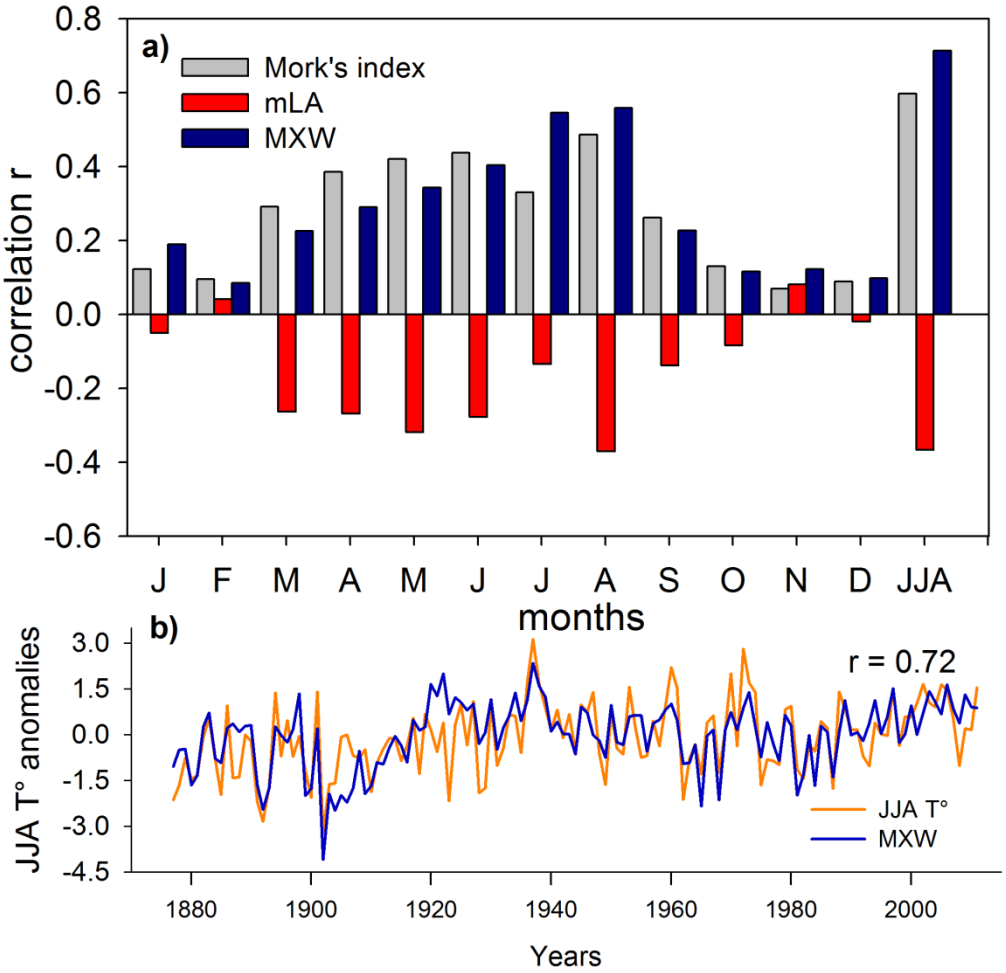

Figure 5 : a) Climate-growth correlation (Pearson's correlation) between CRUTEM4 regional temperatures and intra-annual anatomical features, minimum lumen area (mLA), maximum Mork's index and maximum radial cell wall thickness (MXW). **b)** Comparison between the MXW (blue) and JJA temperature (orange) over the 1875-2011 period.

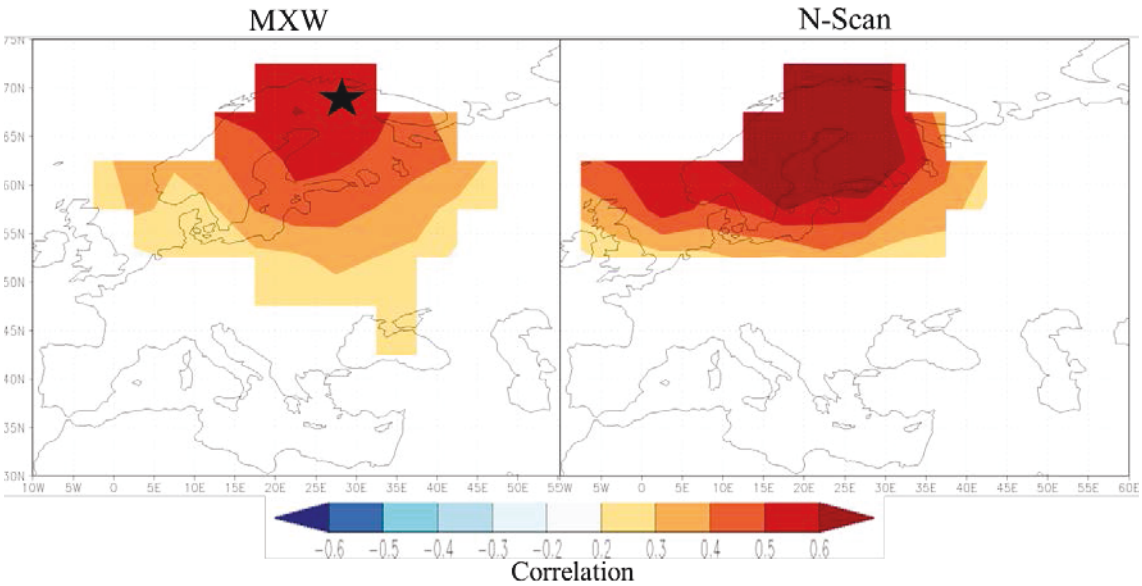

Figure 6: Spatial correlation pattern of detrended MXW (on the left) and N-Scan MXD (on the right) chronologies with JJA temperatures. The star indicates the sites position.

Discussions

Xylem-cell features are the basis of physiological processes influenced by climate during the growing season (Fonti *et al.*, 2010); this gives reason why with tree-ring anatomy it is possible to explore in detail the xylem plasticity (Vaganov *et al.*, 2006; Eilmann *et al.*, 2010) at intra-annual resolution. Earlywood cells in particular are usually affected by climatic conditions just before or at the beginning of the growing season(García-González & Fonti, 2006), on the contrary latewood cells, characterized by thicker wall and reduced lumen area, are connected to the end of the growing season but benefit from carbon assimilation throughout the whole vegetative period (Fonti *et al.*, 2013).

The recent techniques (von Arx *et al.*, 2016) and improvements of dendroanatomical protocols have simplified and reduced the time needed for sample preparation, allowing to build efficiently a well replicated millennium-long cell-chronology and to analyse the multi-proxy records extracted from cell features. Previous researches were limited at maximum four centuries (Panyushkina *et al.*, 2003)

We also proved that from wood anatomical traits it is possible to obtain a surrogate for maximum latewood density measurements.Considering that MXD is connected to the

latewood area of the thickest cell wall thickness and as consequence, also to the minimum cell area (Esper *et al.*, 2014), we hypothesised that maximum latewood cell wall thickness or minimum lumen area could be the most suitable parameters to replace MXD measurements. However not all the cell walls behave the same. We also found that the radial side of maximum cell wall thickness, that is the portion of the cell wall regarding the pith-to-bark direction, presents the highest correlation with maximum latewood density over the entire chronology. In particular, one of the clearest evidences of this common signal regards the period from 1453 to 1457, when both MXW and MXD chronologies presented parallel very low values. This time span coincide to a strong cooling event and likely related to the effect of a large eruption of Kuwae volcano in 1452 (Briffa *et al.*, 1998; Gao *et al.*, 2006). Other common pointer years are also related to volcanic cooling, as in 1902 (Fig.5) with the Santa Maria (Guatemala) eruption (Esper *et al.*, 2013). Running correlations between MXW and MXD chronologies are high and significant over the whole millennium however, in correspondence to lower sample replication (Esper *et al.*, 2014) in the MXW chronology, we observed a decrease. The low correlation values between the two chronologies over the period 1850-1900 can be also related to the inclusion of living samples in the MXW chronology in correspondence to the mature stage of several dead wood. Considering that tracheids face an ontogenetic change in size according the cambial age (Carrer *et al.*, 2015), featuring smaller cells during the first life stage and a progressively widening with the tree size increase, the inclusion of a group of series coming from young trees might introduce a certain amount of noise that the RCS standardization was not able to fully remove.

MXD is well-known as a more efficient parameter to investigate on past climate respect to tree-ring width in northern Fennoscandia (Esper *et al.*, 2010; Konter *et al.*, 2016), and for this reason, it is the most used tree-ring parameter to reconstruct past summer temperatures, at least at high latitudes (Briffa *et al.*, 2001; Esper *et al.*, 2014). Climatic influence on cells at intra-annual level has been broadly investigated (Seo et al., 2011; Pritzkow et al., 2014; Ziaco et al., 2014; Castagneri et al., 2015; Carrer et al., 2016), moreover similarly to MXD measurements it is influenced by JJA temperatures (Panyushkina *et al.*, 2003; Rossi *et al.*, 2006; Fonti *et al.*, 2013). The wide spatial correlation pattern with summer temperature emphasize the high coherence of the MXW climate signal over a large region, suggesting the potential of this anatomical parameter to reconstruct summer temperature over northern Europe.

In conclusion we tested whether anatomical features could be considered valid surrogate of MXD. MXD measurements have indeed several caveats: they can be influenced by specific

laboratory protocols which prevent a straightforward comparison among data produced; then due to the costly facilities needed, that are not accessible for all the labs and finally, sample preparation and data extraction are time consuming (Schweingruber *et al.*, 1978; Sheppard *et al.*, 1996; Schinker *et al.*, 2003). For this reasons we hypothesize that a more standardize but still efficient approach using dendroanatomy, could be applied for future analysis in the same way of MXD measurements.

Due to the high correlation with MXD measurements and due to the broad spatial correlation with summer temperatures, we think that MXW can be considered a valid proxy candidate for future wood-anatomical based climate reconstruction.

References

von Arx G, Carrer M (2014) ROXAS – A new tool to build centuries-long tracheid-lumen chronologies in conifers. *Dendrochronologia*, **32**, 290–293.

von Arx G, Crivellaro A, Prendin AL, Čufar K, Carrer M (2016) Quantitative Wood Anatomy—Practical Guidelines. *Frontiers in Plant Science*, **7**, 781.

Briffa K, Jones P, Schweingruber F, Osborn T (1998) Influence of volcanic eruptions on Northern Hemisphere summer temperature over the past 600 years. *Nature*, **393**, 450–455.

Briffa KR, Osborn TJ, Schweingruber FH, Harris IC, Jones PD, Shiyatov SG, Vaganov E a. (2001) Low-frequency temperature variations from a northern tree ring density network. *Journal of Geophysical Research*, **106**, 2929.

Bryukhanova M, Fonti P (2013) Xylem plasticity allows rapid hydraulic adjustment to annual climatic variability. *Trees - Structure and Function*, **27**, 485–496.

Carrer M, Urbinati C (2006) Long-term change in the sensitivity of tree-ring growth to climate forcing in Larix decidua. *New Phytologist*, **170**, 861–872.

Carrer M, Arx G Von, Castagneri D, Petit G (2015) Distilling allometric and environmental information from time series of conduit size : the standardization issue and its relationship to tree hydraulic architecture. *Tree Physiology*, **35**, 27–33.

Carrer M, Brunetti M, Castagneri D (2016) The Imprint of Extreme Climate Events in Century-Long Time Series of Wood Anatomical Traits in High-Elevation Conifers. *Frontiers in Plant Science*, **7**, 683.

Castagneri D, Petit G, Carrer M (2015) Divergent climate response on hydraulic-related xylem anatomical traits of Picea abies along a 900-m altitudinal gradient. *Tree Physiology*, **35**, 1378–1387.

Denne M (1988) Definition of latewood according to Mork. *Iawa Bull*, **10**, 59–62.

Düthorn E, Holzkämper S, Timonen M, Esper J (2013) Influence of micro-site conditions on tree-ring climate signals and trends in central and northern Sweden. *Trees - Structure*

and Function, **27**, 1395–1404.

Eilmann B, Weber P, Rigling A, Eckstein D (2006) Growth reactions of Pinus sylvestris L. and Quercus pubescens Willd. to drought years at a xeric site in Valais, Switzerland. *Dendrochronologia*, **23**, 121–132.

Eilmann B, Buchmann N, Siegwolf R, Saurer M, Rigling PC (2010) Fast response of Scots pine to improved water availability reflected in tree-ring width and δ 13C. *Plant, Cell and Environment*, **33**, 1351–1360.

Eronen M, Zetterberg P, Briffa KR, Lindholm M, Meriläinen J, Timonen M (2002) The supra-long Scots pine tree-ring record for Finnish Lapland: Part 1, chronology construction and initial inferences. *The Holocene*, **12**, 673–680.

Esper J, Cook ER, Krusic PJ, Peters K, Schweingruber FH (2003) Tests of the RCS method for preserving low-frequency variability in long tree-ring chronologies. *Tree-Ring Research*, **59**, 81–98.

Esper J, Frank DC, Wilson RJS (2004) Climate Reconstructions: Low-Frequency Ambition and High-Frequency Ratification. *EOS*, **85**, 113–115.

Esper J, Krusic PJ, Peters K, Frank D (2009) Exploration of long-term growth changes using the tree-ring detrending program "Spotty." *Dendrochronologia*, **27**, 75–82.

Esper J, Frank D, Büntgen U, Verstege A, Hantemirov R, Kirdyanov A V. (2010) Trends and uncertainties in Siberian indicators of 20th century warming. *Global Change Biology*, **16**, 386–398.

Esper J, Frank DC, Timonen M et al. (2012) Orbital forcing of tree-ring data. *Nature Clim. Change*, **2**, 862–866.

Esper J, Schneider L, Krusic PJ et al. (2013) European summer temperature response to annually dated volcanic eruptions over the past nine centuries. *Bulletin of Volcanology*, **75**, 1–14.

Esper J, Düthorn E, Krusic PJ, Timonen M, Büntgen U (2014) Northern European summer temperature variations over the Common Era from integrated tree-ring density records. *Journal of Quaternary Science*, **29**, 487–494.

Fonti P, Von Arx G, García-González I, Eilmann B, Sass-Klaassen U, Gärtner H, Eckstein D (2010) Studying global change through investigation of the plastic responses of xylem anatomy in tree rings. *New Phytologist*, **185**, 42–53.

Fonti P, Bryukhanova M V., Myglan VS, Kirdyanov A V., Naumova O V., Vaganov EA (2013) Temperature-induced responses of xylem structure of Larix sibirica (pinaceae) from the Russian Altay. *American Journal of Botany*, **100**, 1332–1343.

Fritts HC (1976) *Tree rings and Climate*. Academic Press, London, UK.

Gao C, Robock A, Self S et al. (2006) The 1452 or 1453 A.D. Kuwae eruption signal derived from multiple ice core records: Greatest volcanic sulfate event of the past 700 years. *Journal of Geophysical Research Atmospheres*, **111**.

García-González I, Fonti P (2006) Selecting earlywood vessels to maximize their

environmental signal. *Tree physiology*, **26**, 1289–1296.

Grudd H (2008) Torneträsk tree-ring width and density ad 500–2004: a test of climatic sensitivity and a new 1500-year reconstruction of north Fennoscandian summers. *Climate Dynamics*, **31**, 843–857.

Gurskaya MA, Hallinger M, Eckstein D, Wilmking M (2012) Extreme cold summers in western Siberia, concluded from light-rings in the wood of conifers. *Phyton - Annales Rei Botanicae*, **52**, 101–119.

Helama S, Lindholm M, Timonen M, Eronen M (2004) Detection of climate signal in dendrochronological data analysis: A comparison of tree-ring standardization methods. *Theoretical and Applied Climatology*, **79**, 239–254.

Hughes MK (2002) Dendrochronology in climatology – the state of the art. *Dendrochronologia*, **20**, 95–116.

Jones PD, Briffa KR, Osborn TJ et al. (2009) High-resolution palaeoclimatology of the last millennium: a review of current status and future prospects. *The Holocene*, **19**, 3–49.

Jones PD, Lister DH, Osborn TJ, Harpham C, Salmon M, Morice CP (2012) Hemispheric and large-scale land-surface air temperature variations: An extensive revision and an update to 2010. *Journal of Geophysical Research: Atmospheres*, **117**, n/a-n/a.

Konter O, Büntgen U, Carrer M, Timonen M, Esper J (2016) Climate signal age effects in boreal tree-rings: Lessons to be learned for paleoclimatic reconstructions. *Quaternary Science Reviews*, **142**, 164–172.

Liang W, Heinrich I, Simard S, Helle G, Liñán ID, Heinken T (2013) Climate signals derived from cell anatomy of scots pine in NE Germany. *Tree Physiology*, **33**, 833–844.

Linderholm HW, Björklund J, Seftigen K, Gunnarson BE, Fuentes M (2014) Fennoscandia revisited: a spatially improved tree-ring reconstruction of summer temperatures for the last 900 years. *Climate Dynamics*, **45**, 933–947.

Lindholm M, Eronen M (2000) A reconstruction of mid-summer temperatures from ring-widths of Scots pine since AD 50 in northern Fennoscandia. *GEOGRAFISKA ANNALER SERIES A-PHYSICAL GEOGRAPHY*, **82A**, 527–535.

McCarroll D, Loader NJ, Jalkanen R et al. (2013) A 1200-year multiproxy record of tree growth and summer temperature at the northern pine forest limit of Europe. *The Holocene*, **23**, 471–484.

Panyushkina IP, Hughes MK, Vaganov E a, Munro M a R (2003) Summer temperature in northeastern Siberia since 1642 reconstructed from tracheid dimensions and cell numbers of Larix cajanderi. *Canadian Journal of Forest Research-Revue Canadienne De Recherche Forestiere*, **33**, 1905–1914.

Pritzkow C, Heinrich I, Grudd H, Helle G (2014) Relationship between wood anatomy, tree-ring widths and wood density of Pinus sylvestris L. and climate at high latitudes in northern Sweden. *Dendrochronologia*, **32**, 295–302.

R Core Team (2015) R: A Language and Environment for Statistical Computing. *R Foundation for Statistical Computing Vienna Austria*, **0**, {ISBN} 3-900051-07-0.

Rossi S, Deslauriers A, Anfodillo T (2006) Assessment of cambial activity and xylogenesis by microsampling tree species: An example at the alpine timberline. *Iawa Journal*, **27**, 383–394.

Schinker M, Hansen N, Spiecker H (2003) High-frequency densitometry-a new method for the rapic evaluation of wood density variations. *IAWA Journal*, **24**, 231–239.

Schweingruber FH (2007) *Wood structure and environment*. 279 pp.

Schweingruber F, Fritts H, Braker O, Drew L, Schar E (1978) The Xray technique as applied to dendroclimatology. *Tree-Ring Bulletin*, **38**, 61–91.

Seo JW, Eckstein D, Jalkanen R, Schmitt U (2011) Climatic control of intra- and inter-annual wood-formation dynamics of Scots pine in northern Finland. *Environmental and Experimental Botany*, **72**, 422–431.

Sheppard PR, Graumlich LJ, Conkey LE (1996) Reflected-light image analysis of conifer tree rings for reconstructing climate. *The Holocene*, **6**, 62–68.

Vaganov EA, Hughes MK, Shashkin A V (2006) *Growth Dynamics of Conifer Tree Rings: Images of Past and Future Environments*. Springer Berlin Heidelberg.

Vysotskaya LG, Vaganov EA (1989) Components of the Variability of Radial Cell Size in Tree Rings of Conifers. *IAWA Journal*, **10**, 417–426.

Ziaco E, Biondi F, Rossi S, Deslauriers A (2014) Intra-annual wood anatomical features of high-elevation conifers in the Great Basin, USA. *Dendrochronologia*, **32**, 303–312.

GENERAL CONCLUSIONS

Despite the relevant position among the natural archives, tree rings feature several limitations mostly related to the temporal scale of analysis and the quantity and quality of data obtained. In particular, current research protocols allow to work mainly at annual resolution, without considering the intra-annual level, and keep less importance to anatomical features which are actually the basis of physiological processes influenced by climate (Fonti *et al.*, 2010).

In this thesis I aimed to move a step ahead to fill those gaps by applying two novel approaches: i) using an underrepresented species to detect different climatic information and ii) using dendroanatomy to obtain multi-proxy records with improved time resolution.

Despite it is still a challenging species, common juniper has proved to have high potential. I was successful in building century-long chronologies and to detect a divergent signal across Europe respect coexisting trees. Juniper represent therefore a promising proxy record for snow accumulation at least in the Alps and a species to consider when modelling vegetation responses to climate warming. Forecasts on global carbon uptake, albedo changes in polar biomes or forest dynamics would likely benefit when considering even this widely distributed prostrate/shrubby taxon.

With dendroanatomy I was able to obtain in-depth information at ecophysiological level not detectable with just tree-ring width. These dendroanatomical skills permitted me to explore the mechanisms of forest mortality due to drought and defined that tree death in drought-prone areas is likely due to hydraulic deterioration rather than carbon starvation. The possibility to appreciate subtle changes in anatomical attributed, even without any external evidence, makes this approach a valuable diagnostic tool to forecast forest vulnerability and in face of new climatic scenarios.

Lastly, building a millennium-long chronology and verifying the dendroclimatic potential of some anatomical traits, I highlighted that it is possible to use a surrogate of wood-density. In this sense quantitative anatomy may reduce the time needed for data collection with the added value that we are speaking about a multi-proxy archive. A reconstruction of past climate conditions with wood anatomical parameters even considering an intra-annual resolution, is now possible. This would help to correctly place the actual warming in a longer-term context and assess whether Anthropocene can be considered really unprecedented or just a warming pulse within the normal range of natural climatic variability.

REFERENCES

Fonti P, Von Arx G, García-González I, Eilmann B, Sass-Klaassen U, Gärtner H, Eckstein D (2010) Studying global change through investigation of the plastic responses of xylem anatomy in tree rings. *New Phytologist*, **185**, 42–53.